Evaluate extreme ice loads from freezing rain

for

Newfoundland and Labrador Hydro

Final Report
January 11, 2010

Kathleen F. Jones
Terrestrial and Cryospheric Sciences Branch
Cold Regions Research and Engineering Laboratory
Hanover, New Hampshire

Acknowledgements

Thanks to Robert Morris and Trisha Ralph of Environment Canada for providing weather data for stations in Newfoundland and Labrador as well as nearby stations in Quebec. Johnathan Walsh read through many reels of newspaper microfilm to find stories on ice storm damage, or the lack of stories, on the modeled ice storms. Having done this myself for many other regions in North America, I appreciate someone else taking on this time-consuming nausea-inducing-as-your-eyes-follow-the-slowly-moving-microfilm task for Newfoundland and Labrador.

TABLE OF CONTENTS

LIST OF TABLES

LIST OF ILLUSTRATIONS

1.0 Introduction

Ice and wind-on-ice loads on electric power transmission lines and communication towers are the governing loads on these structures in much of the Canada and the United States. For the 2005 revision of ASCE (American Society of Civil Engineers) Standard 7 *Minimum Design Loads for Buildings and Other Structures* (2005), the Ice Load Task Committee provided a revised map of equivalent uniform radial ice thicknesses from freezing rain with concurrent gust speeds for a 50-year return period. CRREL (Cold Regions Research and Engineering Laboratory) recently completed a project for CEATI Wind and Ice Mitigation Interest Group to map extreme ice loads along the US-Canadian border. For that project we used the same approach for processing Canadian weather and precipitation data, the same ice accretion models, and the same extreme value analysis method as we used to map 50-yr equivalent radial ice thicknesses and concurrent wind speeds in the United States. The inclusion of data from Canada helped to better define ice loads along the northern tier of states in the United States. The map for the eastern United States with equivalent radial ice thicknesses for a 50-yr return period is shown in Figure 1. For this project we will be using that same approach to map ice loads from freezing rain in Newfoundland and Labrador. We will compare our results to those from a study that MRI did for Newfoundland and Labrador Hydro in the 1970s (Richmond and Fegley1973).

2.0 Background

The discussion of the data, models, analyses, and algorithms in this report is taken largely from Jones and Morris (2002), which compared the U.S. and Canadian approaches to mapping extreme ice thicknesses and the concurrent wind speed. Any differences in approach are discussed.

CRREL has developed software and algorithms for processing historical data from weather stations with hourly weather data and 6-hourly or daily precipitation data. Weather data in Canada is provided by Environment Canada (EC). The period of record for those stations typically begins in 1954.

We first merge the weather and precipitation data and prorate accumulated precipitation to each hour based on the type and severity of precipitation. We then extract freezing rain storms, which are assumed to continue as long as freezing rain is falling and, after freezing rain ends as long as the air temperature remains at or below 1^{o}C.

The accretion of ice, expressed as an equivalent radial ice thickness, and wind-on-ice loads are modeled for each storm. We use both the detailed CRREL ice accretion model (Jones 1996a), which does a heat-balance analysis to determine how much of the freezing precipitation impinging on a horizontal cylinder freezes, and the sometimes more conservative Simple model (Jones 1996a,b), which simulates the accretion of ice at a hypothetical site where it is cold enough that all the freezing precipitation freezes.

Model results are checked for ice storms with significant modeled ice thicknesses using contemporaneous newspaper reports. The damage reports are used to determine the footprint of each ice storm where the ice loads and wind-on-ice loads damaged overhead lines, telecommunication towers, and trees.

To generate a long period of record for the extreme value analysis of ice and wind-on-ice loads, the weather stations are grouped into superstations. These groupings are based on the frequency of ice storms, the distribution of damaging ice storms, topography, proximity to large bodies of water, latitude, etc. Ice thicknesses and wind-on-ice loads for a fifty-year return period are determined using the peaks-over-threshold method with the generalized Pareto distribution (Hosking and Wallis 1987). This three-parameter distribution, which allows for a long tail (negative tail shape parameter k) or a finite tail (positive tail shape parameter k) if the data warrants, fits extreme ice thicknesses better than the widely-used two-parameter Gumbel distribution. The parameters of the distribution are determined using probability weighted moments (Wang 1991), with a threshold chosen to give an occurrence rate for the sample of extreme ice thicknesses of about one per year. At locations where freezing rain storms occur relatively rarely, occurrence rates as low as one in ten years are used. Wind speeds concurrent with the 50-yr ice thicknesses are back calculated from the 50-yr wind-on-ice load and the 50-yr ice thickness.

The ice thickness and concurrent gust-on-ice speed zones for the superstations are mapped using 10 mm increments in uniform ice thickness and 5 km/hr increments in gust speed. Ice thicknesses in a zone range from 70% below the nominal value to 30% above. The results of this project will be compared to those presented by Richmond and Fegley (1973) for seven stations in Newfoundland and Labrador (Figure 2).

3.0 Weather data and ice accretion models

Weather data are used as input to ice accretion models that determine the amount of accreted ice using empirical parameters and a physical model of the ice accretion process. The historical weather data files include documentation of the precipitation type and measurements of the precipitation amount, wind speed, air temperature, dew point temperature, and air pressure for each hour. The accuracy of the loads determined by an ice accretion model depends on both the quality of the weather data and the quality of the model, as well as the decisions made by the user in applying the model to the data. Because weather instruments may not work well, or at all, in freezing rain, some of the data that determine the accreted ice thickness may be estimated by the weather observers both during and after freezing rain. Owing to spatial variations in precipitation type and intensity, wind speed, and temperature, actual accreted ice thicknesses can vary significantly over relatively short distances. Thus, using weather data and an ice accretion model to determine ice thicknesses on wires and conductors supplies only an estimate of the equivalent radial ice thickness at any point along a transmission line.

3.1 Weather data

Canadian weather data were provided for this project by Bob Morris and Trisha Ralph of Environment Canada. Data for the specified stations were extracted from the Meteorological Service of Canada National Archives System. The data sets are hourly meteorological observations, some from as early as 1953, with 24-hour precipitation amounts. Data are quality controlled to some extent by Environment Canada, although methods have varied through the years.

We obtained weather data from 28 stations in Newfoundland and Labrador and nearby Quebec. The stations are listed in Table 1, with their location, elevation, the period of record for the daily precipitation data, the total number of years with usable weather data, and comments on the data, including missing years in the precipitation or weather data, years with part-time data, and data errors. A color relief map of the region for this study is shown in Figure 3. The map in Figure 4 shows the locations of the 28 stations. The two automatic stations, Badger and the Argentia station that began operation in 1987, do not collect present weather data so could not be used in this study.

3.2 Ice accretion models

The most important parameters in determining ice thicknesses from weather data are the precipitation rate and wind speed during the freezing rain storm. Unfortunately, anemometers and precipitation gauges may be adversely affected by accreted ice, and sometimes freezing rain storms cause power outages at weather stations. Thus, the expertise and dedication of the weather observers may have a significant effect on the quality of the recorded wind speed and precipitation data. We do not know how much the quality of weather measurements has varied over time or how much it varies from station to station.

The Simple model (Jones 1996b) determines the equivalent uniform radial ice thickness R_{eq} from the amount of freezing rain and the wind speed:

$$R_{eq} = \sum_{j=1}^{N} \frac{1}{\rho_i \pi} \left[(P_j \rho_o)^2 + (3.6 V_j W_j)^2 \right]^{1/2} , \qquad (1)$$

where P_j = precipitation amount (mm) in the jth hour, ρ_o = density of water (1 g/cm^3), V_j = wind speed (m/s) in the jth hour, W_j = liquid water content (g/m^3) of the rain-filled air in the jth hour = $0.067P_j^{0.846}$ (Best 1949), and N = duration (hr) of freezing rain storm. R_{eq} does not depend on the air temperature because it is assumed that all the available precipitation freezes. Then, because the ice is uniformly thick around the wire, R_{eq} does not depend on the wire diameter. Note that the liquid water content W is expressed in terms of the precipitation rate P, implicitly incorporating a fall speed for the raindrops. The relationship used in (1) results in a fall speed V_T (m/s) = $4.15P^{0.154}$. Actual ice accretion shapes vary significantly (Figure 5) depending on the local conditions, thus a general relationship between R_{eq} and the maximum thickness of accreted ice cannot be specified.

The CRREL model (Jones 1996a) is similar to the Simple model, but uses a heat-balance calculation to determine how much of the impinging precipitation freezes directly to the wire and how much of the runoff water freezes as icicles. If it is cold enough and windy enough the ice thicknesses determined by the CRREL and Simple models are the same. However, if the air temperature is near freezing and wind speeds are low, the CRREL model calculates smaller ice thicknesses than the Simple model. In those conditions much of the impinging precipitation may freeze as icicles.

3.3 Data-model interface

To use historical weather data to determine ice thicknesses, a number of decisions must be made about the data that are separate from the model, but affect the results. These include 1) prorating 6-hourly and 24-hourly precipitation amounts to each hour, 2) deciding how much of the precipitation accretes as ice when there are other types of precipitation, such as rain, snow or ice pellets, mixed with or alternating with, freezing rain, 3) correcting the measured wind speed from the height above ground of the anemometer to the height of the wire, 4) dealing with wire orientation to the wind and variability in wind direction, 5) deciding when a freezing rain storm ends. Each of these aspects of determining ice thicknesses from weather data is discussed in this section.

3.3.1 Prorating accumulated precipitation. The weighting factors used to prorate 6- and 24-hourly precipitation amounts to each hour are shown in Table 2. These weights were originally chosen to be the typical precipitation rate in mm/hr for each type of precipitation. The weight assigned to each hour in the weather record is determined by the present weather codes for the hour, with the weight set to zero if there is no precipitation. For example, if the only type of precipitation reported in an hour is light freezing rain, the weighting factor for that hour is 1.8. If in the next hour moderate freezing drizzle is reported with light snow, the weighting factor is (0.3+0.6)/2=0.45. The fraction of the accumulated precipitation attributed to each hour is the weighting factor for the hour divided by the sum of weighting factors for the six or 24 hours in which precipitation accumulated. This fraction is then multiplied by the accumulated amount to estimate the hourly precipitation amount. Table 2 is based on one provided by Tsoi Yip of the Atmospheric Environment Service (AES), which was originally from an unpublished report by MEP for Environment Canada in August 1984. The main difference between Table 2 and the Canadian version is the larger weighting factor for moderate freezing rain, equal to that for moderate rain, here.

3.3.2 Mixed precipitation types. In freezing rain storms the type of precipitation varies from hour to hour, and in any hour there will often be two or even three types of precipitation. We do not attempt a further subdivision of the prorated hourly precipitation amounts, but instead assume that all the precipitation in an hour in which freezing rain falls accretes to the wire as if it were freezing rain. The models are also allowed to accrete precipitation that was described as rain or drizzle (not freezing) if the air temperature is below freezing. These assumptions are conservative. They allow the modeled ice thicknesses to represent the possibly more severe conditions in the vicinity of the weather station, where perhaps all the precipitation is freezing rain rather than the mixture of precipitation types observed at the weather station, or where convective and evaporative cooling are slightly greater than at the weather station. This conservatism also expresses a reluctance to further subdivide the precipitation amounts based on weighting factors that at best are correct on average but cannot represent the mix of varying precipitation types in an hour, of which the observers provide only a glimpse in their once-per-hour observations of the precipitation type.

In both the CRREL and Simple models, ice loads are determined for two cases: 1) allowing ice to accrete only in hours in which the precipitation type is reported as freezing rain or a combination of freezing rain and other types of precipitation and 2) allowing ice to accrete also in hours in which the precipitation type is ice pellets. Freezing rain and ice pellets occur in the precipitation-type transition region of winter storms (Stewart 1992), which typically is bounded by snow on one side and rain on the other. Freezing rain and ice pellets develop in the same meteorological conditions: a layer of warm air over a layer of cold air. Snowflakes, formed in clouds above the layer of warm air, melt as they fall through the warm air. These water drops then cool while falling through the layer of cold air below. For the right combinations of cold and warm layer thicknesses and temperatures, the raindrops may supercool in the cold air layer but remain liquid and ultimately freeze on impact with a structure. However, there are two scenarios in which the precipitation falls as ice pellets rather than freezing rain: 1) if the cold air layer is thick enough and cold enough, the raindrops freeze partially or entirely, forming ice pellets, and 2) if the warm air layer aloft is relatively thin or cold, the snowflakes may not melt completely before falling into the cold air layer. In the first case, structures at higher elevations or high enough above ground may be in freezing rain while ice pellets are observed at weather stations. The inclusion of ice pellets in modeling ice loads at weather stations is intended to estimate ice loads that *may* have occurred on structures near to, but higher than, the weather station. The CRREL ice storm team observed this in a storm in February 1996 in Tennessee, where freezing rain damaged trees and power lines on Lookout Mountain, a suburb of Chattanooga, while ice pellets were falling at the Chattanooga airport.

3.3.3 Anemometer and wire heights above ground. Ice thicknesses on wires are often calculated at 10 m above ground, but may be calculated at any height. Because wind speed increases with height above ground through the earth's boundary layer, the ice thickness also increases with height, as shown by (1). Thus, it can be important to know how far above ground the wind speed is measured. The anemometer height at any weather station has typically varied over time, and also varies from station to station. The rate of increase of wind speed with height depends on the roughness of the terrain and the exposure of the site. In previous ice accretion studies the wind speed was assumed to be proportional to the 1/7 power of the height, following ASCE Standard 7-93 (1993) for exposure C, which is appropriate at these airport weather stations. Thus

$$V_W = V_A \left(\frac{h_W}{h_A} \right)^{1/7} \qquad (2)$$

where V_W and V_A are the wind speeds at the height above ground of the wire h_W and the height above ground of the anemometer h_A, respectively. The relationship in (2) provides only an estimate of the actual average wind profile. Because this wind speed correction to the current nominal 10 m anemometer height was found to be relatively minor in Jones and Morris (2002, Figure 9), in this study the reported wind speeds are assumed to have been measured at 10 m.

A correction is made to hours in which the recorded wind speed is zero in case the zero wind is a result of a frozen anemometer. In these hours the wind speed for the previous hour with a non-zero wind speed is used. Hours that are actually calm are "corrected" erroneously by this procedure, resulting in modeled ice thicknesses that are too high. On the other hand, if ice accreting on the anemometer has caused erroneously low but non-zero winds for a number of hours, the modeled ice thicknesses will be too low.

3.3.4 Wire orientation and wind direction. Both the CRREL model and the Simple model compute the uniform ice thickness on a wire whose orientation changes as necessary so that it is always perpendicular to the wind to give the largest effect of wind-blown rain. This assumption is conservative for power lines, particularly for line routes that are nearly parallel to the prevailing wind direction for freezing rain storms. To determine the variation in ice thickness with orientation, the ice thickness for wires with fixed orientations from north ranging from 0^o to 150^o in 30^o increments are also computed in the Simple model:

$$R_{eq} = \sum_{j=1}^{N} \frac{1}{\rho_i \pi} \left\{ (P_j \rho_o)^2 + (3.6 V_j W_j \sin[\theta - \phi])^2 \right\}^{1/2}, \qquad (3)$$

where θ is the wire direction and ϕ is the wind direction. Unless otherwise stated, the model results presented in this report are for a wire that is always perpendicular to the wind direction.

3.3.5 Storm end. An important aspect of pre-processing the weather data before running ice accretion models is deciding when a freezing rain storm ends. That choice affects both the maximum wind-on-ice load and the maximum ice thickness for the storm. The maximum wind-on-ice load may occur following the ice storm, if a cold front accompanied by higher winds moves into the storm area as freezing rain ends. We end storms at the first hour after freezing rain ends when the air temperature goes above 1^{o}C. This choice sometimes results in ice accreting on top of previously accreted ice that is many days or even weeks old. Ideally, one would model the melting and sublimation of accreted ice; however, that is more difficult than modeling the accretion of ice. Melting by direct or reflected solar radiation or Joule heating and ice shedding before complete melting may be significant.

3.4 Results

Using the methodology outlined in Sections 3.2 and 3.3, we extracted freezing rain storms from the weather data at the 26 useful stations in the study region, prorated accumulated daily precipitation amounts to each hour, and made any necessary corrections to the data. These data were then used in the CRREL and Simple ice accretion models to estimate for each storm the amount of ice, in terms of the equivalent uniform radial ice thickness, that accreted on a 1-in. (25.4-mm)diameter wire, perpendicular to the wind direction, at 10 m above ground. The wind-on-ice load was calculated throughout each storm assuming a drag coefficient C_D = 1. Time series of the weather conditions and the modeled ice loads and wind-on-ice loads for two events at St. John's are shown in Figure 6.

The storm in 1958 in Figure 6a was called the worst sleet storm in St. John's since the late 1920s. Thousands of people were without power for up to two weeks with hundreds of poles and miles of wire on the ground. The top panel shows the daily accumulated precipitation prorated to each hour, along with the number of hours in each day with snow (S), rain (R), or freezing rain (ZR). The second panel shows that temperatures were only a few degrees below freezing, while the wind speeds in the third panel varied between 5 and 15 m/s. The bottom two panels present the model results. Freezing rain was the dominant precipitation type in the first three days and during that time the models accreted more than 30 mm of ice, with slightly more ice accreting in the Simple model than the CRREL model in the relatively warm conditions in the middle of day 59 (February 28). The modeled ice loads increased again at the end of day 63 (March 4), with the Simple model accreting substantially more ice than the CRREL model with both air and dew point temperatures at freezing. The CRREL and Simple model wind-on-ice loads in the bottom panel are essentially equal until March 4 when the CRREL model forms icicles, which provide an increased projected area. Vertical loads are higher in the Simple model while horizontal loads are higher in the CRREL model. Local variations in the ice load in the St. John's area in this storm could also be generated by locally varying precipitation amounts, precipitation types, and wind speeds. Ice was reported to be thicker on wires and poles in the more exposed Higher Levels.

An event two years earlier in 1956, beginning on April 12 and ending April 15 (Figure 6b), was not confirmed. No reports were found in the *Telegram*, and *The Daily News* reported only on a snow storm sweeping across the island and delaying trains and airplanes. As in the 1958 storm, precipitation varied between freezing rain, snow, and rain with temperatures and wind speeds in the same range. The model results in the fourth panel show ice accreting primarily at the end of the event, even as freezing rain turned to rain. The modeled ice accretion amounts of 20 to 25 mm may have melted rapidly in those conditions. Temperatures elsewhere on the Avalon Peninsula were no colder than at St. John's.

4.0 Storms

To balance the inherent uncertainties in modeled ice thicknesses and to provide a qualitative description of historical freezing rain storms to better understand the climatology of these storms in the region, we also compile information from newspaper accounts of damaging freezing rain storms. For this study we had three Newfoundland and Labrador Hydro publications (Shawmont Newfoundland Ltd 1970, Richmond and Fegley 1973, NLH 1984b) as well. These sources are not expected to supply quantitative information on equivalent radial ice thicknesses, but they do provide crucial information on the severity and extent of storms. We also compiled information on reported glaze ice thicknesses on Passive Ice Meters from the NLH Climatological Monitoring Program for the nine years for which the annual reports were available.

4.1 Qualitative damage information

We chose storms based on the modeled ice thicknesses, and obtained qualitative information about them. At each station we used four criteria for choosing these storms: 1) the accretion of *X* mm or more of ice only from freezing rain by the CRREL model, at one or more stations, or 2) the accretion of at least *X* mm of ice only from freezing rain by the Simple model at one or more stations, or 3) the accretion of at least *X* mm of ice from freezing rain or ice pellets by the CRREL model at one or more stations, 4) the accretion of at least *X* mm of ice from freezing rain or ice pellets by the Simple model at one or more stations. The value of *X* was 12 mm, except at St. John's, Gander, Bonavista, and Port aux Basques, where it was 18 mm because of the relatively frequent high modeled ice loads at those stations. The second criterion is used to investigate the difference between the CRREL and Simple models. The third and fourth criteria are used to investigate the justification for allowing ice pellets to accrete as well as freezing rain, and to pick up storms in which there may be a band of freezing rain that is not observed at the weather stations. These are all test storms that *may* be damaging ice storms.

These criteria resulted in 117 ice storms to research in which the ice thickness at one or more stations exceeded the threshold thickness for that station. Newfoundland and Labrador Hydro staff searched for newspaper articles on these storms in the St. John's *Telegram* as well as weekly newspapers across the province. For some storms no articles on ice storms or any other weather events were found. To supplement this information we requested newspaper articles for some storms from the Corner Brook daily *Western Star* from the microfilm archives at the National Library of Canada in Ottawa. Desiree Hopkins at the Clarenville library searched paper copies of the Clarenville *Packet* for additional information on some storms with significant modeled ice loads at Bonavista. Finally we obtained any additional newspaper stories from local daily and weekly newspapers that were available online. Because of time constraints we did not request newspaper coverage from cities in Quebec (e.g. Sept Iles) that might include articles on ice storms in the Natashquan, Lake Eon and Havre St. Pierre areas.

4.2 Passive ice meter data

We compiled information on reported glaze ice thicknesses on Passive Ice Meters (PIMS) from the NLH Climatological Monitoring Program from 1978/79 through 1986/87 (NLH 1979, 1980, 1981, 1982, 1983, 1984, 1985, 1986, 1987). The annual report was not available for the first year of the program in the winter of 1985/1986. Butt (1986) provides a description of the PIM program using the design for the platform from Quebec provided Jean LaFlamme. The annual summaries report the maximum ice thickness in each month at each station for which values were reported in that month. Neither Butt (1986) or the summaries say how the observers at each PIM measured the ice thickness and whether the measured values are checked or processed. Thus, the reports should be considered to be maximum thicknesses, rather than equivalent radial thicknesses. It is not clear if the larger reported values are the maximum dimension of the cross section of the ice-covered rod and include the rod diameter. Values smaller than the rod diameter are obviously of the ice alone and are likely maximum radial ice thicknesses. It is also possible that the reported values are the maximum dimension minus the rod diameter and represent twice the maximum thickness.

A total of 31 stations (Figure 7) were used, some for only a few years. For this freezing rain study we compiled all the reported glaze ice thicknesses in a table. Glaze ice can also form from in cloud icing, however, so these ice accretions do not necessarily result from freezing rain. The ice thicknesses are plotted in the seven panels of Figure 8 that group the stations by region. Keeping the possible measurement variations in mind, it is interesting to note the largest reported glaze ice thicknesses are at Hamden with 8 cm reported in 1978/79, followed by 6 cm at Point Arthur, Plum Point, and Yankee Point in 1982/83, and 5 cm at Goose Bay in 1981/82. The largest values for the Avalon Peninsula do not exceed 3 cm.

4.3 Damaging ice storms

For the 117 modeled severe storms in the study region we mapped the modeled ice thicknesses and determined the footprint of the storm using information from newspaper articles from cities in the region. We confirmed significant ice loads on trees, power lines, or communication towers in only 34 storms. Summaries of the damage associated with those storms are presented in Table 3. This table includes the start and end dates of each storm and descriptions of the storm characteristics and damage from the qualitative information. This description sometimes includes ice thicknesses, which generally should not be interpreted as equivalent radial thicknesses.

The information from Richmond and Fegley (1973) attributed to Young and Shell (1971) on eight damaging ice storms is reported in a separate column. Our approach in extracting freezing rain storms, modeling the accretion of ice, and identifying severe storms picked seven of the eight Young and Shell storms. The exception was a storm that occurred January 22-24, 1964 that they describe as resulting in 5-inch diameter glaze ice accretions on conductors in the Conception Bay area. It is shown in italics in Table 3. On the 22nd at St. John's, 2 mm of ice accreted during nine hours of freezing rain, which was followed by two days with temperatures a few degrees above freezing and rain and fog. The only other nearby station is Argentia. Temperatures there never dropped below freezing and were slightly warmer than at St. John's. It was foggy with a little rain. This ice storm apparently occurred between the weather stations.

Two other storms were not chosen by our storm criteria and are shown in italics in the table. Newspaper reports acquired for the CEA study on the U.S.-Canadian border region for a January 12-20, 1982 storm mentioned winds gusting to 80 mph snapping ice-laden power lines in Newfoundland, and Labrador City being declared a disaster area. Our initial assumption that the disaster declaration in Labrador City was associated with an ice storm is probably incorrect. The Wabush Lake data shows snow, extreme cold, and moderate winds. At St. John's 15 mm of ice accreted on January 19-20 with wind speeds as high as 10 m/s. A few mm ice accretion at Bonavista, Burgeo, and Gander was accompanied by hourly winds as high as 19 m/s while St. Lawrence and Stephenville had snow. While this storm did not reach the high 18 mm criterion for St. John's that was used to limit the number the number of storms we investigated, 15 mm of ice would be expected to damage power lines. We do not have information from newspapers to delineate the storm footprint.

Another damaging storm occurred in December 1994 in the region between Gander and St. John's. Hurricane-force winds and 24 cm of snow in less than 24 hours left 50,000 utility customers without power. The modeled ice load at St. John's for that storm was just 7 mm with hourly winds up to 18 m/s in 10 hours of freezing rain preceded by two days of snow. In Gander the storm was primarily freezing rain with 5 mm of ice accreting and hourly winds as high as 16 m/s. The relatively small ice accretions from freezing rain may indicate that sticky snow accreting on the wires and conductors, or on trees that that broke onto the power lines, contributed to the outages.

These storm footprints have been compiled in a GIS database. Maps of each ice storm footprint along with the modeled ice thicknesses are provided in Appendix B with a map of all the storm footprints and the proposed transmission line route in Figure 9. The storm footprints were compiled to determine regions with similar severe icing climatologies for forming superstations for the extreme value analysis (see section 5.1).

The relatively few confirmed damaging ice storms (34 out of 117) is puzzling. For comparison, in the study of the U.S.-Canadian border region, 70 of the 108 modeled storms were confirmed. Because we are intentionally conservative in some of our model runs, allowing reported ice pellets to accrete as if they were freezing rain, having a third of the modeled ice storms not be damaging ice storms is not surprising. However in this study we confirmed only 29%. There are a few possible reasons: 1) Most of the newspapers in the province are weekly newspapers that may report only ice storms that occur at the right time in the news cycle, 2) there may be a significant delay in the weekly newspaper reports so we might need to search for ice storm coverage weeks after the storm, 3) the daily newspapers in St. John's and Corner Brook may focus their reporting locally, 4) the transmission and distribution line systems may be stout enough to withstand significant ice loads because of system upgrades following the 1970 and 1984 ice storms, and 5) excessive conservatism in the models.

The first three items deal with damaging storms that occurred but for which we just did not find coverage, either because it was not there or because we failed to look in the right newspaper at the right time. We do not know how frequently that occurred. Historical outage records for Newfoundland and Labrador Hydro, United Towns, Newfoundland Power, and the other utilities in the province might provide supplementary information.

To attempt to deal with the robust electrical grid hypothesis in (4) we also have included reports of thick ice accretions on wires, even if there was no outage, in delineating the storm footprint. However, the lack of tree damage with thick ice but no outages is hard to explain. In our experience branches break with equivalent radial ice thicknesses as small as 5 to 10 mm. Perhaps the trees in Newfoundland are those that are strong enough and have the branching structure (Greene, Jones, and Proulx 2007) to thrive in the windy conditions there and thus can also withstand significant ice loads.

To address the excessive conservatism possibility in (5) we examined the hourly weather data for some of the unconfirmed storms, and found that the models were sometimes accreting significant amounts of ice in hours in which the temperature was slightly below freezing with rain reported rather than freezing rain. We have assumed that a report of rain at subfreezing temperatures is just a coding error; that the reported rain is actually freezing rain. Perhaps that is not the case here. Therefore we reran the models not allowing rain at subfreezing temperatures to freeze to the wires. The resulting ice loads were significantly different for some storms at some stations. Revised ice loads are plotted versus the largest *N* original loads for Bonavista and Gander in Figure 10. *N* is the number of years in the period of record; 47 for Bonavista and 56 for Gander. Four of five cases at Bonavista with revised ice loads less than half of the original ice loads had no reported damage in the Bonavista Peninsula. The fifth case was not a storm we investigated. All these storms occurred in the 5-year period between 2001 and 2006, perhaps indicating an instrument problem.

In earlier studies we used discrepancies between modeled ice thicknesses and qualitative information to revise our data-model interface (Jones 1998) and determine whether to use the CRREL or Simple model and freezing rain only or freezing rain and ice pellets in mapping extreme ice thicknesses. We have concluded that using the Simple model and accreting only freezing rain gives the most consistent results. Therefore, in spite of the low confirmation rate in this study, we continue to rely on the results from the Simple model accreting only freezing rain in estimating extremes.

5.0 Extreme ice thicknesses and concurrent wind-on-ice speeds

We used the modeled ice thicknesses at the weather stations to determine ice thicknesses with a 50-yr return period. We have found both the peaks-over-threshold method (Simiu and Heckert 1995, Hosking and Wallis 1987, Walshaw 1994, Wang 1991, Gross et al. 1994, and Abild et al. 1992) and the concept of superstations (Peterka 1992) to be useful in the extreme value analysis.

5.1 Superstations

The superstation concept is presented in Peterka (1992) for extreme wind speeds. The 50-yr wind map in the 1993 revision of ASCE Standard 7 shows small regions in the Midwest with high winds. Peterka argued that these small-scale variations in the extreme wind speed were not real but were due to sampling error from determining the parameters of the extreme value distribution from relatively short data records. He suggested that the records of extreme winds, from different weather stations with the same wind climate, could be appended to each other to form a superstation with a much longer period of record. This long period of record supplies many more extremes to use in the extreme value analysis and thus produces better estimates of the parameters of the extreme value distribution. The limitation on forming the superstation is the requirement that the maximum annual winds from the different stations in the superstation should be uncorrelated. If extreme winds at two stations are correlated, then including the second station supplies no new information on the extreme wind climate.

If there were 500 years of weather data at each of the stations in the study region, reasonably accurate estimates for ice thicknesses for a 50-yr return period could be made without grouping the stations into superstations. However, sampling errors in the estimation of extreme loads can be significant for the current electronic data records of weather stations in this region which range from 12.5 up to 55.5 years in duration and average 33 years. At any weather station the probability that an ice thickness with a 50-yr return period has occurred increases as the period of record increases. However, large ice thicknesses with a long return period may have occurred at a station with a short period of record, and conversely, only short recurrence interval ice thicknesses may have occurred at a station with a longer period of record.

To obtain the longest possible period of record, as many stations as possible are included in each superstation, consistent with the available information on the climatology of ice storms in the region. Superstations are shown in Figure 11. The groupings are based on the compilation of information from the 34 storms that were confirmed (Figure 9), the terrain of the region and station elevation (Figure 3 and Table 1),). The superstation groupings are not based on the extreme ice thicknesses at individual stations.

5.2 Peaks-over-threshold method

Researchers often use the epochal method to determine the parameters of an extreme value distribution. They pick the maximum value for each year in the period of record, and then use these annual maxima to determine the parameters of a type I (Gumbel), II (Frechet) or III (reverse Weibull) extreme value distribution. Note that a Gumbel distribution is based on 1) assuming that the probability of exceeding a value approaches the exponential form as the magnitude of the value gets large, and 2) assuming that the average number of events per year is large (Nash 1966). If these two assumptions are not satisfied, a Gumbel distribution cannot be assumed a priori for the series of annual extremes. This is discussed further in Jones and White (2002).

We think that the peaks-over-threshold (POT) approach is better for dealing with ice thicknesses for the following reasons:

- At a given location freezing rain storms may occur infrequently and some winters will have no measurable freezing rain. In those years the maximum ice thickness is zero, which would have to be considered part of the extreme population in the epochal method. At locations where freezing rain is relatively rare, the epoch must be longer than one year to obtain a sample of true extremes.

- In other years there may more than one severe ice storm, each of which may generate larger ice thicknesses than the most severe storms in milder years. The epochal method would not include these severe but not-worst-that-year storms in the estimation of the parameters of the extreme value distribution.

These problems are avoided using the POT method because loads are chosen as members of the extreme population if they exceed a specified threshold, which may be defined by specifying an average occurrence rate. The excess of the value over this threshold is used to determine the two additional parameters of the generalized Pareto distribution (GPD):

$$\begin{aligned} F(x) = P(X \le x | x \ge u) &= 1 - \left[1 - \frac{k(x-u)}{\alpha}\right]^{1/k} \qquad k \ne 0 \\ &= 1 - \exp\left[\frac{-(x-u)}{\alpha}\right] \qquad k = 0 \end{aligned} \tag{4}$$

The threshold is u, the shape parameter is k and α is the scale parameter. The cases $k = 0$, $k < 0$, and $k > 0$ correspond to the extreme value distribution types I (shortest infinite tail), II (longer infinite tail), and III (finite tail length, $x < \alpha/k$). Typically k ranges between -0.5 and 0.5. If the data are correctly described by a GPD, then k is not dependent on the value chosen as the threshold, as long as the threshold is high enough.

We used probability weighted moments (Abild et al. 1992, Wang 1991, Hosking and Wallis 1987) to determine the distribution parameters k and α. This method relies less on the high extremes in the sample in determining the best fit than, for example, the method of moments. Estimates of the GPD parameters are provided by:

$$k = \frac{4b_1 - 3b_0 + u}{b_0 - 2b_1}$$
$$\alpha = (b_0 - u)(1 + k)$$

where (5)

$$b_0 = \frac{1}{l} \sum_{i=1}^{l} x_{(i)}$$
$$b_1 = \frac{1}{l} \sum_{i=1}^{l} \frac{i-1}{l-1} x_{(i)}$$

(Wang 1991), where the $x_{(i)}$ are the ordered sample, $x_{(1)} \leq x_{(2)} \leq ... \leq x_{(l)}$ of loads greater than the threshold *u*.

A variety of methods can be used to define the threshold *u*. It should be high enough that only true extremes are used to estimate the parameters of the GPD, but low enough that there are sufficient data so sampling error is not a problem. Some authors specified the threshold as a percentile of the number of cases. For example, Walshaw (1994) used a threshold at about the 95th percentile of his 10 years of hourly maximum wind gusts. Sometimes the threshold is determined on a physical basis (Abild et al. 1992). For Newfoundland and Labrador, we used an occurrence rate of 1 storm/year. In the interior of Labrador that resulted in a threshold ice thickness of only 2 mm, compared to almost 10 mm in eastern Newfoundland.

Once the parameters of the distribution have been determined, the load x_T corresponding to a specified return period *T* is calculated from

$$x_T = u + \frac{\alpha}{k}\left[1 - (\lambda T)^{-k}\right] \quad (6)$$

where λ is the occurrence rate (number per year) of values exceeding the threshold.

5.3 Correlation

The correlation of the sample of extreme ice thicknesses for each pair of stations in each superstation should be checked by calculating the Spearman rank-order correlation coefficient R_s (Press et al. 1987). The strength of the correlation is given by the square of the correlation coefficient. A high negative correlation for a pair of stations indicates that ice loads at one station typically occur with no ice at the other station in the pair. Because of time constraints and the typically minor effect of excluding pairs of somewhat correlated stations from superstations (e.g. Jones and Morris 2002, Table 7; Jones 2003 Table 6), this was not done for this project.

5.4 Wind-on-ice speeds

The amount of ice that accretes on a wire is affected by the speed of the wind that accompanies the freezing rain. Wind speeds during freezing rain are typically moderate, ranging between 3 and 8 m/s. In Newfoundland and Labrador winds with freezing rain tend to be higher, with the average hourly wind at St. John's at about 8 m/s. The ice that accretes on a wire may last for days or even weeks after the freezing rain ends, as long as the weather remains cold. Thus, the ice-laden wires may be exposed to higher winds that occur after the storm. We determine the wind speeds to use in combination with extreme ice thicknesses from the modeled wind-on-ice loads at the weather stations.

The summary information for each freezing rain storm includes the maximum wind-on-ice load at the maximum uniform ice thickness (a conditional maximum) as well as the maximum wind-on-ice load that occurred at any time during the storm (the absolute maximum). We use the peaks-over-threshold method to calculate the parameters of the distribution of extreme wind-on-ice loads for the superstations. By assuming that the maximum wind-on-ice load in each storm occurs with the maximum ice thickness, which is somewhat conservative, the concurrent wind-on-ice speed V_c can be calculated from the N-yr wind-on-ice load F_N and the N-year ice thickness R_{eqN}:

$$V_c = \sqrt{\frac{2W_N}{\rho_a C_D (D + 2R_{eqN})}}, \qquad (7)$$

where ρ_a is the density of air, D is the diameter of the bare wire, and C_D is the drag coefficient. V_c is the wind speed that when used in combination with the ice thickness for an N-year return period gives the wind-on-ice load for an N-year return period. Wind loads are calculated using a drag coefficient $C_D = 1$ in both models, however the computation of the load is done differently in the two models. The Simple model wind load is based on the compact wire plus ice diameter, equal to $D + 2R_{eq}$. The CRREL model wind load is based on the average cross-sectional dimension of the ice-covered wire, taking into account the spacing (45 icicles/meter), length L_i and diameter D_i of the icicles. The cross-sectional area of icicles is $45D_iL_i$ in each meter so the cross-sectional width used in the wind load calculation is $D + 2t + 0.45D_iL_i$, where t is the uniform thickness of the ice that freezes immediately to the wire. This is larger than $D + 2R_{eq}$ when there are icicles. Thus, for the CRREL model, V_c accounts crudely for the increase in wind drag on the iced wire because of icicles, while retaining an ice thickness expressed in terms of the equivalent uniform radial ice thickness.

V_c is an hourly wind speed, rather than a 3-s gust speed or a fastest-mile wind speed. It is obtained from the 1- or 2-minute average wind speeds that are reported each hour at the weather stations. Gust speeds are recorded at military weather stations in the United States whenever there is a rapid change in wind speed with at least a 10-knot difference between the high and low speeds. In a previous study, these gust wind speeds at a number of Army and Air Force weather stations were used to calculate G_c, the concurrent gust-on-ice speed. The ratio between G_c and V_c was then calculated:

$$f_{gust} = G_c / V_c = 1.34. \qquad (8)$$

We use f_{gust} to estimate G_c from V_c for each station and superstation.

6.0 Results

6.1 Extreme value analysis

The results of the extreme value analysis using ice thicknesses from the Simple model at 10 m above ground for a 50-yr return periods are presented in Table 4 for the superstations and individual stations. For each superstation the sample of extremes and the fitted generalized Pareto distribution are plotted in Figure 12. In each plot the tail shape parameter is reported. All values are less than zero indicating a relatively fat tail for the distribution, and thus a faster increase in equivalent radial ice thickness with return period than allowed by the Gumbel distribution.

Equivalent radial ice thicknesses for a 50-yr return period reported by Richmond and Fegley (1973) for seven stations are shown in red in Table 4. The period of record for the stations in that report ranged from 6 years at Deer Lake and Daniel's Harbour to 19 years at St. John's and Goose Bay. They used the MRI icing model to determine the ice accumulation from the worst storm each year, but do not specify how that worst storm was picked, or the values for the user-specified parameters in the MRI model. The mean and standard deviation of the annual maxima were then used to determine the parameters of the Gumbel distribution from which the 50-yr ice thicknesses were calculated. In the preceding column in Table 4 are the 400-yr ice thicknesses from the Simple model. Note that the Richmond and Fegley 50-yr values exceed these 400-yr values by factors ranging from 1.2 (St. John's) to 3.0 (Battle Harbour), with an average of 2.2.

Concurrent gust speeds are calculated for each return period using (7) and (8). Typically these speeds vary slightly with return period, increasing at some stations, decreasing at others, or remaining essentially constant. The speeds in Table 4 are from the averages of the concurrent wind speeds calculated from the ice thicknesses and wind-on-ice loads for 50-, 100- and 200- and 400-year return periods.

6.2 Mapped ice thicknesses and concurrent wind speeds

Ice thicknesses (mm) from freezing rain for a 50-yr return period at 10 m above ground with concurrent gust speeds (km/hr) are mapped in Figure 13. The Avalon, Bonavista and Burin Peninsulas have 50-yr point ice thicknesses of 35 mm. In western Newfoundland and coastal Labrador and nearby Quebec R_{eq} decreases to 20 mm, and to 10 mm in interior Labrador. Because there was no apparent trend in concurrent wind speeds the average concurrent gust speed of 95 to 125 km/hr is used everywhere. The lower end is from the Simple model with its compact ice accretion while the upper end is based on the larger projected area associated with icicle formation in the CRREL model.

6.3 Spatial effect

The map in Figure 13 is for ice loads at a point, such as a communication tower or a particular span of a transmission line. However, transmission lines are linear structures and thus are exposed to ice storms that occur anywhere along the length of the line. Similarly a transmission line system is exposed to severe storms that occur anywhere in the service area. Ice thicknesses of 35 mm will accrete on the conductors of transmission lines somewhere in the Avalon Peninsula more frequently than on a particular span near, say, Mount Pearl. This phenomenon is called the spatial effect (Golikova et al. 1983, Jones 2003) and applies to thunderstorms, tornados, and hurricanes as well as to ice storms.

Because the conductors of the proposed transmission line are at about 45 m above ground, we also ran the model for that level, using the 1/7 power law to adjust the measured wind speeds from the assumed 10-m high anemometer to 45 m. We compared these point ice loads at 45 m to spatial ice loads at the same height above ground, determining the spatial values by compiling the modeled equivalent radial ice thicknesses from all the stations in a region, sorting chronologically, and then picking the largest value for each event. For an N year overall period of record, from the first start date to the last end date, the N largest values were used in the spatial extreme value analysis. This was done for the four stations on the Avalon, Bonavista and Burin Peninsulas, the 11 stations in western Newfoundland, the six stations along the Labrador and Quebec coasts, and the five stations in interior Labrador. Those same stations were also grouped into superstations to calculate point ice loads for the same regions. These point and spatial values are compared in Table 5 for 50- and 200-year return periods. The 50-yr spatial values are between 22 and 36% higher than the point values. This variation is probably due in part to the number of stations and the size of each region (how well we are sampling the region) and the period of record at each station compared to the maximum period of record for the region (how many stations are reporting in each event). This spatial factor is within the range of 1 to 1.7 calculated in Jones (2005).

7.0 Site-specific effects

7.1 Wind

Wind-blown rain may contribute significantly to the ice load on a structure. The wind flux term in (1) is comparable to the falling rain term at a wind speed of about 5 m/s. Structures at sites that are typically windier than the airport weather stations may accrete more ice than structures at the airport. Furthermore, since wind speed typically increases with height above ground, more ice is expected to accrete on ground wires than on the conductors of the same line and on the highest conductor in a vertical configuration than on the lower conductors. These effects are taken into account in ASCE Standard 7 with a height factor and a topographic factor applied to the ice thickness. The height factor is

$$f_z = \left(\frac{z}{33}\right)^{0.10} \quad , \tag{10}$$

where z is the height above ground in feet. The topographic factor is $K_{zt}^{\ 0.35}$, where K_{zt} is determined from Section 6 of ASCE Standard 7 (ASCE 2005) for isolated hills, ridges and escarpments. In complex terrain, anemometers installed along the transmission line route may be required to determine the wind regime during the icing season. If the wind direction is parallel to the spans, the accreted ice thickness will be less than the model estimates and no increase in ice thickness with height above ground is expected.

7.2 Temperature

The air temperature may vary at any location during a freezing rain storm and across the region affected by the storm. For near-freezing temperatures, even small variations in temperature can have a significant effect on the fraction of the impinging precipitation that freezes to a structure and on the rate of freezing, which controls the shape of the accretion. At relatively warm temperatures, icicles may account for a significant portion of the accreted ice. At colder temperatures, on the other hand, the impinging precipitation may freeze where it hits, accumulating in an eccentric accretion that would tend to rotate torsionally flexible ground wires and single conductors, with the ice eventually forming a cylindrical sleeve around the wire. At intermediate temperatures the impinging water will flow before freezing, resulting in thicker ice on the sides or bottom of the wire than on the top. Examples of the variety of ice accretion shapes are shown in Figure 5. Following an ice storm the temperature may remain below freezing longer at higher elevations than at the airport weather stations. Where it remains cold, structures may see higher wind-on-ice loads than the hypothetical structure at the airport.

Joule heating from the current in conductors may have a significant effect on the amount of ice that accretes. For the impinging precipitation to freeze to a conductor, the heat of fusion (40 cal/gram) must be removed, which typically occurs by convective and evaporative cooling. If sufficient heat is generated in the conductor, it will remain ice free. More realistically, the amount of heat generated in the conductor may be enough to decrease the initial rate of freezing and make more water available for icicle formation. This larger volume of dripping water affects the aspect ratio of the icicles, with long thin icicles caused by low freezing rates and short fat icicles by high freezing rates. The shape of the accretion affects both the further accretion of ice and also the rate of ice shedding when the storm ends and the weather warms. Ice accretions on ground wires may tend to be more compact than those on conductors because of the absence of Joule heating in ground wires.

7.3 Wind direction

The modeled ice thicknesses in this report are for transmission line spans that are perpendicular to the direction of the wind that accompanies the freezing rain. Spans that are parallel to the wind direction will have significantly lower ice loads on the conductors and shield wires because of the smaller flux of water perpendicular to the orientation of their axis. In regions like Newfoundland that tend to be windy, the difference in ice loads for spans with different orientations can be pronounced. Wind direction histograms for St. John’s, Bonavista, Argentia, and St. Lawrence are shown in Figure 14. Notice that the winds are generally from the east with significant northerly components except at Argentia.

7.4 Hawke Hill

We evaluated the effect of wind and temperature variations by comparing St. John’s conditions with those at Hawke Hill. Asim Haldar provided wind and temperature data from seven freezing rain events at Hawke Hill in 2008 and wind data from three events in 1995-1996. The raw wind speeds for March-April 2008 and the calculated hourly averages for all events are plotted in Figure 15 along with the St. John’s hourly wind speeds. The Hawke Hill anemometers are at 10 m and 50 ft (15 m). Assuming a 1/7 power law for wind speed variation with height above ground results in 15 m winds 6% higher than 10 m winds on average. Average hourly temperatures at Hawke Hill and the St. John’s hourly values are shown in Figure 16 for March-April 2008. The raw Hawke Hill wind directions are plotted with the hourly St. John’s values for March-April 2008 in Figure 17. The wind direction at Hawke Hill appears to be consistent with that at the airport.

A direct comparison of the Hawke Hill and St. John’s winds for the events in Figure 15 is in Figure 18. Note the scatter in the relationship, some of which might be from the Hawke Hill data being from different anemometers at different locations and heights above ground. However, the scatter might also represent an intrinsically low correlation between wind speeds at St. John’s and Hawke Hill. The best fit line through the origin in this wind speed relationship is

$$V_{HH} = 1.44 V_{SJ}, \qquad (11)$$

where V_{HH} is the average hourly wind speed at Hawke Hill and V_{SJ} is the hourly wind speed at St. John’s. This fit looks better by eye than the fit that is not constrained to go through the origin.

A direct comparison of the Hawke Hill and St. John’s temperatures for the events in Figure 16 is also shown in Figure 18. The best fit temperature relationship is

$$T_{HH} = -1.8 + T_{SJ} \ , \tag{12}$$

where T_{HH}(°C) is the average hourly temperature at Hawke Hill and T_{SJ}(°C) is the hourly temperature at St. John's. The Hawke Hill and St. John's temperatures are highly correlated with R^2=0.96.

In an attempt to model the accretion of ice at Hawke Hill, to represent locations on the Avalon Peninsula where freezing rain storms are more severe than at St. John's, we used the relationships in (11) and (12) to extract ice storms from the St. John's data and model the accretion of ice in freezing rain. The continuation of ice storms was assessed using the T_{HH} temperature and ice accreted with V_{HH} wind speeds. We ran two cases. In the first, precipitation coded as rain at St. John's in hours with T_{HH} <0 is assumed to be snow or ice pellets at Hawke Hill so does not accrete on the wires and conductors. In the second that precipitation is treated as freezing rain at Hawke Hill and processed like other hours with freezing rain. The results of these analyses along with the original results at St. John's are shown in Figure 19. The vertical axis is limited to 80 mm in all three plots, so that the differences between (a) and (b) are clear. Case (c), which treats cold rain as freezing rain, results in 34 storms with R_{eq} > 50 mm, with R_{eq} > 100 mm in eight of those storms, and R_{eq} > 200 mm in one storm. Ice loads this high and this frequent seem unlikely, so we will tentatively rely on the results in Figure 19b to represent icing at locations like Hawke Hill that are generally colder and windier than St. John's in freezing rain.

For a sanity check on our Figure 17b results, we used photos from Hawke Hill for ice storms between 2004 and 2006 provided by Kyle Tucker. We did not attempt to estimate equivalent radial ice thicknesses from the photographs. We obtained the maximum Simple model R_{eq} for the date of each photo, both for the St. John's data and the pseudo Hawke Hill data. The photos and the modeled equivalent radial ice thicknesses are provided in Appendix C. For most but not all dates (e.g. 3/14/2005) the pseudo-Hawke Hill values are significantly greater than the St. John's values. In some cases the actual ice accretion appears to have a much larger R_{eq} than either calculated result (e.g. 3/21/2006). In other cases both modeled ice thicknesses appear to be greater than the photographs indicate (e.g. 3/12/2004).

What would be the result of using the pseudo Hawke Hill data in an extreme value analysis? The 50-yr equivalent radial ice thickness from the Simple model at 10 m is 58 mm compared to 38 mm for St John's and 81 mm obtained by Richmond and Fegley (1973) for St. John's. The 50-yr value for an Argentia-Hawke Hill superstation is 53 mm compared to 34 mm for the Argentia-St. John's superstation.

8.0 Conclusions

We modeled the accretion of ice from freezing rain on wires and conductors in the Newfoundland and Labrador region using the available period of record for hourly weather data and daily precipitation data and the CRREL and Simple ice accretion models. To check the model results we used reports on previous storms provided by Newfoundland and Labrador Hydro as well as daily and weekly newspapers in the province. We suspect that the relatively low confirmation rate from this qualitative information of the freezing rain storms that generate significant modeled ice loads is due to the concentration of the population in towns near the coast and the limited coverage of daily newspapers in St. John's and Corner Brook of the rest of the island. We found essentially no storm coverage for Labrador. We compiled the PIM data for reported glaze ice thicknesses in each month at each station. Because the measurements are some measure of the maximum ice dimension rather than the equivalent radial ice thickness and because the dates of the measurements are not provided we ultimately did not rely on the data to check model results.

We continued to rely on the Simple model results, accreting only precipitation in hours with freezing rain. Ice loads from freezing rain in Newfoundland and Labrador appear to decrease from east to west across Newfoundland and into Labrador. Equivalent radial ice thickness for a 50-yr return period at 10 m above ground range from 35 to 10 mm with concurrent gust speeds in the 95 to 125 km/hr range. At 45 m above ground, the approximate conductor height for the planned transmission line, equivalent radial ice thicknesses calculated for regions are about 30% higher than the point values in that region. Using a loose relationship between Hawke Hill and St. John's winds and a close temperature relationship, allowed us to estimate equivalent radial ice thicknesses at locations in the Avalon Peninsula that, like Hawke Hill, are windier and colder than St. John's. The 50-yr ice thickness at pseudo Hawke Hill is 54% higher than the St. John's ice thickness at 10 m. The photographs of ice on the PIM at Hawke Hill suggest that in cloud icing may be a significant factor in the accretion of glaze ice there.

All of these estimates are significantly smaller than the 50-yr ice thicknesses reported by Richmond and Fegley (1973). Only the 86-mm 400-yr equivalent radial ice thickness at 10 or 15 m above ground at pseudo Hawke Hill is higher than Richmond and Fegley's (1973) 50-yr equivalent radial ice thickness of 81 mm from freezing rain for St. John's.

This analysis addresses only ice accretion from freezing rain. In cloud icing is known to cause large ice loads on towers and wires in the Long Range Mountains, and may also contribute to significant icing elsewhere in the province. The planned approach is to use the cloud cover, temperature, and dew point data from coastal stations to estimate liquid water content in subfreezing clouds that are at ground level in the Long Range Mountains (Thorkildson et al, in review). With typical droplet concentrations and estimated or measured wind speeds for each icing event we can calculate a likely range of rime ice loads on conductors perpendicular to the wind direction.

9.0 References

Abild, J., E.Y. Andersen and L. Rosbjerg (1992) The climate of extreme winds at the Great Belt, Denmark, *J. of Wind Engineering and Industrial Aerodynamics*, **41-44**, pp 521-532.

ASCE (1993) *Minimum Design Loads for Buildings and Other Structures*, ASCE Standard 7-93, New York, 134 pages.

ASCE (2005) *Minimum Design Loads for Buildings and Other Structures*, ASCE Standard 7-05, Reston, Virginia, 388 pages.

Best, A.C. (1949) The size distribution of raindrops. *Q. J. Royal Met. Soc*., 75, pp 16-36

Butt, D. (1991) Ice observations in Newfoundland and Labrador, *Proceedings of the Third International Workshop on Atmospheric Icing of Structures,* Vancouver 1986, Canadian Climate Program, pp 287-292.

Golikova, T.N., B.F. Golikov and D.S. Savvaitov (1983) Methods of calculating ice loads on overhead lines as spatial constructions, *Proceedings of the First International Workshop on Atmospheric Icing of Structures*, CRREL Special Report 83-17, pp 341-346.

Greene, D.F., Jones, K.F., and Proulx, O.J. (2007) The effect of icing events on the death and regeneration of North American trees, Chapter 6 in *Plant Disturbance Ecology* (E. Johnson and K. Miyanishi, eds) pp 181-214.

Gross, J., A. Heckert, J. Lechner and E. Simiu (1994) Novel extreme value estimation procedures: Application to extreme wind data, *Extreme Value Theory and Applications*, J. Galambos et al. (eds.), pp 139-158, Kluwer Academic Publishers, Netherlands.

Hosking, J.R.M. and J.R Wallis (1987) Parameter and quantile estimation for the generalized Pareto distribution, *Technometrics*, **29**, no. 3, pp 339-349.

Jones, K.F. (1996a) Ice accretion in freezing rain, CRREL Report 96-2, Cold Regions Research and Engineering Laboratory, Hanover, New Hampshire. http://www.crrel.usace.army.mil/techpub/CRREL_Reports/reports/CR96_02.pdf

Jones, K.F. (1996b) A simple model for freezing rain ice loads, *Proceedings of the 7th International Workshop on Atmospheric Icing of Structures*, Chicoutimi, Canada, pp 412-416.

Jones, K.F. (1998) Comparison of modeled ice loads in freezing rain storms with damage information, *Proceedings of the 8th International Workshop on Ice Accretion on Structures*, pp 163-168.

Jones, K.F. (2003) *Ice storms in the St. Lawrence Valley region*, ERDC report TR-03-1.

Jones, K.F. and R. Morris (2002) Canadian Electricity Association *Investigation of the Differences in the Application of the Canadian and U.S. Methodology for Estimates of Ice Loads for a 50-yr Return Period.*

Jones, K.F. and H.B. White (2002) The estimation and application of extremes, *Proceedings of the ASCE Conference on Electrical Transmission in a New Age*, pp 32-47, Omaha, Nebraska, September 9-12, 2002.

Jones, K.F. (2003) Spatial factors for extreme ice and extreme wind: Task 1 Literature review on the determination of spatial factors (T033700-3316B), CEA Technologies Inc, October 2003.

Jones, K.F. (2005) Spatial factors for extreme ice and extreme wind: Task 2 Calculation of spatial factors from ice and wind data (T033700-3316B-2), CEA Technologies Inc, January 2005.

Nash, J.E. (1966) Applied Flood Hydrology, in *River Engineering and Water Conservation Works*, edited by R. B. Thorn, Butterworth, Inc, Washington, D.C. pp 63-110.

NLH (1979) Newfoundland and Labrador Hydro Report on 1978/79 Climatological Monitoring Program, prepared by Engineering & Construction Division Transmission Line Design Group, 78 pages.

NLH (1980) Newfoundland and Labrador Hydro Report on 1979/80 Climatological Monitoring Program, prepared by Engineering & Construction Division Transmission Line Design Group, 66 pages.

NLH (1981) Newfoundland and Labrador Hydro Report on 1980/81 Climatological Monitoring Program, prepared by Engineering & Construction Division Transmission Line Design Group, 54 pages.

NLH (1982) Newfoundland and Labrador Hydro Report on 1981/82 Climatological Monitoring Program, prepared by Engineering & Construction Division Transmission Line Design Group, 107 pages.

NLH (1983) Newfoundland and Labrador Hydro Report on 1982/83 Climatological Monitoring Program, prepared by Engineering & Construction Division Transmission Line Design Group, 49 pages.

NLH (1984) Newfoundland and Labrador Hydro Report on 1983/84 Climatological Monitoring Program, prepared by Engineering & Construction Division Transmission Line Design Group, 44 pages.

NLH (1985) Newfoundland and Labrador Hydro Report on 1984/85 Climatological Monitoring Program, prepared by Engineering & Construction Division Transmission Line Design Group, 32 pages.

NLH (1986) Newfoundland and Labrador Hydro Report on 1985/86 Climatological Monitoring Program, prepared by Engineering & Construction Division Transmission Line Design Group, 34 pages.

NLH (1987) Newfoundland and Labrador Hydro Report on 1986/87 Climatological Monitoring Program, prepared by Engineering & Construction Division Transmission Line Design Group, 39 pages.

NLH (1984b) Report on April 9-14/84 sleet storm damage, September 1984, 78 pages.

Peterka, J.A. (1992) Improved extreme wind prediction for the United States, *J. of Wind Engineering and Industrial Aerodynamics*, **41-44**, pp 533-541.

Press, W.H., B.P. Flannery, S.A. Teukolsky and W.T. Vetterling (1987) *Numerical Recipes*, Cambridge University Press, Cambridge.

Richmond, M.C. and Fegley, M.J. (1973) Meteorological study of the Gull Island-Stephenville-Holyrood transmission line routes, prepared for Teshmount Consultants, Ltd by Meteorology Research, Inc., 86 pages.

Shawmont Newfoundland Ltd (1970) Report on ice damage to transmission lines during February 27-28, 1970, for Newfoundland and Labrador Power Commission, April 1970, 124 pages.

Simiu, E. and N.A. Heckert (1995) *Extreme wind distribution tails: A "Peaks over Threshold" Approach*, National Institute of Standards and Technology Building Science Series 174, U.S. Government Printing Office, Washington D.C., 72 pages.

Stewart, R.E. (1992) Precipitation types in the transition region of winter storms, *Bulletin American Meteorological Society*, **73**, no. 3, pp 287-296.

Thorkildson, R., K.F. Jones, and M. Emery (in review) In cloud icing in the Columbia Basin, submitted to *Monthly Weather Review*.

Walshaw, D. (1994) Getting the most from your extreme wind data: A step by step guide, *J. of Research of the National Institute of Standards and Technology*, **99**, pp 399-411.

Wang, Q.J. (1991) The POT model described by the generalized Pareto distribution with Poisson arrival rate, *J. of Hydrology*, **129**, pp 263-280.

Young, H.F. and J.P. Shell (1971) Icing damage to transmission facilities in Newfoundland, Canadian Electrical Association Transmission Meeting, Quebec, October 25-28, 1971.

Newspapers (various dates)

St. John's *Telegram*
St. John'*s Daily News*
Corner Brook *Western Star*
Clarenville *Packet*
Labrador City Aurora
Gander Beacon
Harbour Breton *Foghorn*

Stephenville *Georgian*
Channel Port aux Basques *Gulf News*
Lewisporte *Pilot*

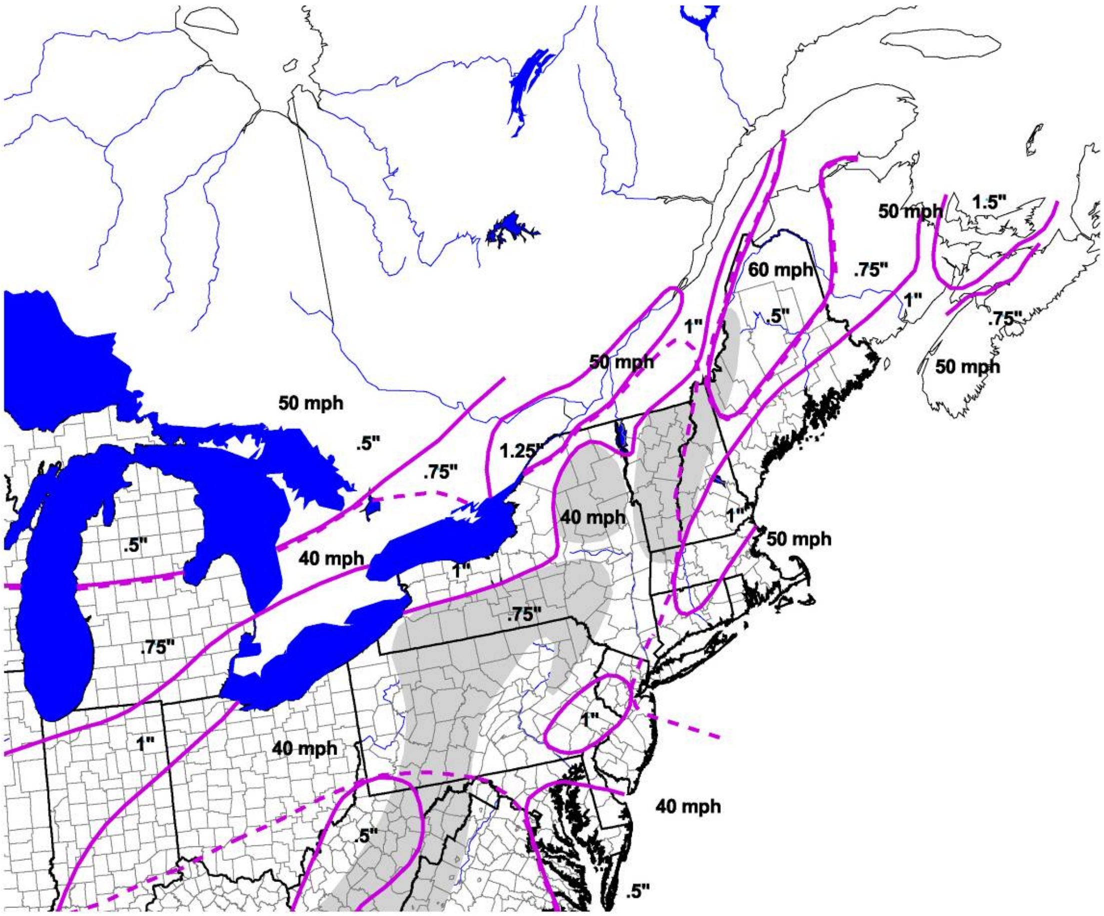

Figure 1. Ice thicknesses and concurrent wind speeds for a fifty year return period in the eastern United States, using stations in Canada

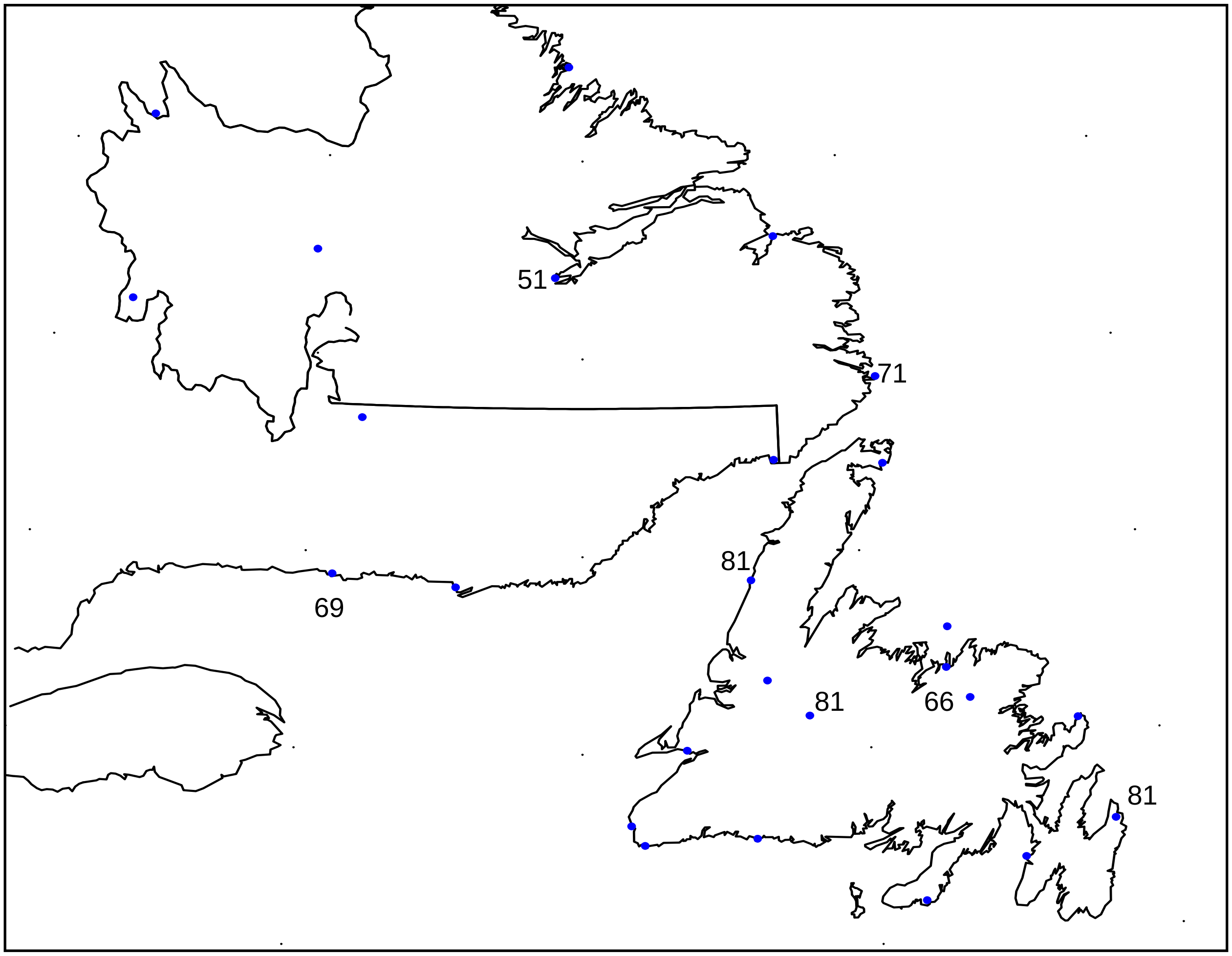

Figure 2. Glaze ice thicknesses (mm) from freezing rain for a 50-yr return period (Richmond and Fegley, 1973)

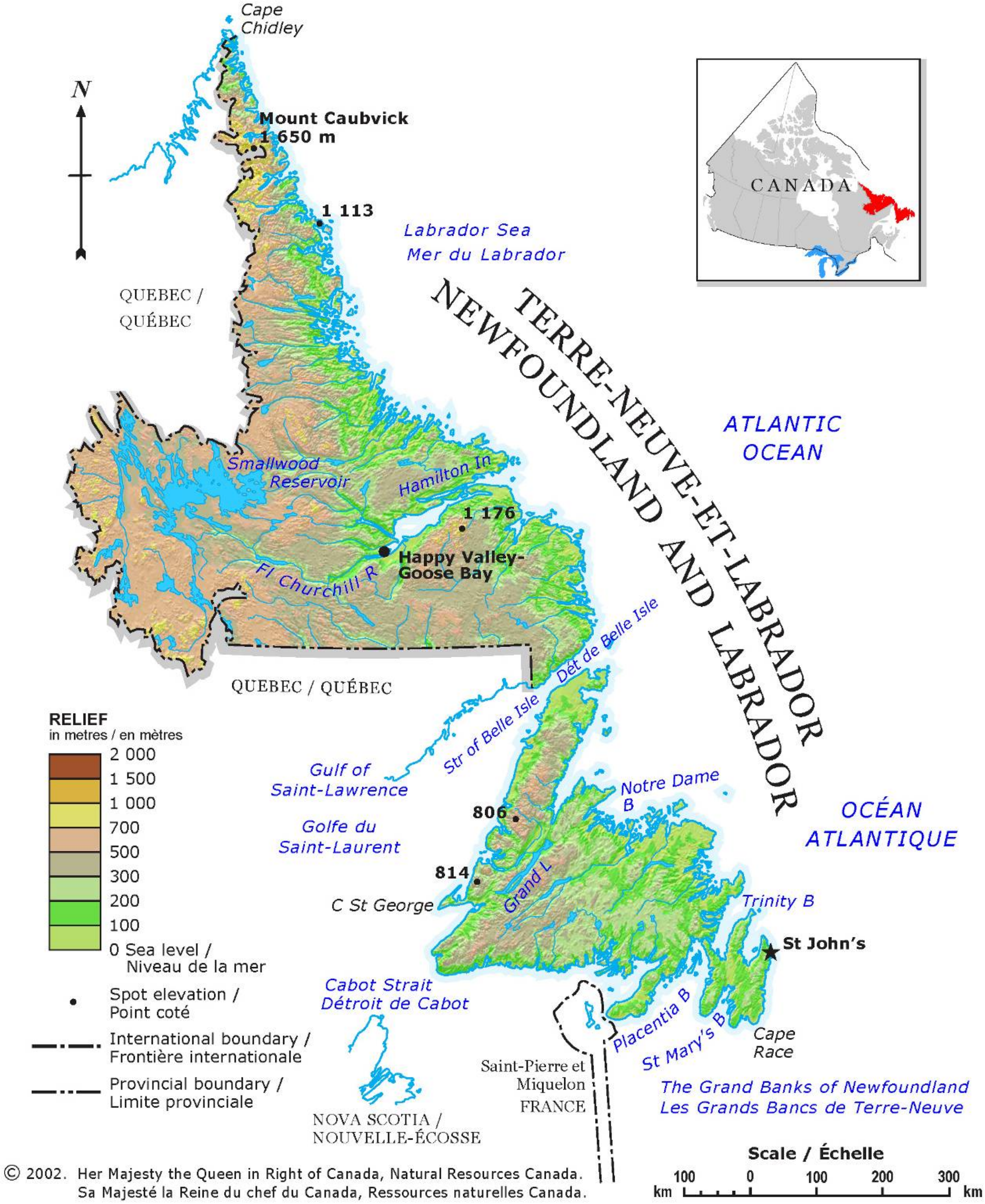

Figure 3. Color relief map of Newfoundland and Labrador

Figure 4. Locations of the 28 weather stations in Table 1.

Figure 5. Some of the variety of shapes of ice accreted from freezing rain (photos, CRREL).

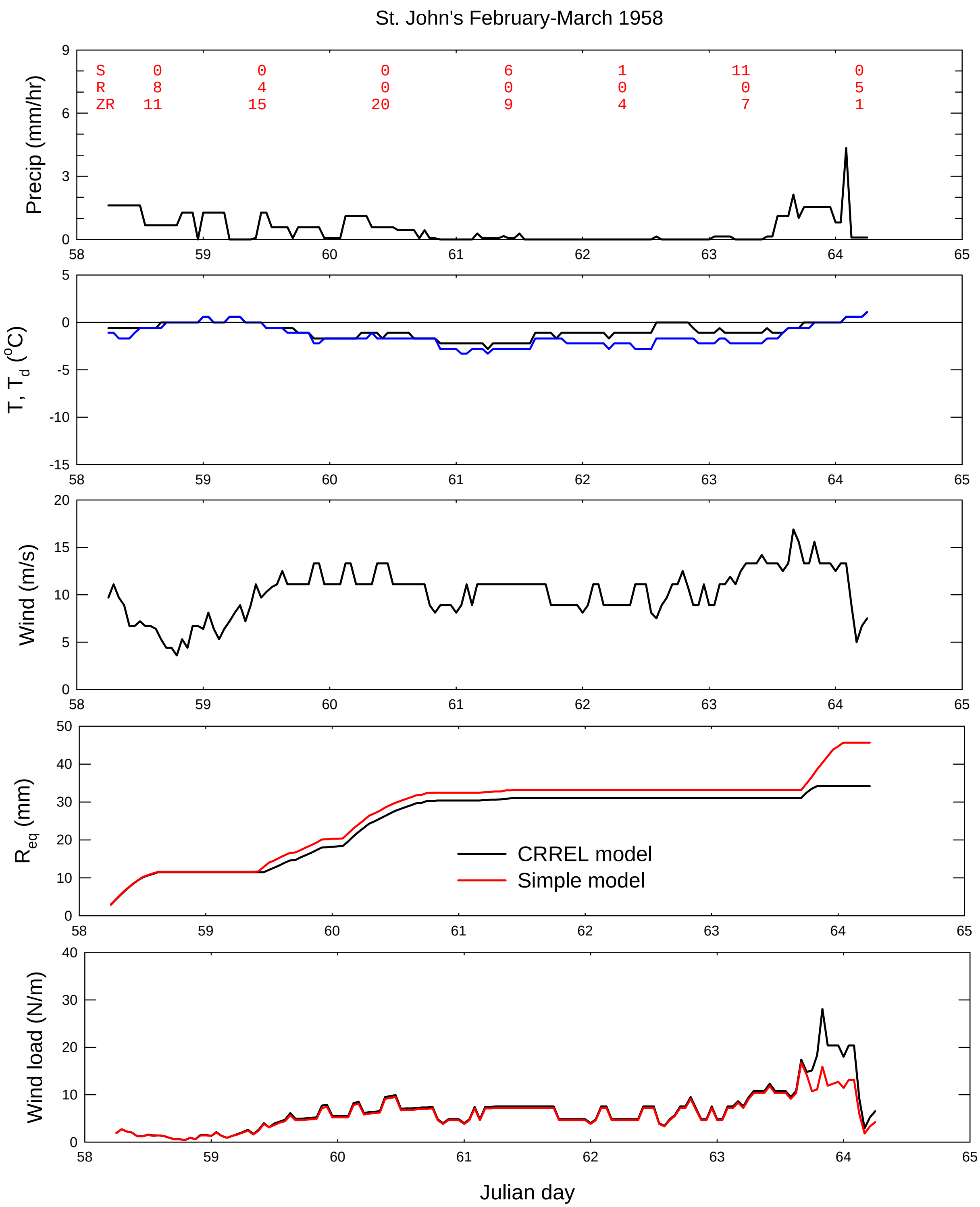

Figure 6. a)Freezing rain storm from February 27 to March 5, 1958

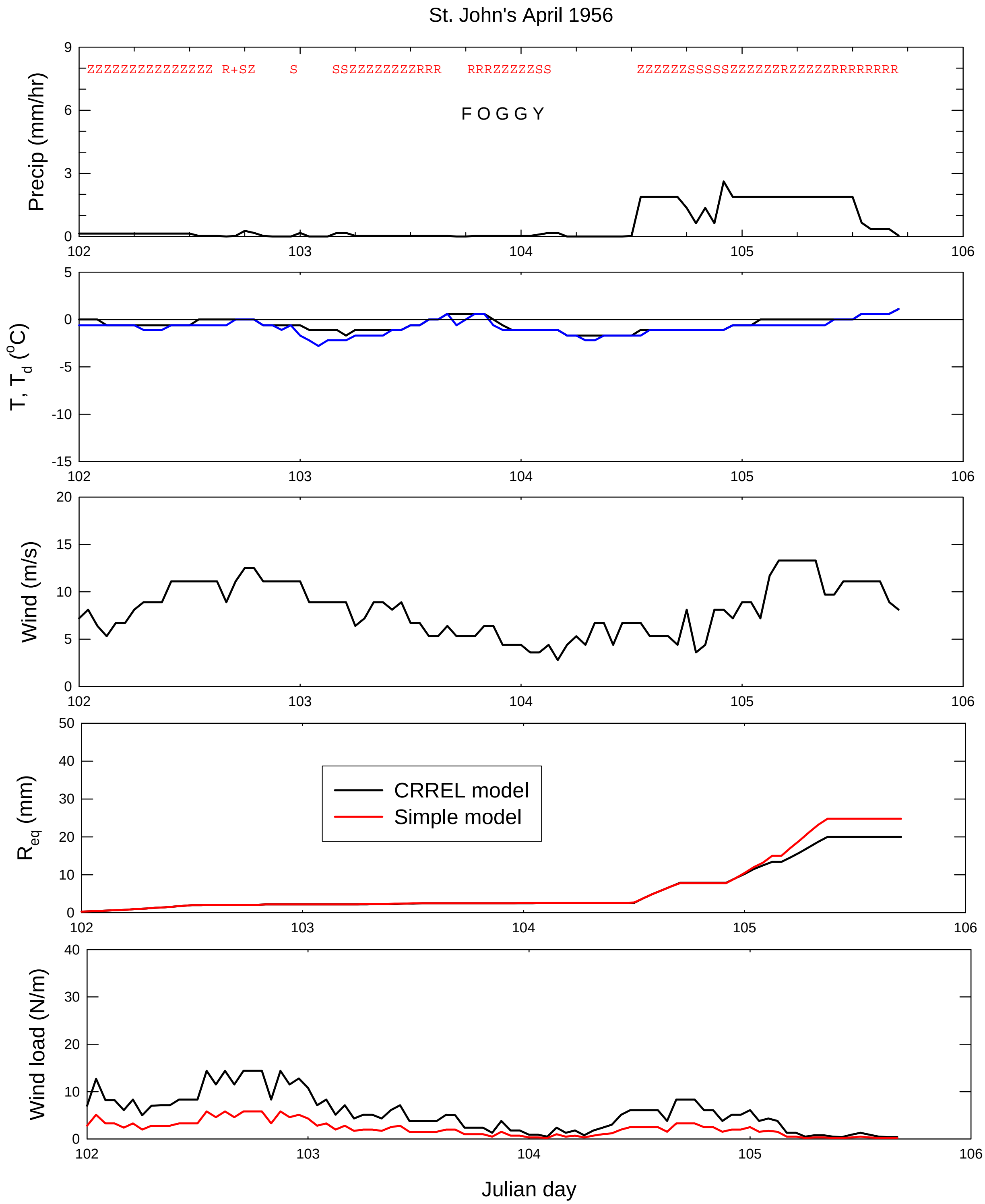

b) Freezing rain event in April 1956

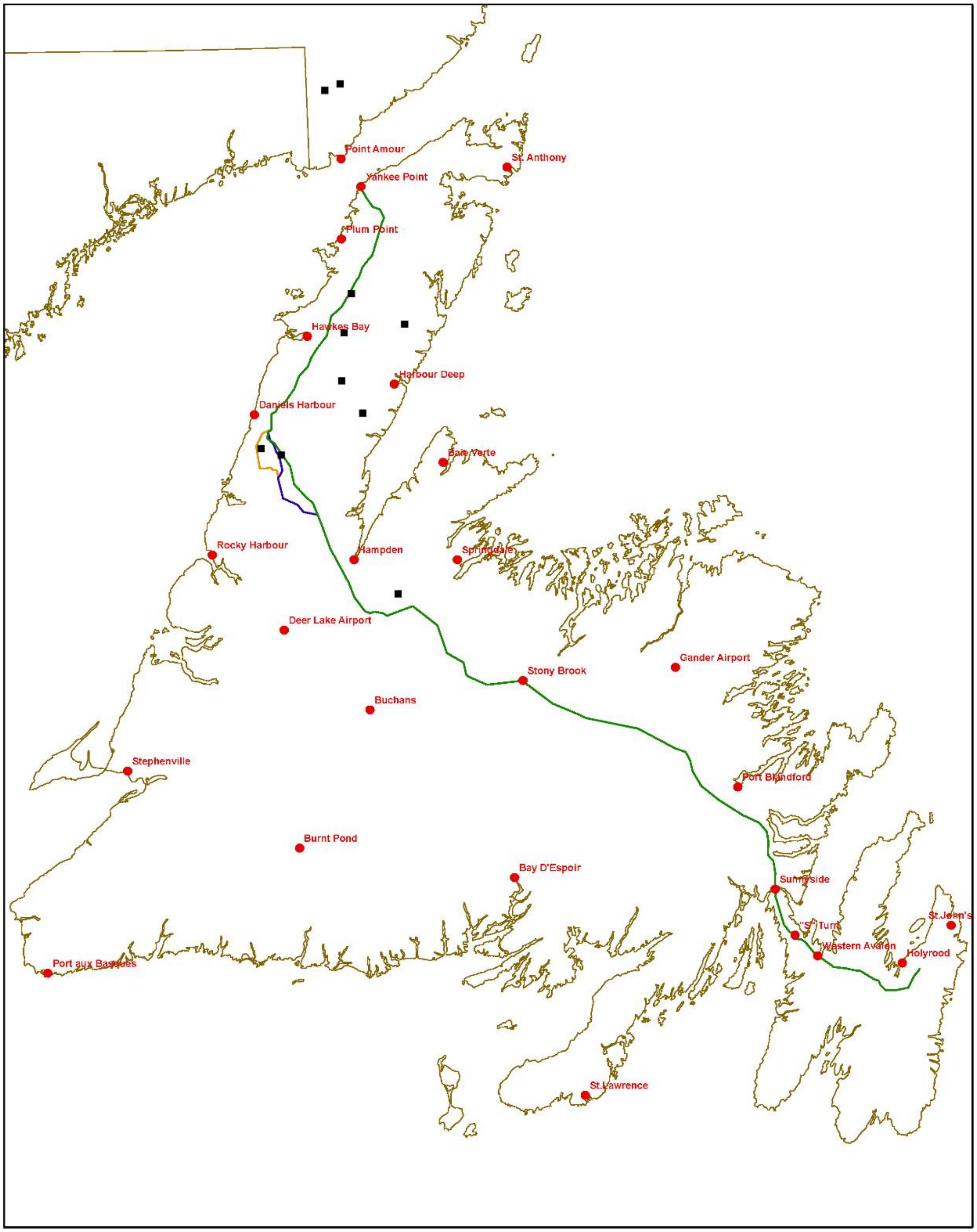

Figure 7. Passive ice meter (PIM) stations. Long Harbour, Brigus Junction, and Dildo on the Avalon Peninsula and Gros Morne, inland of Rocky Harbour, are not shown.

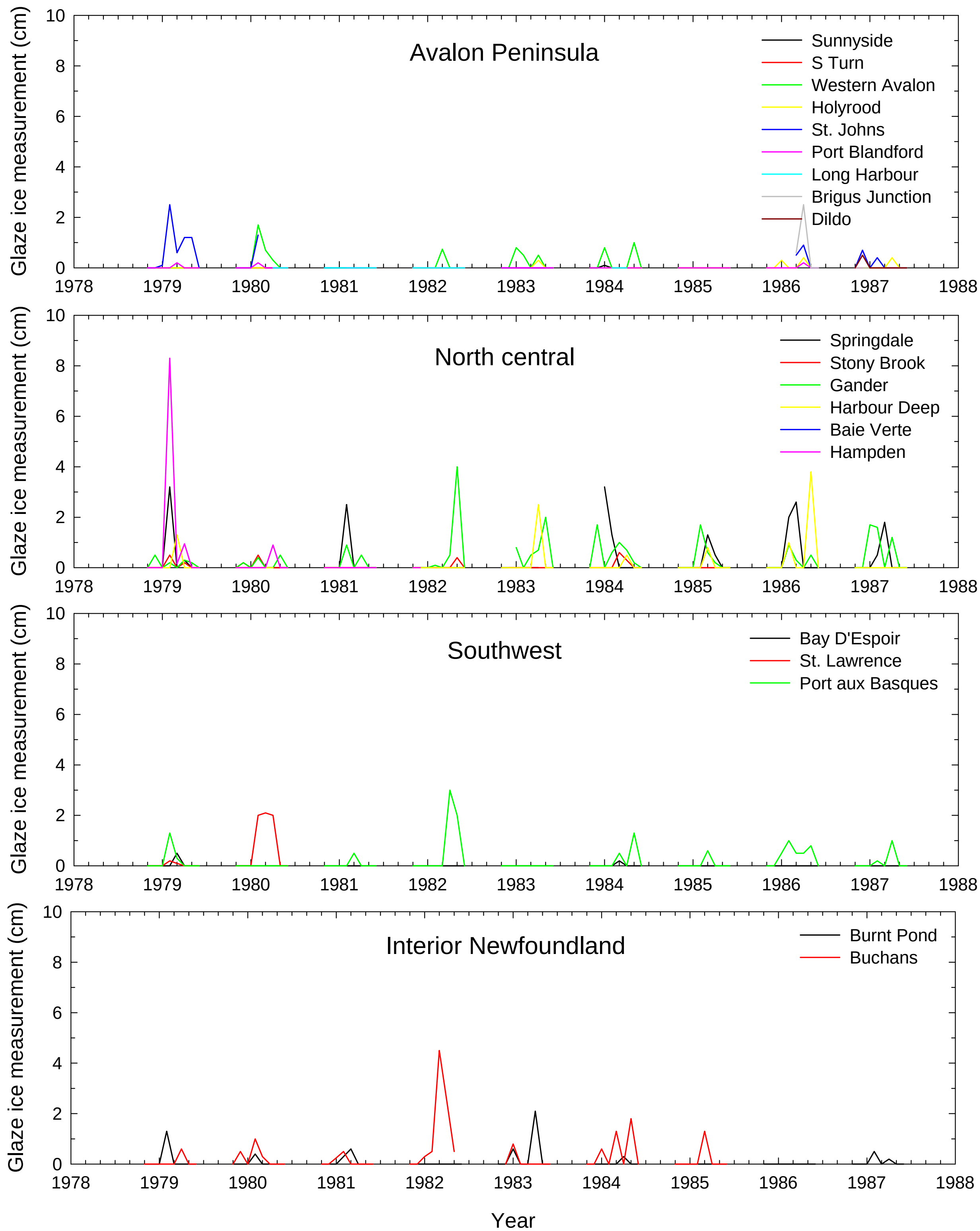
Avalon Peninsula
Sunnyside
S Turn
Western Avalon
Holyrood
St. Johns
Port Blandford
Long Harbour
Brigus Junction
Dildo
North central
Springdale
Stony Brook
Gander
Harbour Deep
Baie Verte
Hampden
Southwest
Bay D'Espoir
St. Lawrence
Port aux Basques
Interior Newfoundland
Burnt Pond
Buchans
Glaze ice measurement (cm)
Year
0
2
4
6
8
10
1978
1979
1980
1981
1982
1983
1984
1985
1986
1987
1988

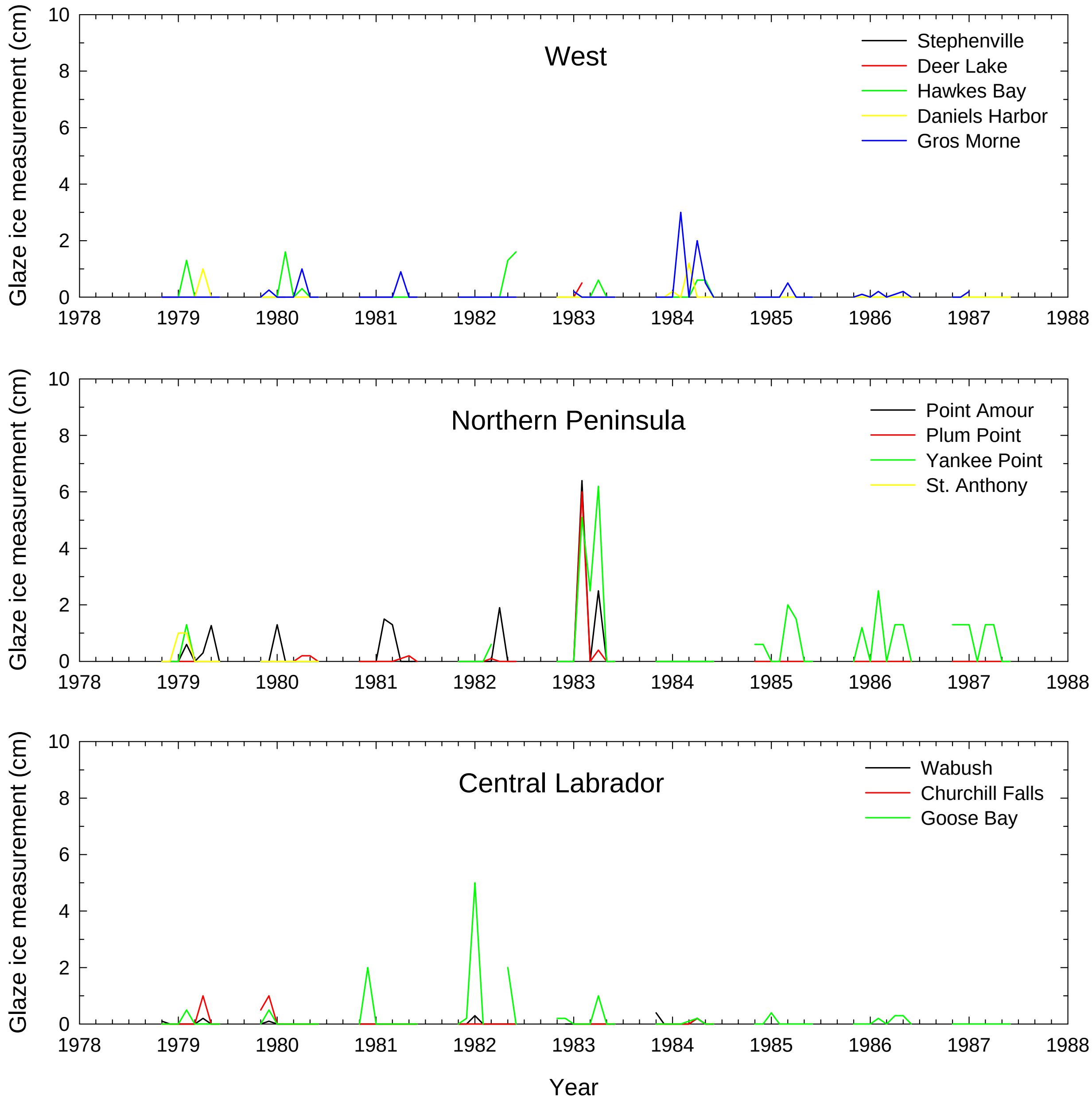

Figure 8. Reported maximum glaze ice thicknesses from Passive Ice Meters

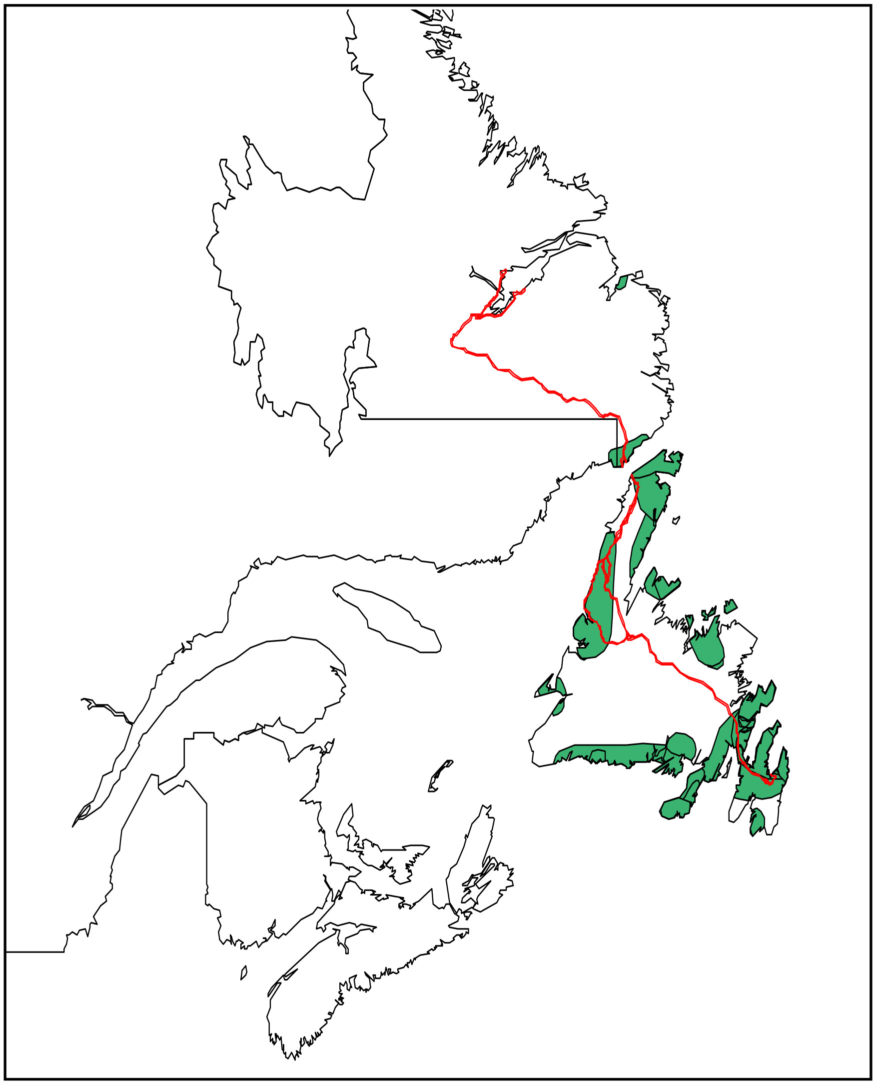

Figure 9. Compilation of damaging freezing rain storms, 1953-2008. The proposed alternative transmission line routes are in red.

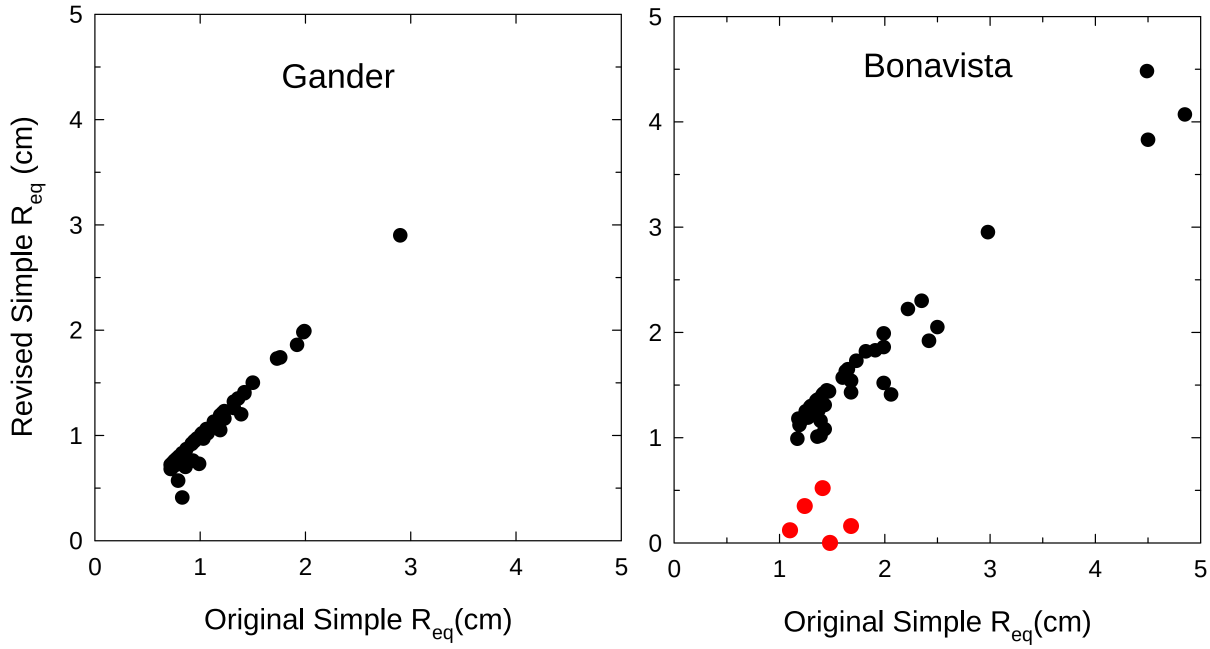

Figure 10. Revised versus original ice loads (Simple model) for Gander (largest 56) and Bonavista (largest 47). The events at Bonavista marked by red circles occurred between April 2001 and February 2006.

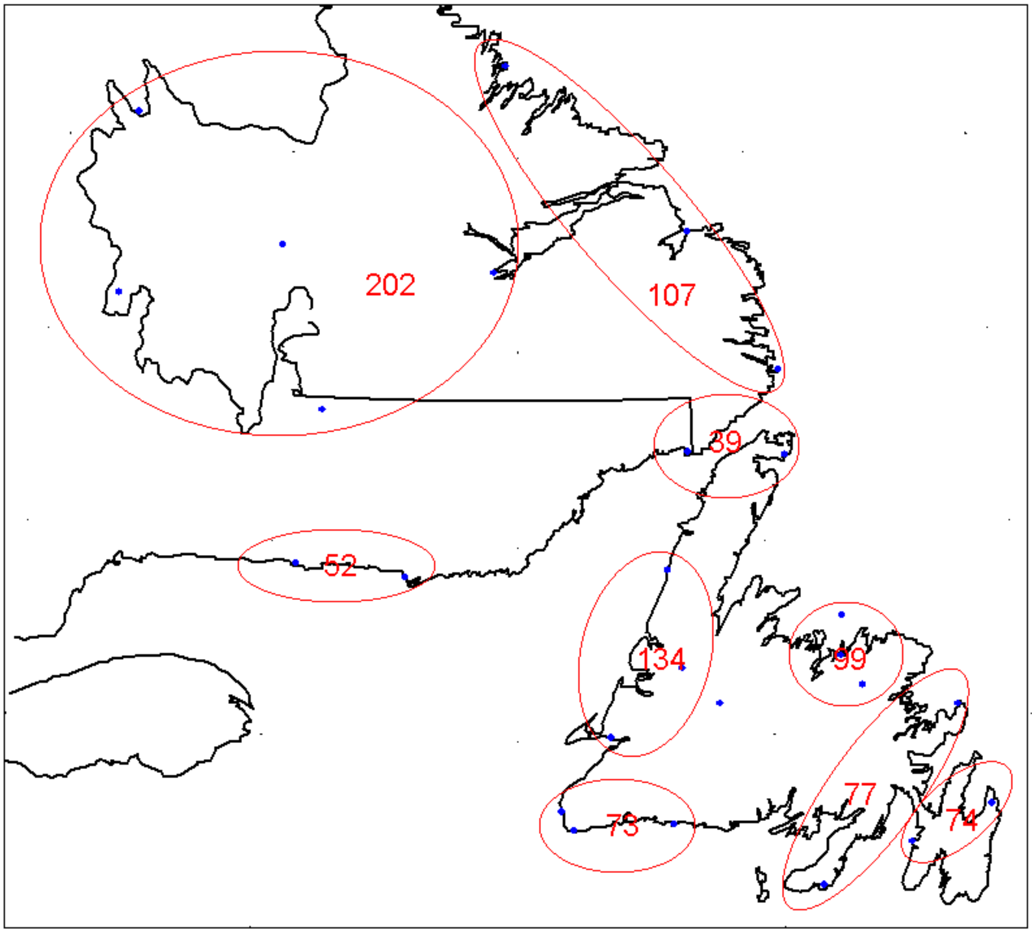

Figure 11. Superstations for the study region with the length of the period of record in years.

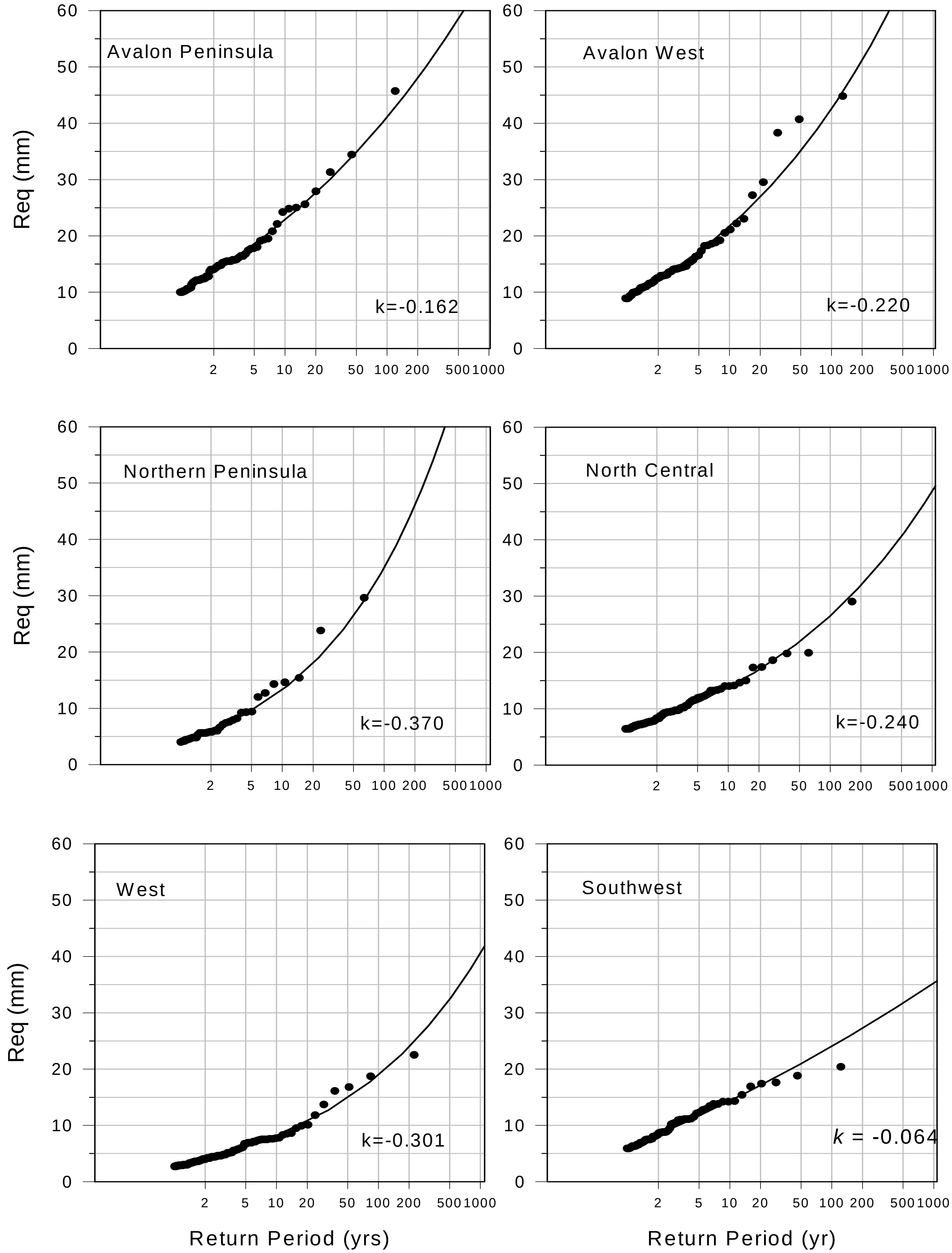
Avalon Peninsula
k=-0.162
Avalon West
k=-0.220
Northern Peninsula
k=-0.370
North Central
k=-0.240
West
k=-0.301
Southwest
k = -0.064
Req (mm)
0
10
20
30
40
50
60
2
5
10
20
50
100
200
500
1000
Return Period (yrs)
Return Period (yr)

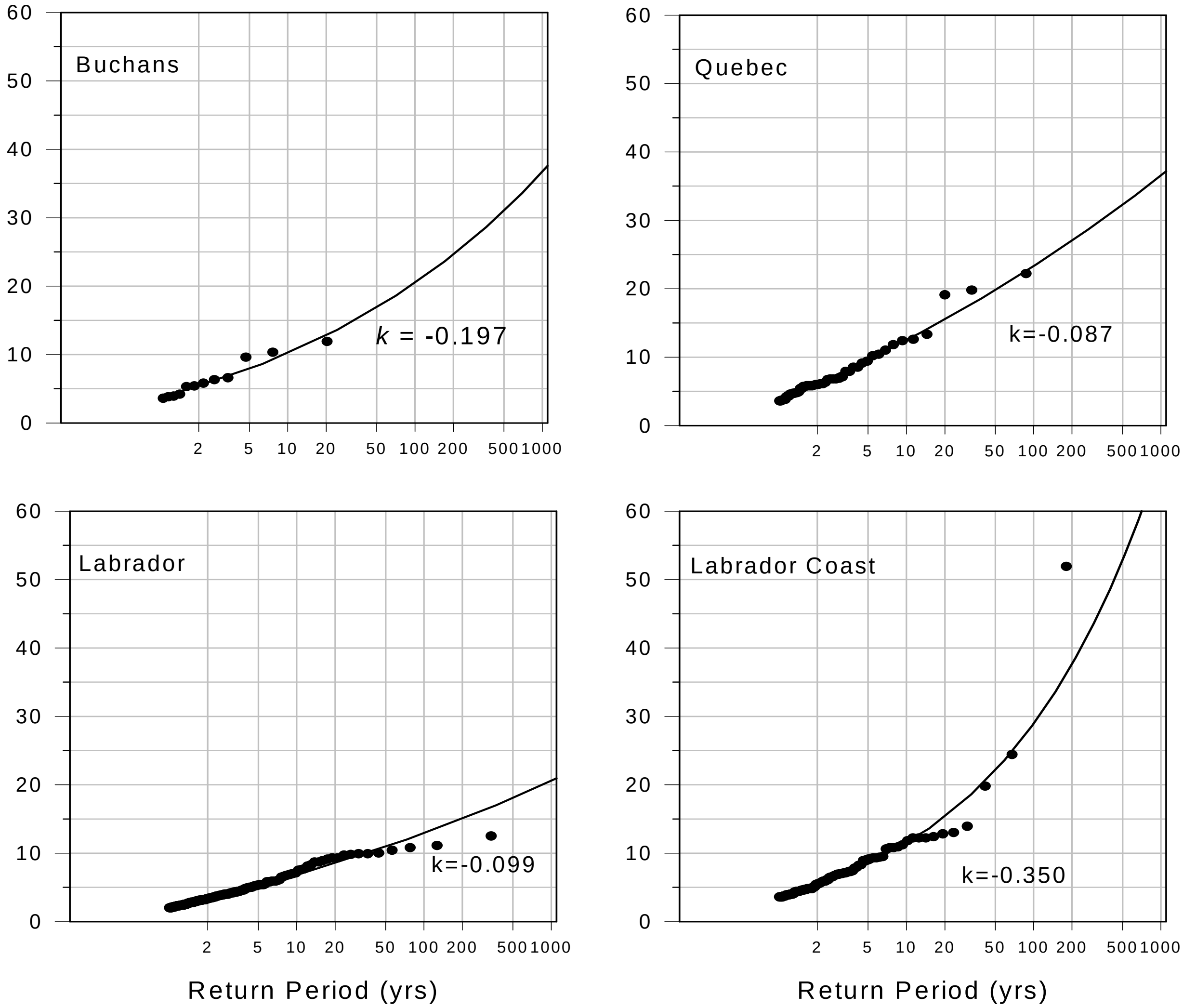

Figure 12. Generalized Pareto distribution fitted to the sample of extremes for each superstation. The tail shape parameter *k* is shown for each fit.

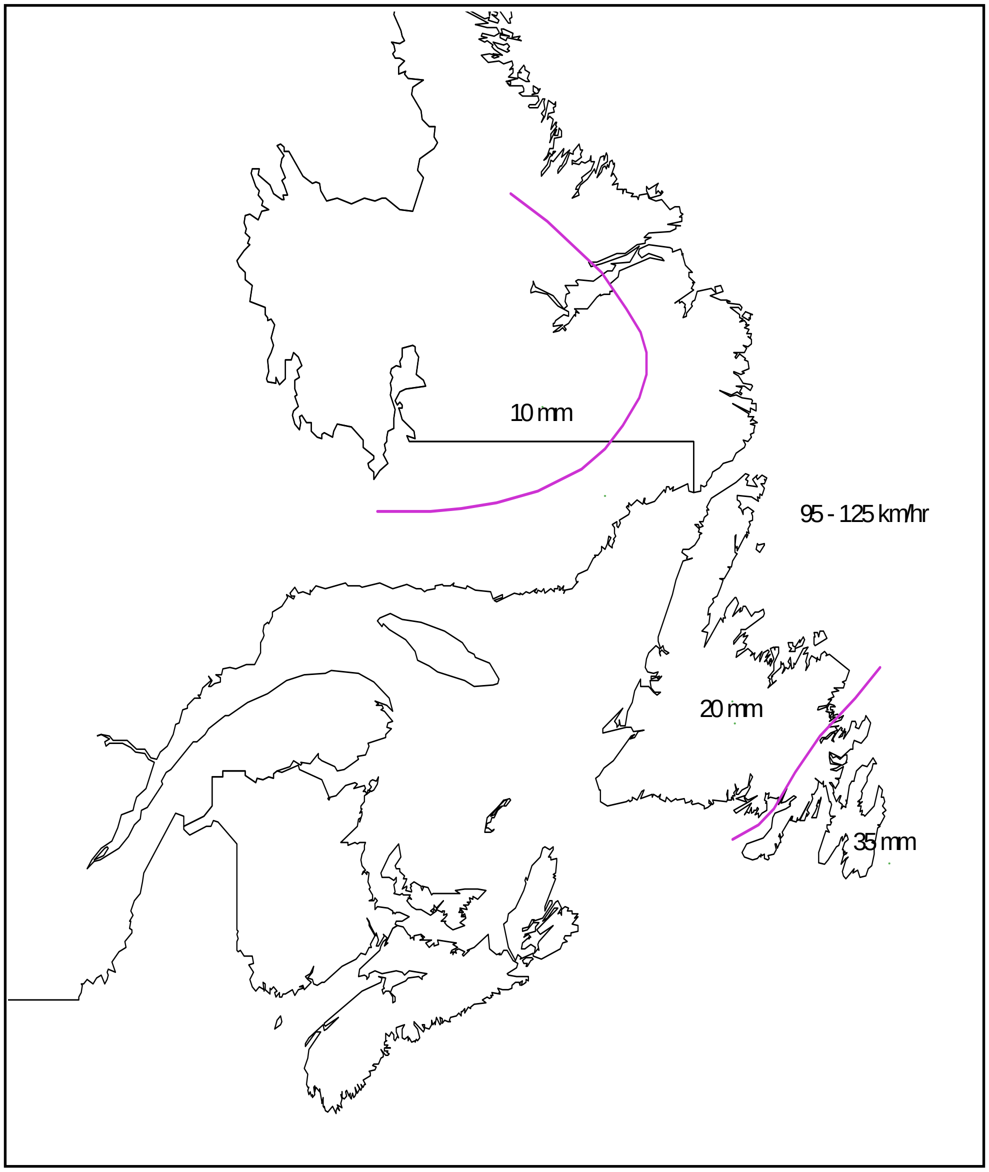

Figure 13. Ice thicknesses from freezing rain for a 50-yr return period with concurrent gust speeds

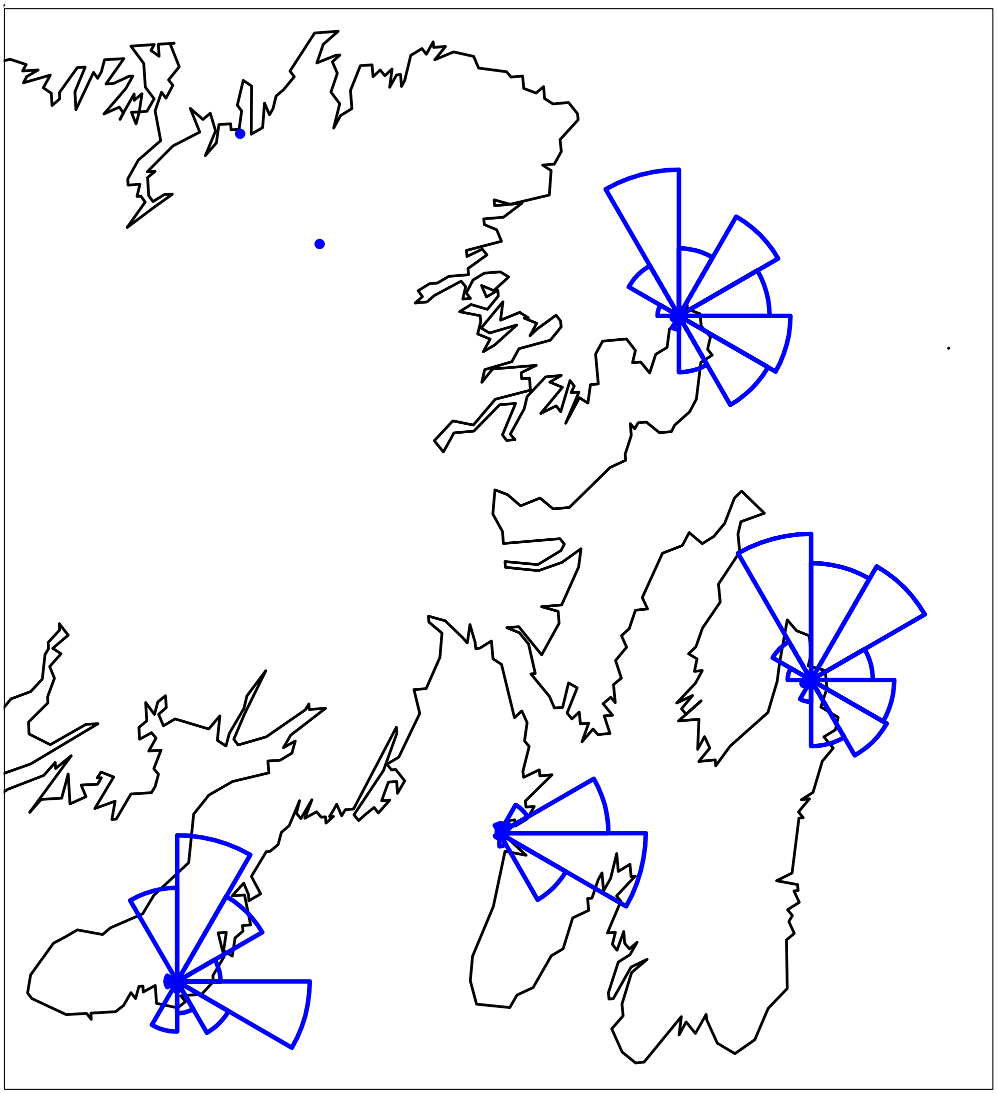

Figure 14. Wind direction histograms for Bonavista, St. John's, Argentia, and St. Lawrence for hours with freezing rain.

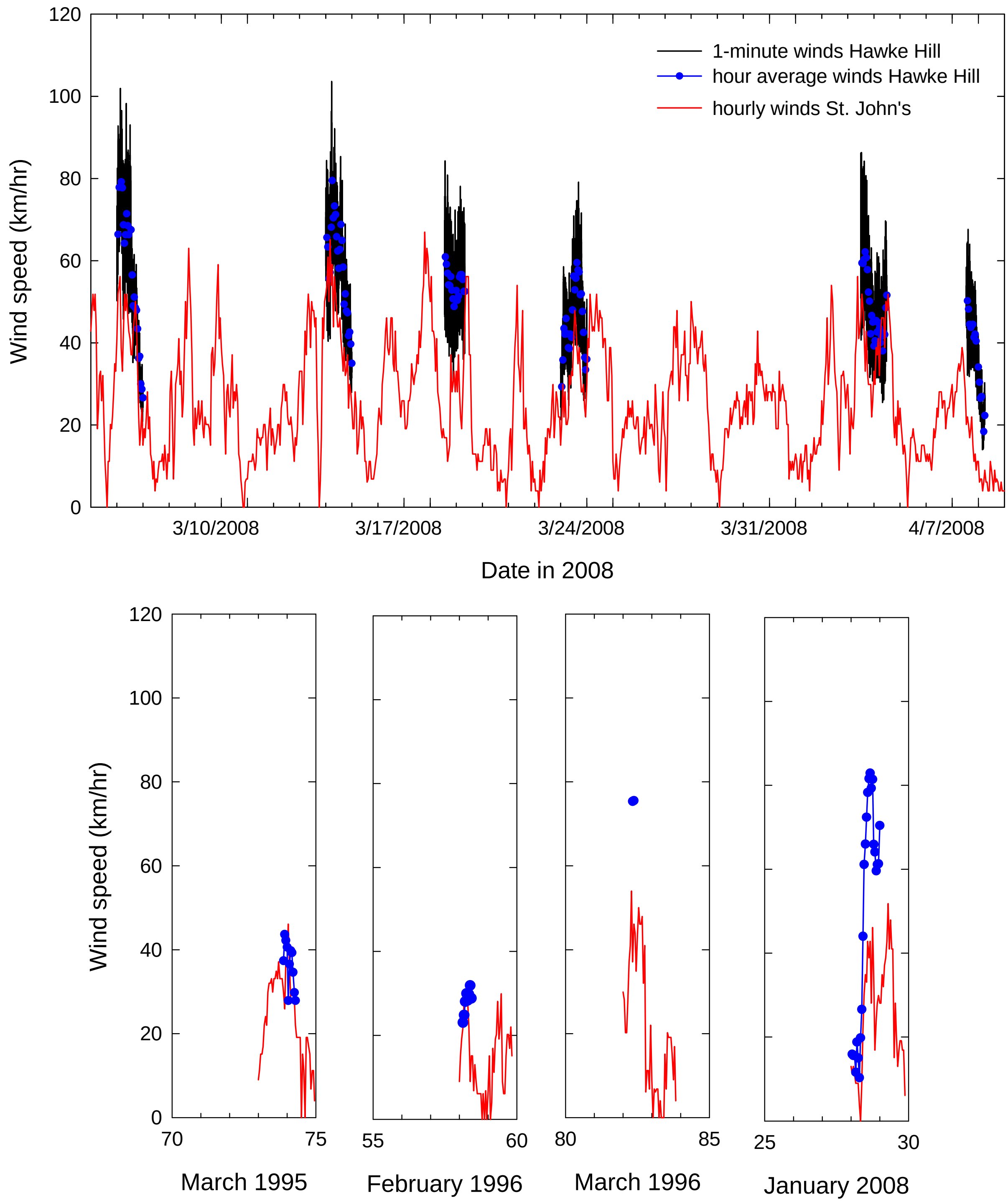

Figure 15. Time series of wind speeds at St. John's and Hawke Hill during freezing rain storms.

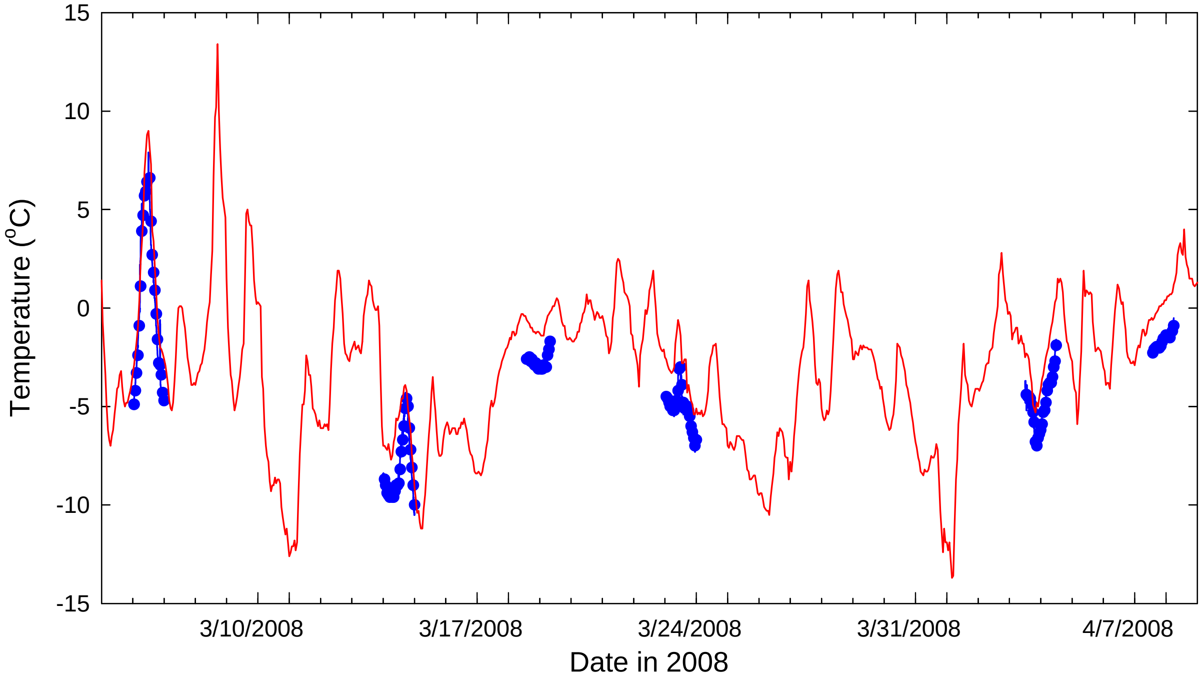

Figure 16. Times series of temperatures at St. John's and Hawke Hill, March and April 1998

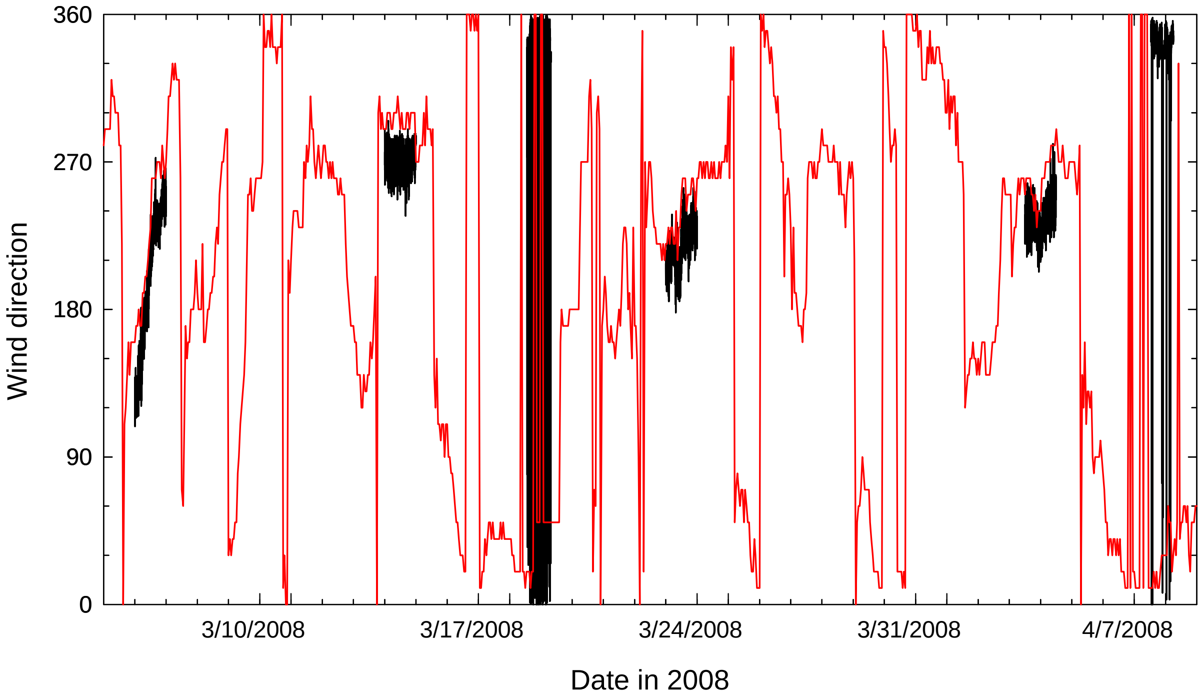

Figure 17. Time series of wind directions at St. John's and Hawke Hill, March and April 1998.

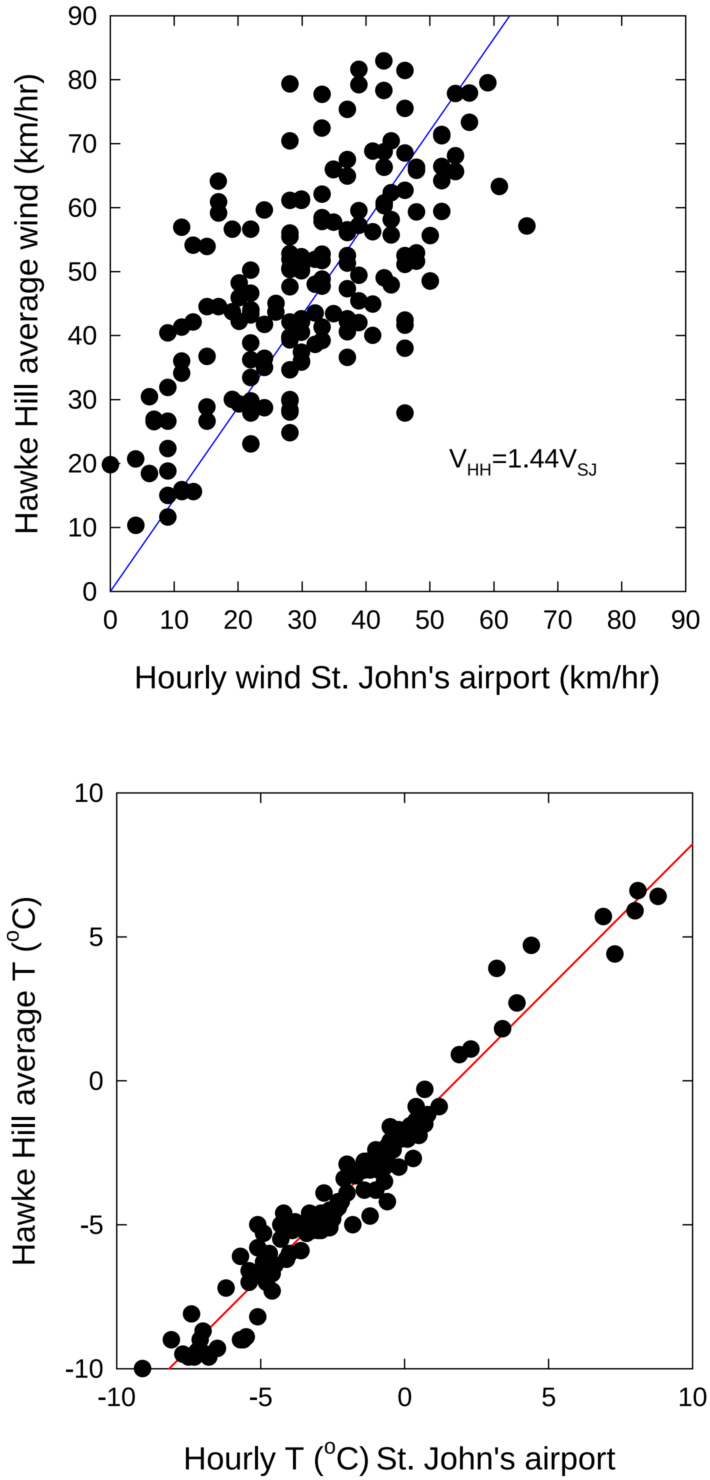

Figure 18. Hawke Hill and St. John's wind speeds and temperatures

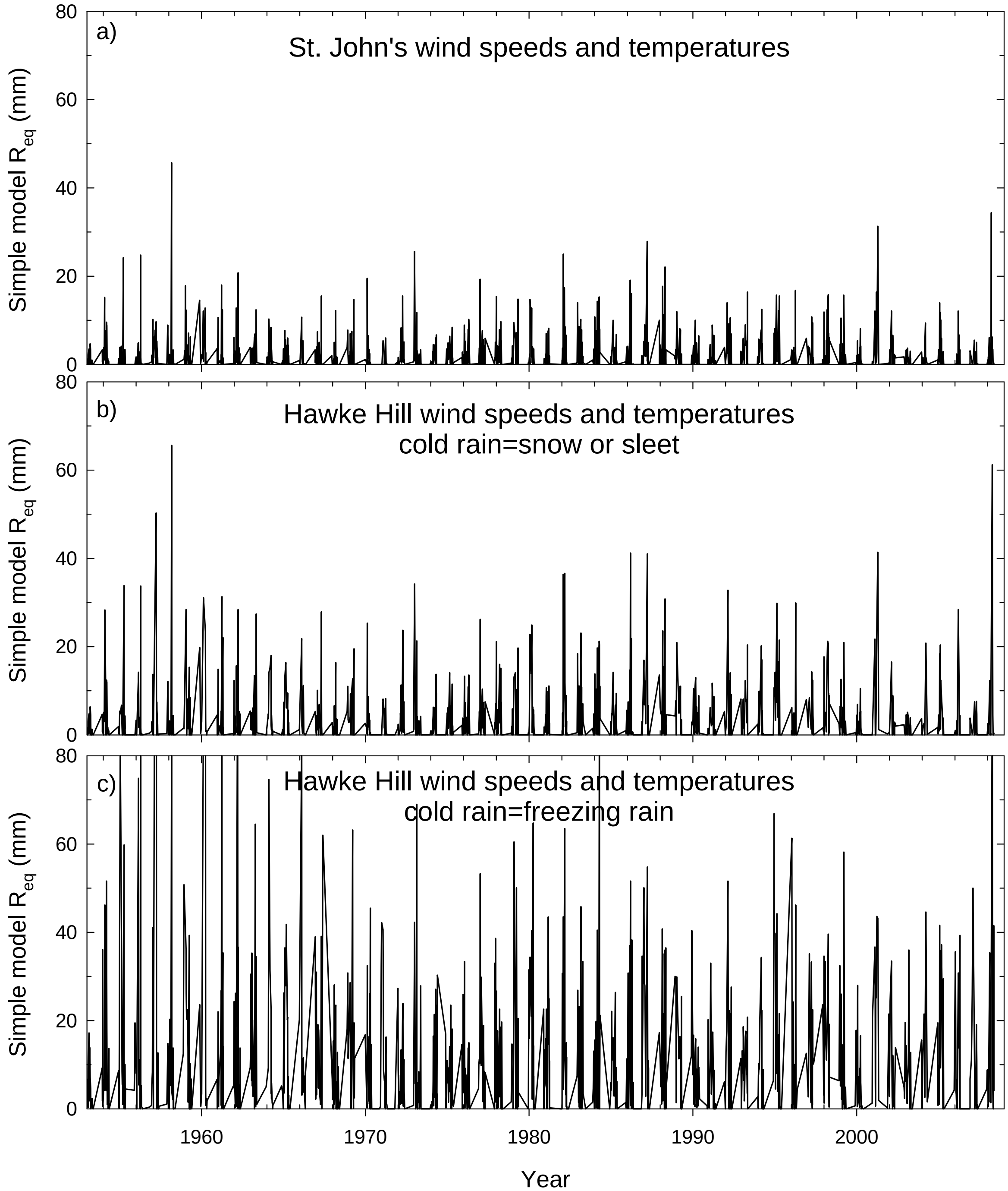

Figure 19. Time series of equivalent radial ice thicknesses a) St. John's data, b) calculated Hawke Hill temperatures and wind speeds with cold rain treated as snow or ice pellets, c) same as (b) but with cold rain treated as freezing rain.

Table 1. Weather stations in Newfoundland and Labrador

Location Name	Climate ID	Province	Latitude	Longitude	Elev (m)	POR (# yr)	Start	End	Zone	comments
~~ARGENTIA (AUT)~~	~~8400104~~	~~NFLD~~	47.29	-53.99	13	0	01-1987	07-2008	AST	pt 07-10/2000, 11/2001-01/2002; no present weather data-don't use
ARGENTIA A	8400100	NFLD	47.30	-54.00	14	17.5	01-1953	05-1970	AST	pt 04-05/1970
~~BADGER (AUT)~~	~~8400301~~	~~NFLD~~	48.97	-56.07	105	0	12-1986	07-2008	AST	pt -06/1993, 06-09/1994, 03-04/1995, 07/1995, 09-12/1995, 03-06/1996; no present weather data-don't use
BATTLE HARBOUR LOR	8500398	NFLD	52.25	-55.60	9	25	10-1957	10-1983	AST	pt 01-03/1968, 01-03/1969
BONAVISTA	8400600	NFLD	48.67	-53.11	26	47	11-1959	06-2006	AST	pt 08/1999, 03/2006
BUCHANS A	8400700	NFLD	48.85	-56.83	276	12.5	01-1953	06-1965	AST	
BURGEO	8400798	NFLD	47.62	-57.62	11	25	11-1966	06-1995	AST	pt 10/1991- (deleted)
CARTWRIGHT	8501100	NFLD	53.71	-57.04	14	53	01-1953	07-2008	AST	6-hly data -01/1955 (deleted); 3-hly data -05/1963; pt 02-08/1999 (deleted)
CHURCHILL FALLS A	8501132	NFLD	53.55	-64.10	440	24.5	11-1968	03-1993	AST	pt 01/1977, 03/1993 (deleted)
COMFORT COVE	8401259	NFLD	49.27	-54.88	99	29	01-1967	02-1996	AST	3-hly 04/1983-; no data 7-10/1995, 1/1996
DANIELS HARBOUR	8401400	NFLD	50.24	-57.58	19	36.5	01-1953	07-2008	AST	pt -12/1965 (deleted), 10/1991-10/1996 (deleted), 1/3-2/10/98 (deleted), 2/11-28/00 (deleted), no pcp 4/98 (deleted)
DEER LAKE A	8401501	NFLD	49.22	-57.40	22	42.5	07-1965	07-2008	AST	no pcp 12/1996-01/1997 (deleted)
GANDER INT'L A	8401700	NFLD	48.95	-54.58	151	55.5	01-1953	07-2008	AST	
GOOSE A	8501900	NFLD	53.32	-60.42	49	55.5	01-1953	06-2008	AST	
HOPEDALE (AUT)	8502400	NFLD	55.45	-60.22	12	29	01-1953	07-2008	AST	pt -02/1955 (deleted), 3-hly-06/1963, no data 09/1984-01/1994; no pw 02/1994-
PORT AUX BASQUES	8402975	NFLD	47.57	-59.15	40	34	06-1966	07-2008	AST	pt 10/1991-05/1998 (deleted), no pcp 12/1995 (deleted)
ST ANDREWS	8403300	NFLD	47.77	-59.33	11	13.5	01-1953	05-1966	AST	
ST ANTHONY	8403400	NFLD	51.37	-55.58	17	13	01-1953	12-1965	AST	
ST JOHN'S A	8403506	NFLD	47.62	-52.74	141	55.5	01-1953	07-2008	AST	
ST LAWRENCE	8403615	NFLD	46.92	-55.38	49	30	02-1966	02-1996	AST	3-hly data 04/1983-
STEPHENVILLE A	8403800	NFLD	48.53	-58.55	26	55.5	01-1953	07-2008	AST	
TWILLINGATE	8404000	NFLD	49.68	-54.82	5	14	01-1953	01-1967	AST	no data 03-04/1953
WABUSH LAKE A	8504175	NFLD	52.93	-66.87	551	46.5	01-1961	07-2008	AST	no pcp 11-12/2003 (deleted)

Location Name	Climate ID	Province	Latitude	Longitude	Elev (m)	POR (# yr)	Start	End	Zone	comments
BLANC-SABLON A	7040813	QUE	51.45	-57.18	37	25.5	09-1982	07-2008	AST	3-hly for part of each day - 07/1996 and 01/1997; pt 11/2007-2/2008 (deleted)
HAVRE-SAINT-PIERRE A	7043018	QUE	50.28	-63.60	38	13	12-1983	07-2008	EST	pt - 02/1995 (deleted) except 12/1994
LAKE EON	7043740	QUE	51.87	-63.28	561	22	05-1955	06-1977	EST	no data 03/1977; pt 03-04/1957 (deleted)
NATASHQUAN A	7045400	QUE	50.18	-61.82	11	39	01-1957	06-2008	EST	less than 3-hly data - 02/1969 (deleted); 3 hly data for half of each day - 04/1997;
SCHEFFERVILLE A	7117825	QUE	54.80	-66.82	522	54	01-1953	07-2008	EST	no pcp 10/1993, 12/1993-04/1994 (deleted); no data 10-11/1979; pt 10/1993-01/1994 (deleted); sporadic missing hours 10-11/1994

key: pt = part time
no pcp = no precipitation data
3-hly data = weather data every 3rd hour
no pw = no present weather data = type of precipitation not reported

Table 2. Weighting factors for prorating 6- and 24-hourly precipitation amounts

Precipitation Intensity/Type	*Rain*	*Rain showers*	*Drizzle*	*Freezing rain*	*Freezing drizzle*	*Snow*	*Snow grains*	*Ice pellets*	*Snow showers*	*Snow pellets*	*Hail*
Light	1.8	1.8	0.1	1.8	0.1	0.6	0	1.8	0.6	0.6	1.8
Moderate	5.1	5.1	0.3	5.1	0.3	1.3			1.3	1.3	5.1
Heavy	13.0		0.8			2.5					

Table 3. Confirmed freezing rain storms

Start		End	Location	Description	Young and Shell
3 13 1955	-	3 22 1955	St. John's area	United Towns EC lost 3 poles from heavy ice; one area served by NPL is dark; wires torn off 8 houses; little trouble for CNT because of no wind	
2 27 1958	-	3 5 1958	Avalon Peninsula	worst sleet storm in St. John's in at least 30 yrs, since 4 days in the late 1920s; 1000s wo power for up to 2 weeks; 100s of poles and miles of wire down; every power line at the Goulds switching plant broke; Bowring Park is a mass of broken trees; roads into St. John's blocked by poles and trees; CNT's transNF cable damaged; telegraph cable short circuited by power wire embedded in it; ice as thick as 8" in the Higher Levels; iron ore mines on Bell Island idled for up to 2 weeks; 2 radio towers on Mt. Pearl toppled by ice with another leaning; 9 lb of ice on 8-ft long wire	4" diameter ice on conductors in St. John's area from more than 1" of rain in 6 days; winds generally above 20 mph
2 7 1962	-	2 12 1962	Avalon Peninsula; St. Lawrence area	1000s of power lines crashed to the ground with inches of glittering silver thaw on the Avalon Peninsula where most communication is also out; 500 poles down and transmission line broken; as bad as the 1958 storm on Bell Island with ice up to 2" thick; 90% of CNT's wires are down in one section of the Avalon Peninsula; ATC and NPL helping UT with equipment and men, but only half as many poles available now as in 1958	forests on the Avalon and Bonavista Peninsulas severely damaged; 3" thick glaze on structures in the St.Lawrence area
2 16 62	-	2 19 1962	Gander area	snow storm and winds above 60 mph knocked out power at Gander; electricity was off for hours	3" diameter glaze near Gander; 1 mile of transmission line failed; 30 hrs of freezing drizzle
1 22 64	*-*	*1 24 1964*	*Conception Bay area*	*St. John's: 2 mm ice on 1/22 then fog, rain and $T>0^oC$* *Argentia: 3 hours fog, no precip $T>0^oC$*	*5" diameter glaze*
1 1 1965	-	1 10 1965	Gander, La Scie, areas	freezing rain resulted in up to 10" of ice on the CNT tower at Twillingate; this is the worst at Twillingate since 1959 when the island was hit by severe glitter; not as severe at Flower's Cove and St. Anthony for CNT	1.5" diameter glaze at Gander; 15" diameter glaze in La Scie
12 20 1965	-	1 24 1966	Trinity and Conception Bay areas	No ice storm damage mentioned in *Telegram*	6" diameter glaze with 30-40 mph winds
2 5 1970	-	2 12 1970	St. John's area	ice straining trees and power lines; broken branches; NLP and NTC busy with loose wires from heavy ice; 4 blown feeders caused 1.5 hr outage; worst sleet storms were 1958 and 1962; not as much damage now because lines are built to withstand icing	

Start	End	Location	Description	Young and Shell
2 27 1970	- 3 3 1970	Bonavista and Burin Peninsulas and NW Avalon Peninsula	NLH has 37 steel towers collapsed with 33 miles of transmission line down under weight of 6-8" of ice; this is 3 to 5 times what is normally expected; sleet storm of catastrophic proportions; complete blackout in Sunnyside area; CNT has 135 crossarms down	5 to 6" diameter glaze ice on transmission line near Sunnyside
2 14 1971	- 2 15 1971	west coast	ice snaps power and phone lines and trees; 138 kV and 230 kV lines damaged; power out for more than 4 hours; rain washes out bridges	4 to 5" glaze ice in the Humber Valley and across the northwest coast; 2 double circuit 69kV lines damaged by differential stretching; 2 conductors on long span of NLPC T205 west of Grand Lake came down
12 22 1972	- 2 3 1973	Avalon and Bonavista Peninsulas	freezing rain with wind in eastern NF downs trees and power lines; 1 of 2 transmission lines to St. Johns knocked out by heavy ice; conductors along 4 miles crossing the Isthmus of Avalon down with 5" of ice on parallel line; like the Feb and Mar 1970 storms	
12 30 1976	- 1 27 1977	northern Avalon Peninsula	beautiful silver thaw; limbs and phone and power lines laden with ice; power outage from fire at substation possibly caused by storm; other outages possibly caused by lines banging together	
2 1 1979	- 2 28 1979	Northern and Baie Verte Peninsulas	NLH has ice 6" in diameter on poles and windy, breaking crossarms and cracking poles; power out for more than 2 days; accumulation is 20 times normal since lines are designed for 3-4" ice without wind or 2" with wind	
2 28 1981	- 3 21 1981	Baie Verte Peninsula and Fogo Island	phones out for a week from ice twisting poles and breaking wires	
1 12 1982	*- 1 20 1982*	*Unspecified Newfoundland*	*Winds gusting to 80 mph snapped ice-laden power lines in Newfoundland. Labrador City declared a disaster area; however, Wabush Lake data shows snow, extreme cold and moderate wind speeds*	

Start		End	Location	Description	Young and Shell
4 7 1984	-	4 17 1984	northern Avalon Peninsula	heavy ice and high winds in worst sleet storm in more than 25 yrs caused power failures for more than 250,000 residents; worse than 1958 storm; 14 steel structures collapsed and 500 to 600 poles down; 2 AM towers on Kinnount Rd destroyed-one shook to pieces and the other sheared off at base under 6" of ice; ice falling from various towers onto structures below; trees down	
2 28 1986	-	3 5 1986	Avalon Peninsula	freezing rain causes havoc with distribution system; ice and trees on wires; worse outside of St. John's because of the longer spans	
3 27 1986	-	3 30 1986	St. John's area	ice-covered branches snapping wires; 2 major power outages but no troubles on main transmission line	
2 14 1988	-	2 21 1988	south coast	1.5" of glitter on everything brings down phone and power lines	
4 9 1988	-	4 16 1988	northern Avalon Peninsula and eastern Bonavista Peninsula	freezing rain, wet snow and high winds cause widespread power outages that might be as bad as the 1984 storm; 4" of ice on towers and cables; TL217 has tower collapse and TL#201malfunctioned; 6 transmission towers will need to be replaced	
3 4 1991	-	3 8 1991	Burin Peninsula	heavy freezing rain knocked out power	
3 9 1992	-	3 11 1992	Burin Peninsula	heavy ice loads and storm force winds bring down 80 to 100 power poles; drop lines down; phone poles also down but those wires could be spliced on the ground;	
4 5 1992	-	4 10 1992	St. John's area	power outages from wet snow, rain and 60-70 km/hr winds; more than 25 poles down; weight of ice and wind causes shorts; NH lost 3 lines; salt contamination from high winds	
12 7 1994	*-*	*12 10 1994*	*Gander to St. Johns*	*50,000 without power from hurricane force winds and 24 cm of snow in less than 24 hours*	
1 17 1995	-	2 16 1995	South of Conne River to Harbor Breton	heavy buildup of ice brought down power transmission lines; 3 H-frame structures went down under weight of ice and crossarms were damaged on 2 others; backup system in Harbor Breton did not start, so no water all day	
3 1 1995	-	4 12 1995	St. John's area	heavy ice and high winds wreaked havoc; tree damage	
2 26 1998	-	3 10 1998	Avalon, Bonavista and Connaigre Peninsulas and Bay de Verde area	freezing rain left 77,000 of NP's 175,000 customers without power; there were also massive outages in 1959, 1984 and 1994; fairly massive hard ice that can't be broken off; Baie de Verde area with 60 poles down under 15" of ice was hardest hit with 300 customers out for more than 48 hours;	

Start				End			Location	Description	Young and Shell
4	4	1998	-	4	5	1998	St. John's, St. Vincent's and St. Lawrence areas	ice about 1' thick splinters poles and causes extensive tree damage; 120 poles down on the Burin Peninsula; 20,000 without power some for more than a day	
1	3	1999	-	2	27	1999	Port au Port Peninsula	1.5 to 2" of ice all around the wires cracked crossarms and some poles; ice covered trees falling on wires; 1600 NP customers without power; NP says that ice in this area is abnormal	
12	25	2003	-	2	5	2004	Blanc Sablon to Red Bay	hard to repair lines because of snow storm	
2	4	2004	-	3	16	2004	St. John's area	heavy slush and high winds cause power outage	
1	13	2005	-	3	9	2005	St. John's area	ice buildup and high winds bring down power lines in blizzard; trees on wires; worst storm in last few years	
12	19	2005	-	2	6	2006	Northern Peninsula and Stephenville and Blanc Sablon areas	freezing rain, snow and wind causes havoc with fallen lines and broken poles and 100s without power; trees weighed down; power restored slowly	
1	21	2007	-	3	11	2007	Cartwright	thick layer of ice from freezing rain in a blizzard knocked out power for 300; 2 lines down; ice as thick as 6" on wires *(likely snow accretion)*	
5	19	2007	-	5	21	2007	Northern Peninsula	high winds and freezing rain downed power lines with significant damage to distribution lines; NH has 30 damaged or broken poles; drop lines ripped off houses; 1300 customers out at peak with 700 out for more than 3 days;	
3	9	2008	-	4	5	2008	St. John's and Bay St. George areas	freezing rain and high winds damage power and phone lines; crossarms cracked	

Table 4. Results of extreme value analysis

					400-yr RP R_{eq} (mm)		50-yr RP R_{eq} (mm)				*Concurrent gust (m/s)*	
Superstation	**POR (yr)**	Station	Elev (m)	POR (yr)	Simple	RF(1973)	CRREL	Simple	**CRREL**	**Simple**	***CRREL***	***Simple***
Avalon Peninsula	**74**	ARGENTIA	14	17.5			11	13	**29**	**34**	***38***	***23***
		ST JOHN'S	141	56.5	66	81	30	38				
Labrador Coast	**107**	BATTLE HARBOUR LOR	9	25	24	71	12	15	**19**	**22**	***32***	***28***
		CARTWRIGHT	14	53			26	29				
		HOPEDALE (AUT)	12	29			9	13				
Northern Peninsula	**39**	BLANC-SABLON	37	25.5			26	30	**20**	**26**	***47***	***27***
		ST ANTHONY	17	13			14	21				
Avalon West	**77**	BONAVISTA	26	47			29	40	**28**	**35**	***47***	***32***
		ST LAWRENCE	49	30			23	26				
Buchans	**13**	BUCHANS	276	12.5	29	81	16	17	**16**	**17**	***30***	***32***
Southwest	**73**	PORT AUX BASQUES	40	34			17	22	**18**	**21**	***45***	***31***
		ST ANDREWS	11	13.5			10	11				
		BURGEO	11	25			18	19				
North central	**99**	COMFORT COVE	99	29			14	16	**20**	**22**	***25***	***23***
		GANDER INT'L	151	55.5	50	66	22	26				
		TWILLINGATE	5	14			11	11				
West	**134**	DANIELS HARBOUR	19	36.5	30	81	15	15	**15**	**15**	***27***	***24***
		STEPHENVILLE	26	55.5			15	15				
		DEER LAKE	22	42.5	29	69	15	15				
Quebec	**52**	HAVRE-SAINT-PIERRE	38	13			23	28	**18**	**20**	***29***	***18***
		NATASHQUAN	11	39			17	18				
Labrador	**202**	GOOSE	49	55.5	20	51	12	12	**10**	**11**	***26***	***24***
		LAKE EON	561	22			12	16				
		SCHEFFERVILLE	522	54			8	9				
		WABUSH LAKE	551	46.5			10	9				
		CHURCHILL FALLS	440	24.5			12	12				

Table 5. Spatial and point loads (Simple model) compared at 45 m above ground.

		spatial values							point values					
	N stations	**N years**	**threshold R_{eq} (mm)**	**# per year**	**tail shape k**	**R_{eq50} (mm)**	**R_{eq200} (mm)**	**N years**	**threshold R_{eq} (mm)**	**# per year**	**tail shape k**	**R_{eq50} (mm)**	**R_{eq200} (mm)**
Avalon	4	55.5	16.6	1.01	-0.282	57	87	150	11.6	1	-0.217	42	61
Western Newfoundland	11	55.5	11.8	1.01	0.062	29	35	331	5.8	1.01	-0.143	23	31
Coastal Labrador and Quebec	6	53	8.6	1	0.101	33	39	184	4.3	1.02	-0.270	27	43
Interior Labrador	5	55.5	5.0	0.96	0.084	15	18	202	2.2	1.01	-0.052	12	17

Appendix A. Symbols and acronyms

b_0, b_1	average and weighted average of sample of extremes
C_D	drag coefficient of ice-covered wire
D	diameter of wire
D_i	diameter of icicles
f_{gust}	G_c/V_c
$F(x)$	cumulative distribution of x
F_n	N-yr return period wind-on-ice load on a 1-in. wire
G_c	gust speed equivalent to V_c
h_A	height of anemometer above ground
h_W	height of wire above ground
k	shape parameter for generalized Pareto distribution
L_i	length of icicles
N	number of hours
p_i	plotting position of ith value in sample of extremes
P	precipitation rate
R_{eq}	equivalent uniform radial ice thickness
R_{eqN}	N-yr return period equivalent uniform radial ice thickness
r_s	Spearman rank order correlation coefficient
t	thickness of ice frozen directly to the wire in the CRREL model
T	return period
u	threshold for generalized Pareto distribution
V	wind speed
V_A	wind speed at height of anemometer
V_T	terminal velocity of raindrops
V_W	wind speed at height of wire
V_C	1-min hourly wind speed associated with R_{eq50} and F_{50}
$x_{(i)}$	ith extreme value
x_T	T-year return-period value
W	liquid water content
Z	height above ground
α	scale parameter for generalized Pareto distribution
λ	occurrence rate of extreme loads
π	3.14159
ρ_a	density of air
ρ_i	density of glaze ice
ρ_o	density of water
θ	wind direction
φ	wire direction

ASCE	American Society for Civil Engineering
CRREL	Cold Regions Research and Engineering Laboratory
GPD	Generalized Pareto distribution
POT	Peaks-over-threshold
UTC	Universal Coordinate Time

Appendix B. Storm maps

Each of the ice storms investigated for this project and confirmed to have been severe enough to damage power lines, trees, or communication towers, or result in notable ice accretions on power lines is mapped in this appendix. For each storm one map shows the modeled ice thicknesses from the CRREL and Simple models and the other map shows the region with damaging or notable ice loads. The format of the ice thicknesses, which are reported in millimeters, is:

CRREL model freezing rain only/Simple model freezing rain only
CRREL model freezing rain and ice pellets/Simple model freezing rain and ice pellets

So, if the model results are all different from each other there will be four numbers reported. For example, at St. Anthony in the 1/1 – 10/65 storm the model runs gave
6/15
10/19 .
Indicating more ice accreted by the Simple model than the CRREL model, and somewhat more ice accreted when ice pellets were treated as freezing rain. If the CRREL and Simple model results are essentially the same, only one number is reported in that row. So for the 2/7 – 12/62 event at Gander
10
44 .
Because the storm footprint did not include Gander, the 10 mm obtained by accreting ice from only freezing rain is the more believable result. If all four results are the same, which occurs frequently, only one number is reported, e.g. 1 mm of ice at Buchans for 3/13 – 22/55.

There may also be multiple events at a station in the period of time covered by one storm. In that case the storm totals are reported in order, with a superscript identifying the storm. This occurred, for example, at St. John’s in the 2/13 – 27/62 storm with
12
18
in the first event and
2
12
in the second.

If 0 is reported for a station, then freezing rain was observed but less than 0.5 mm of ice accreted. If there is no number at a station, there were no reports of freezing rain or ice pellets in that time period. Stations with an **x** over the station location did not have sufficient weather data for that time period to model the accretion of ice from freezing rain.

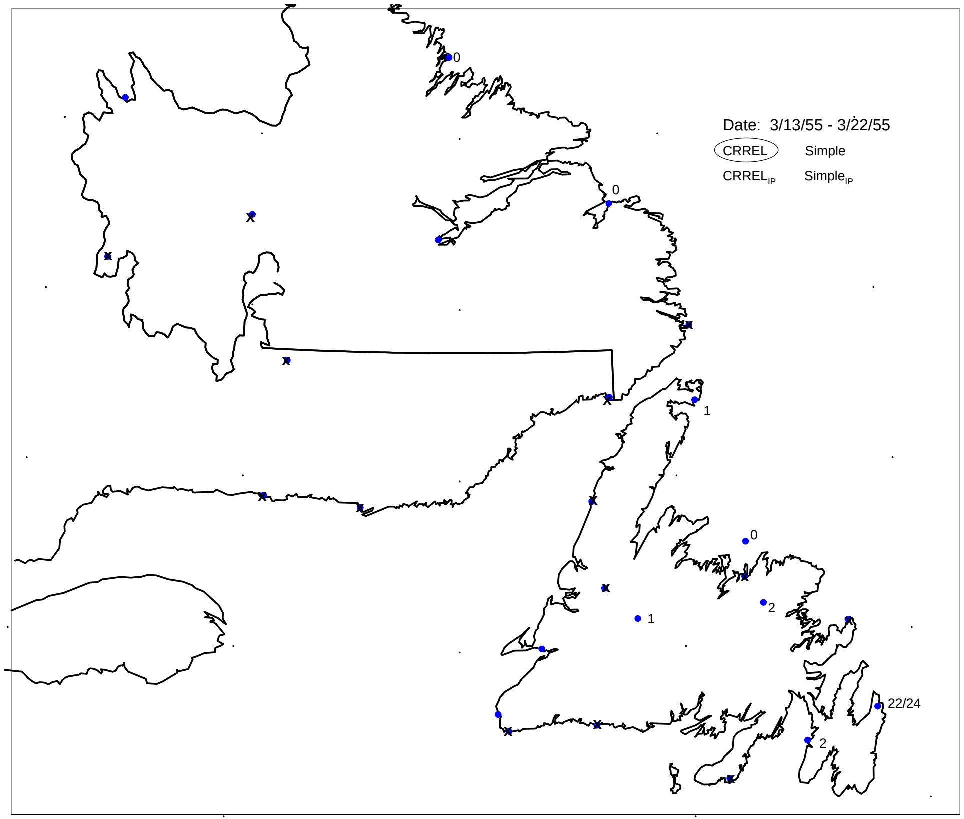
Date: 3/13/55 - 3/22/55
CRREL
Simple
CRREL$_{IP}$
Simple$_{IP}$
0
0
1
0
1
2
22/24
2

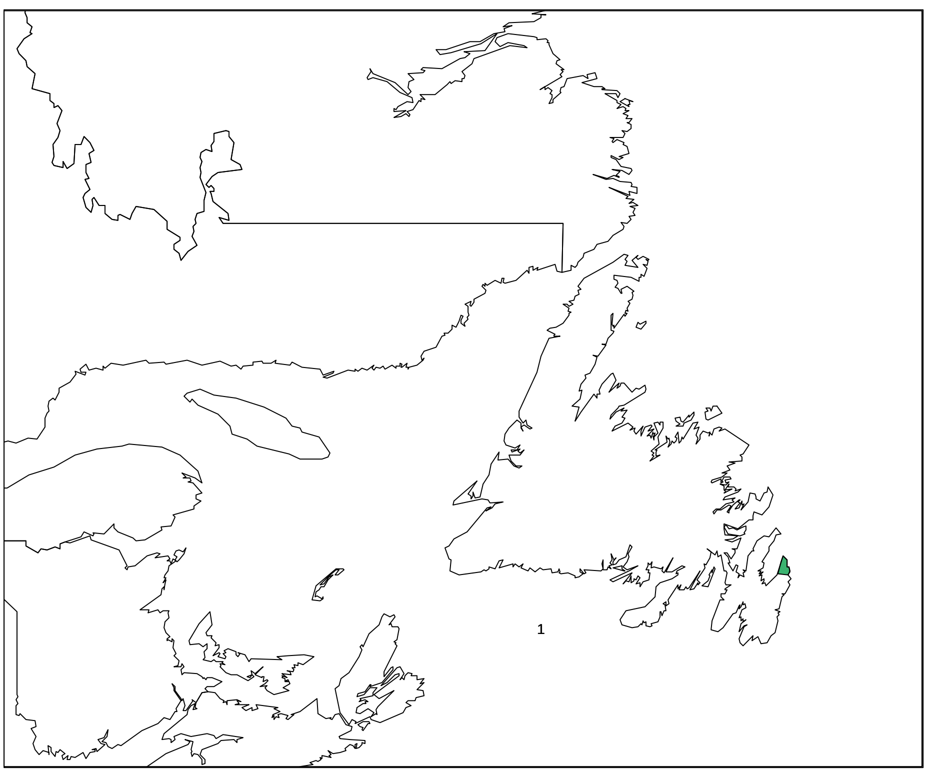
1

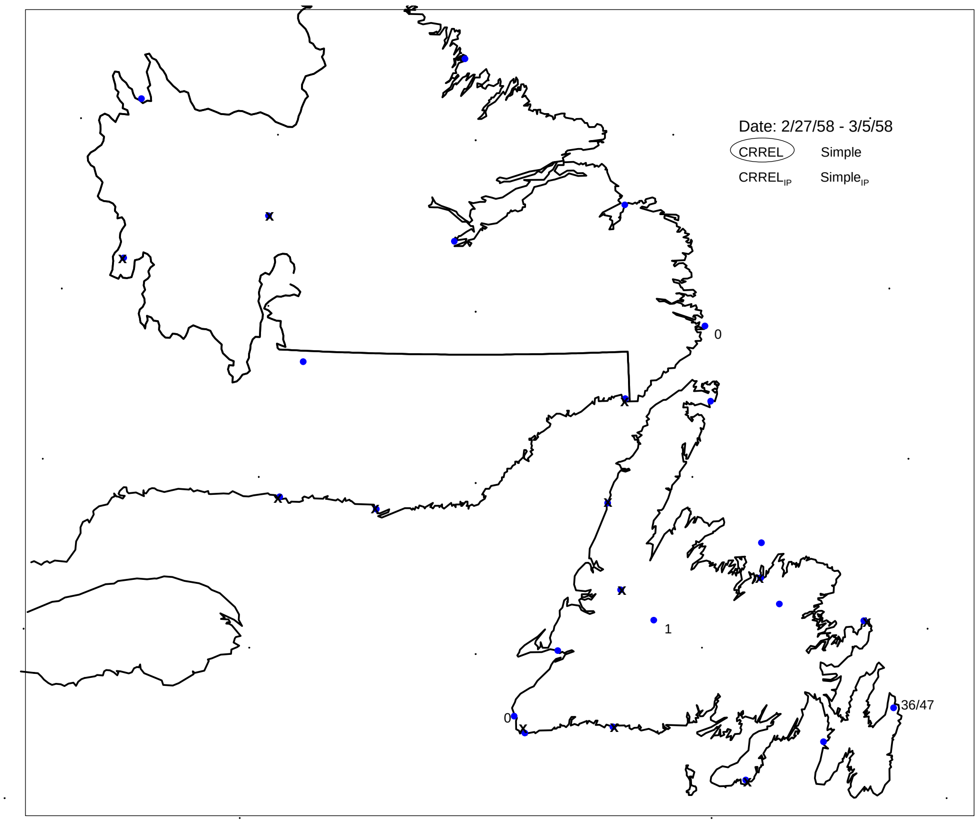
Date: 2/27/58 - 3/5/58
CRREL
Simple
$CRREL_{IP}$
$Simple_{IP}$
0
1
0
36/47


1

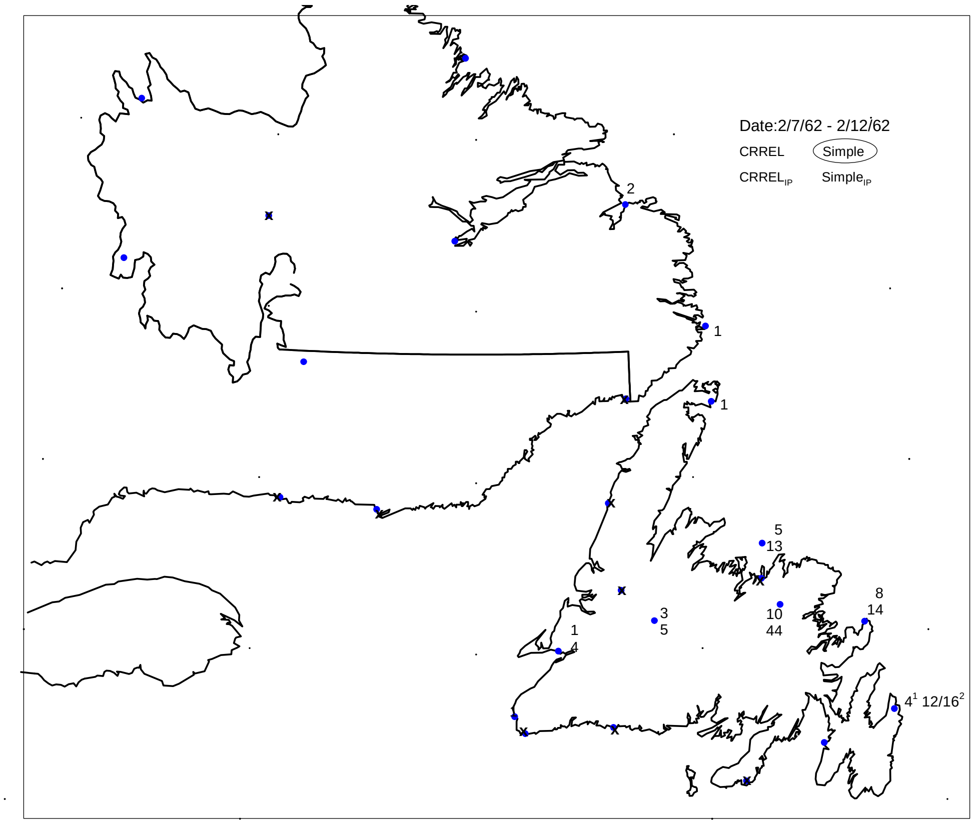
Date:2/7/62 - 2/12/62
CRREL
Simple
CRELIP
SimpleIP
2
1
1
5
13
8
14
3
5
10
44
1
4
41 12/162

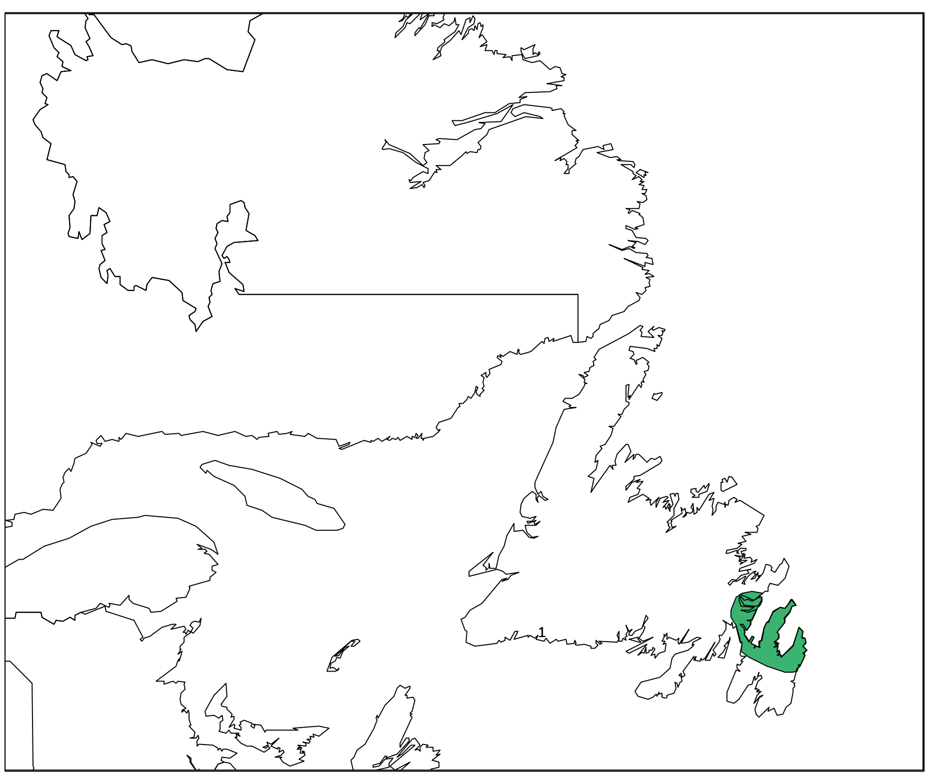
1

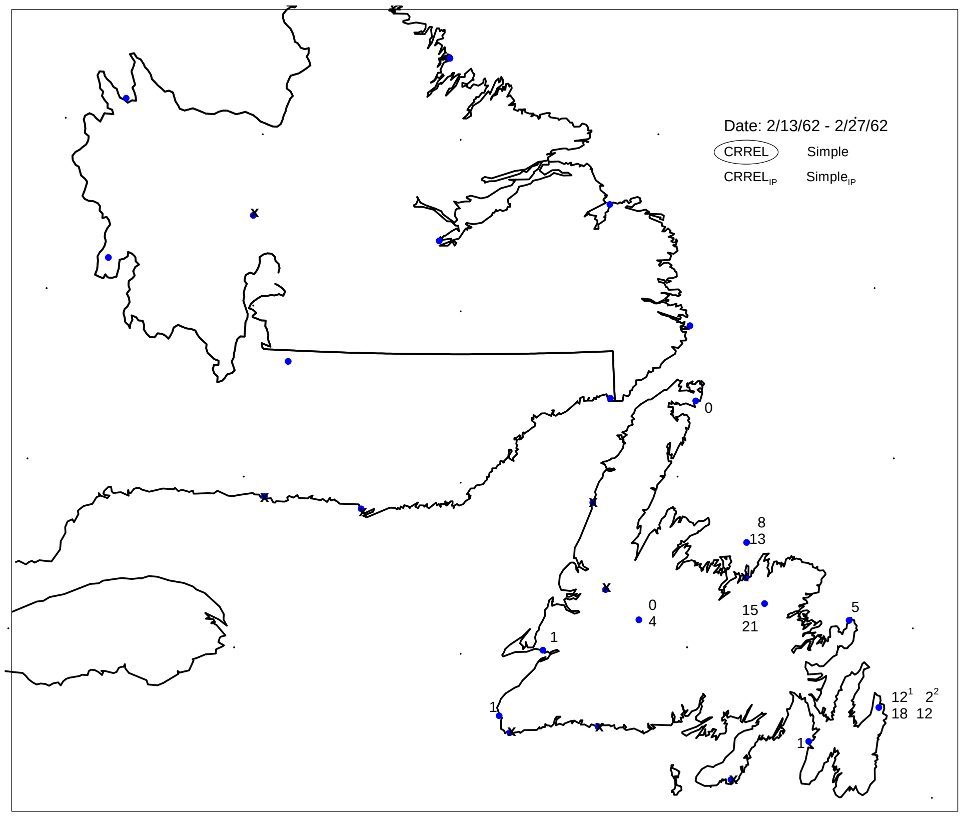
Date: 2/13/62 - 2/27/62
CRREL
Simple
CRELIP
SimpleIP
0
8
13
0
4
15
21
5
1
1
12 1 2 2
18 12
1


1

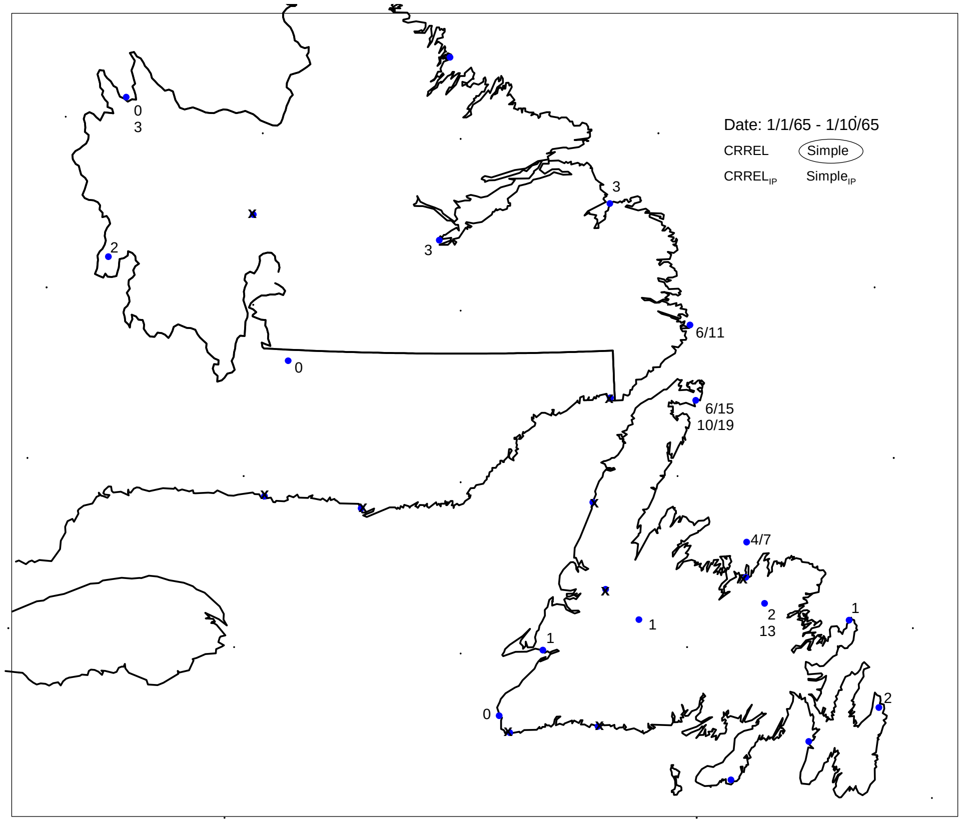
Date: 1/1/65 - 1/10/65
CRREL
Simple
CRREL$_{IP}$
Simple$_{IP}$
0
3
2
3
3
0
6/11
6/15
10/19
4/7
2
13
1
1
1
0
2

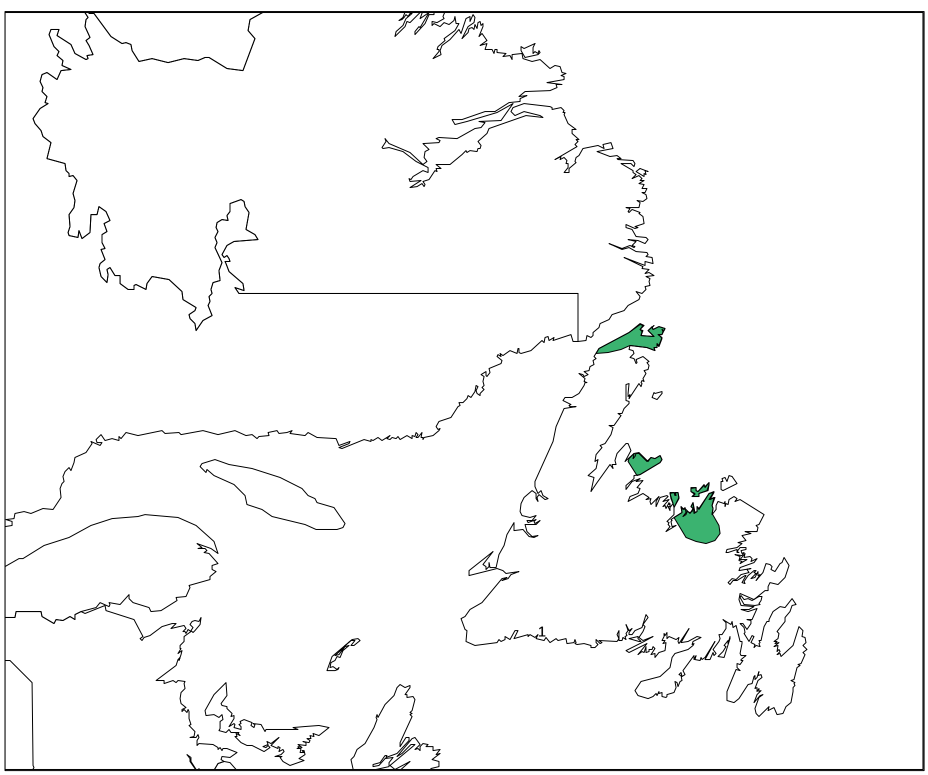
1

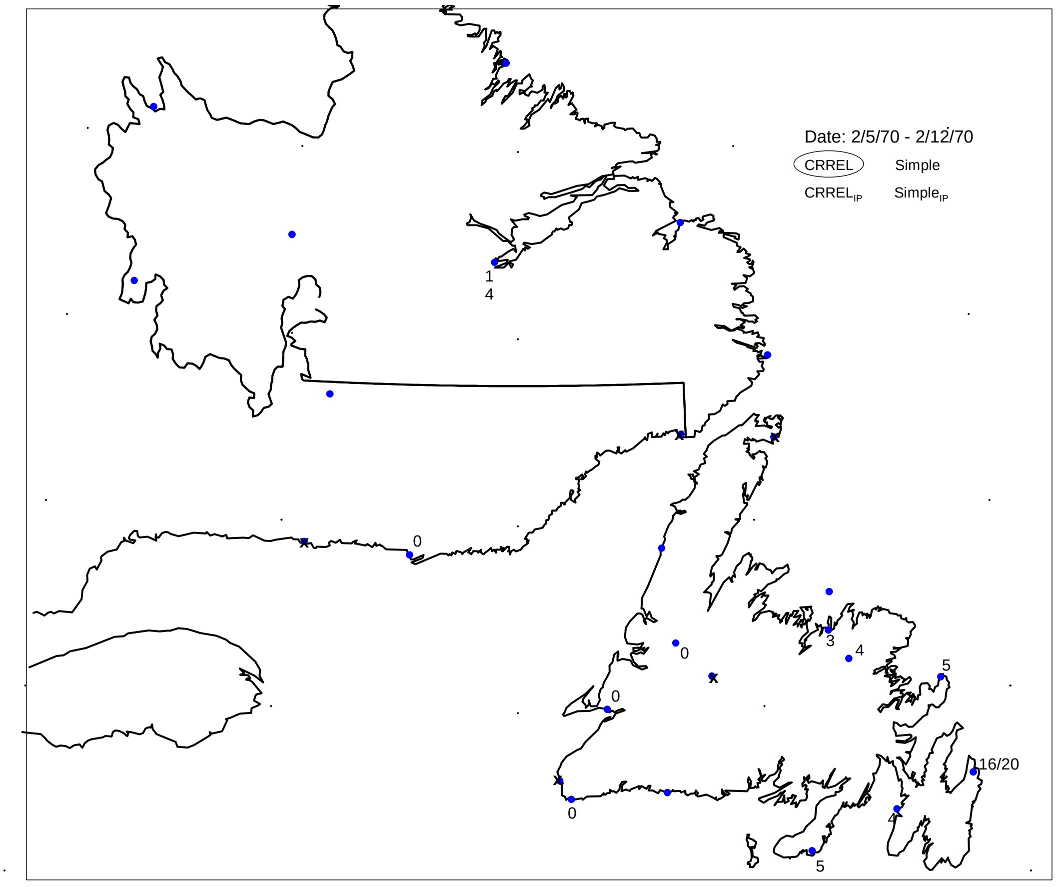
Date: 2/5/70 - 2/12/70
CRREL
Simple
CRELL$_{IP}$
Simple$_{IP}$
1
4
0
0
3
4
5
0
16/20
0
4
5


1

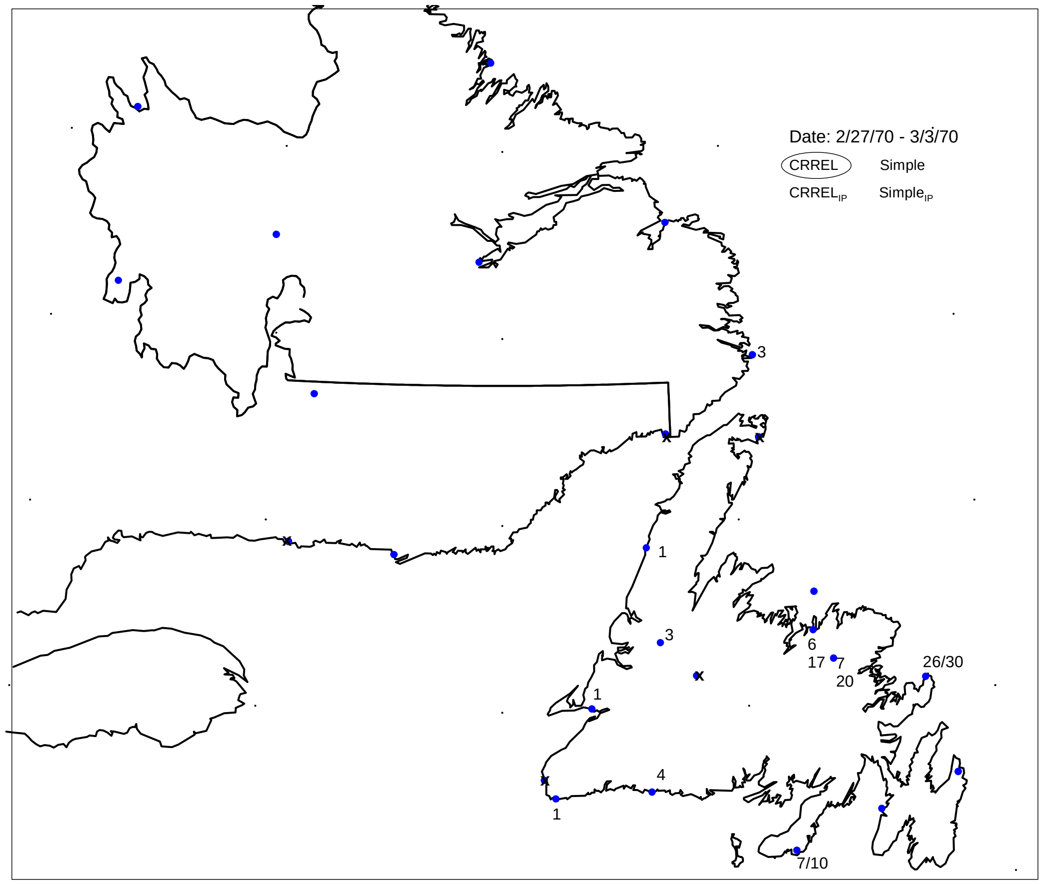
Date: 2/27/70 - 3/3/70
CRREL
Simple
$CRREL_{IP}$
$Simple_{IP}$
3
1
3
6
17
7
20
26/30
1
4
1
7/10

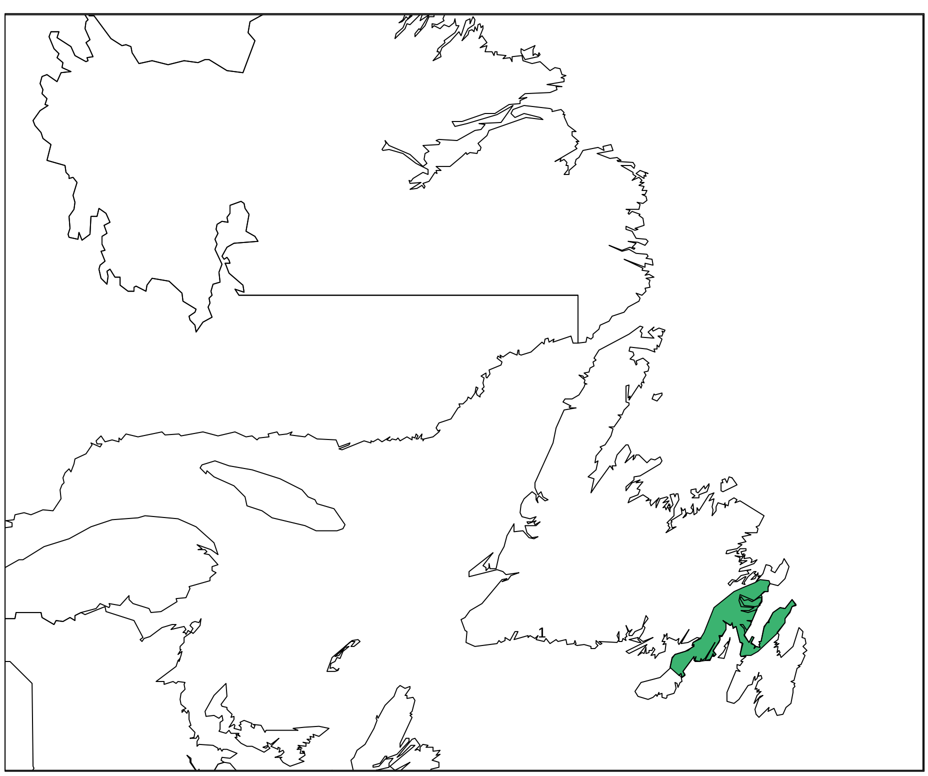
1

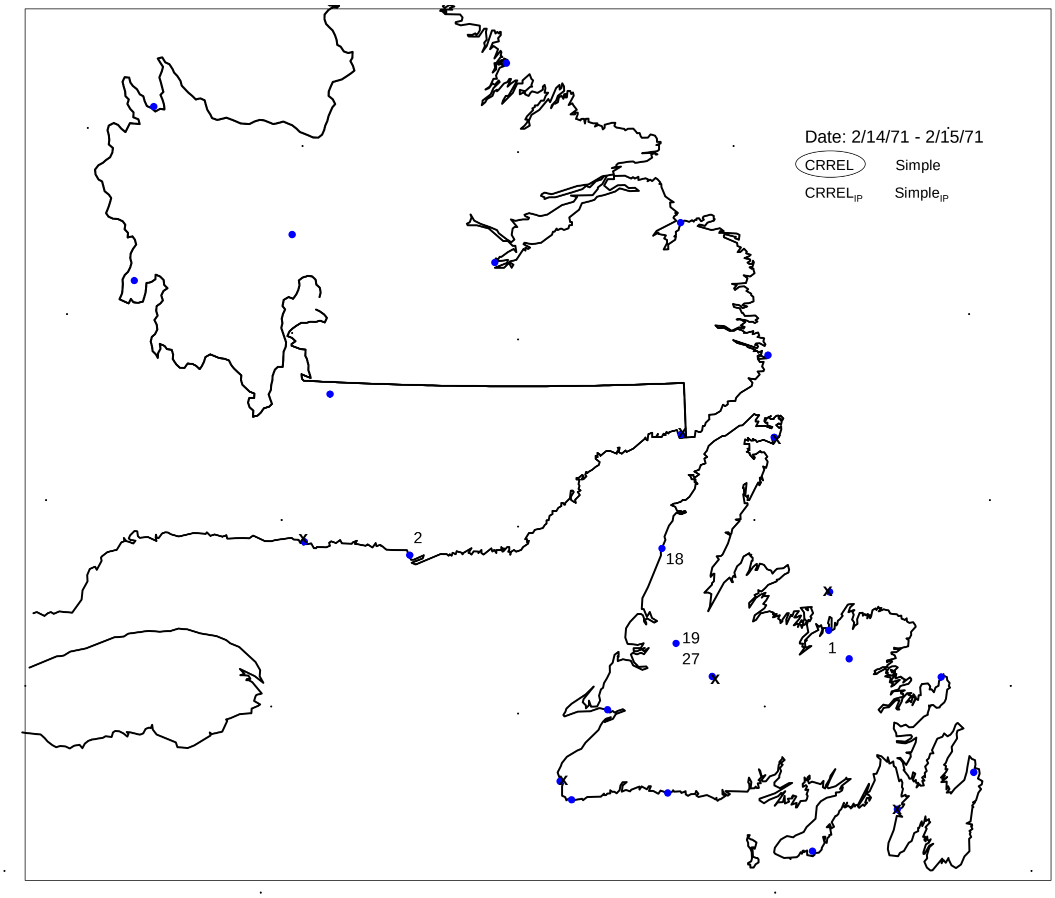
Date: 2/14/71 - 2/15/71
CRREL
Simple
$CRREL_{IP}$
$Simple_{IP}$
2
18
19
27
1

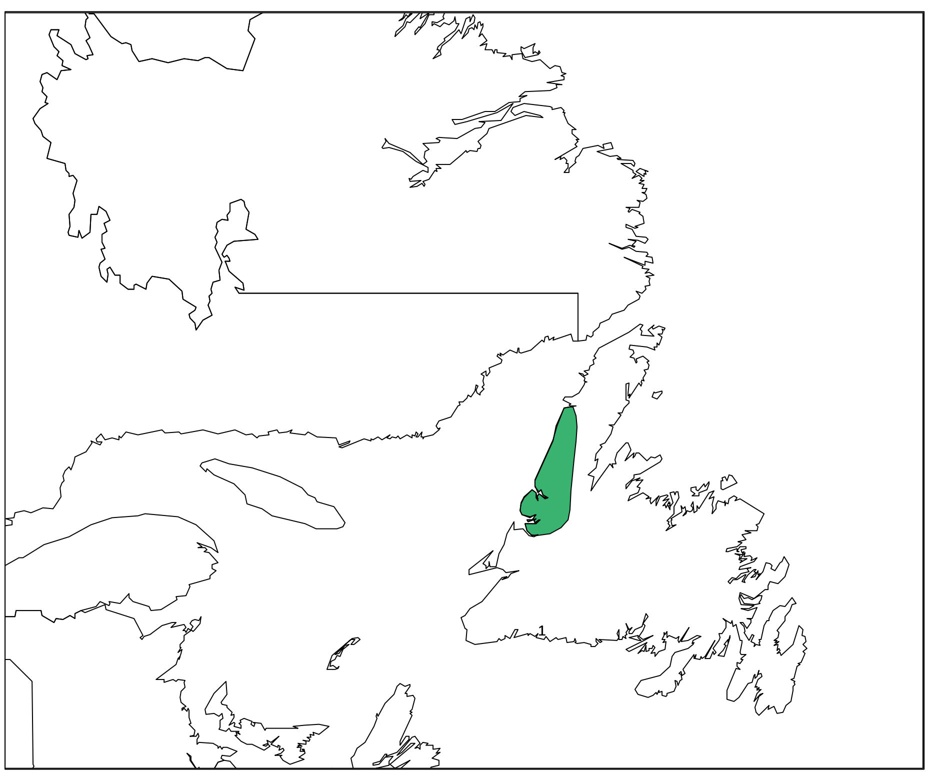
1

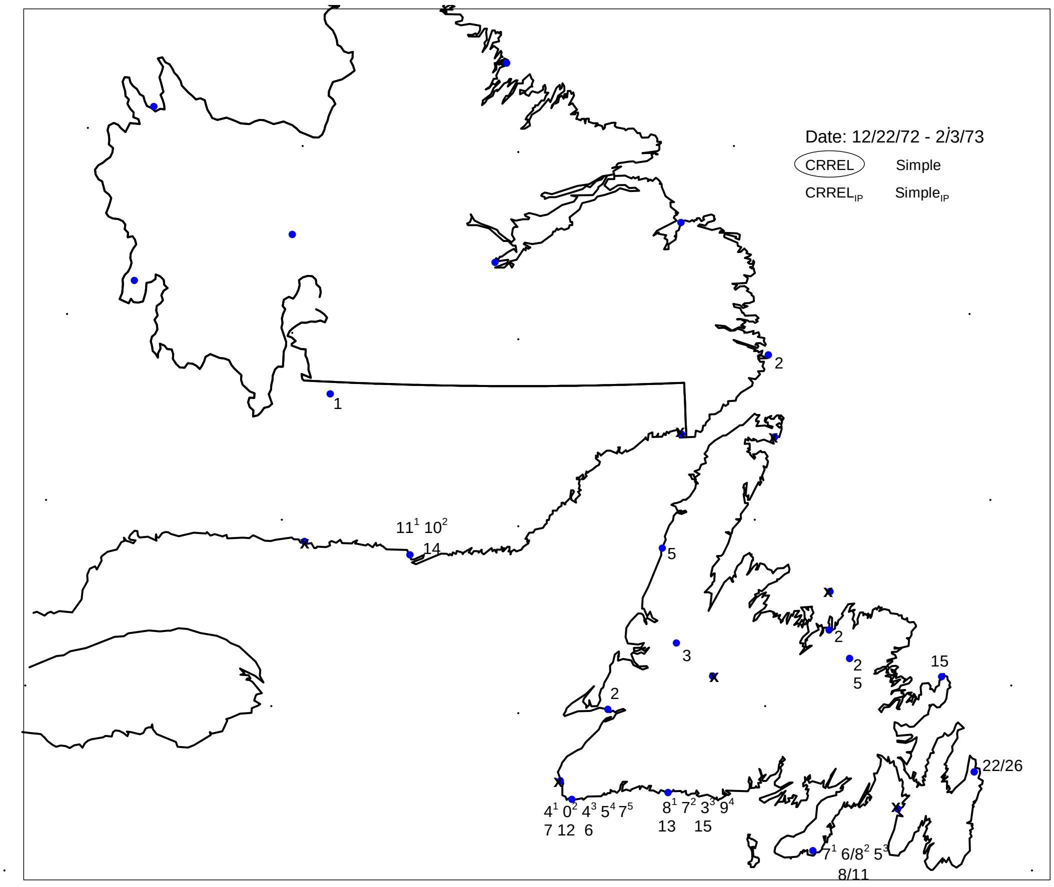
Date: 12/22/72 - 2/3/73
CRREL
Simple
CRELIP
SimpleIP
2
1
11¹ 10²
14
5
3
2
2
5
15
2
22/26
4¹ 0² 4³ 5⁴ 7⁵
7 12 6
8¹ 7² 3³ 9⁴
13 15
7¹ 6/8² 5³
8/11

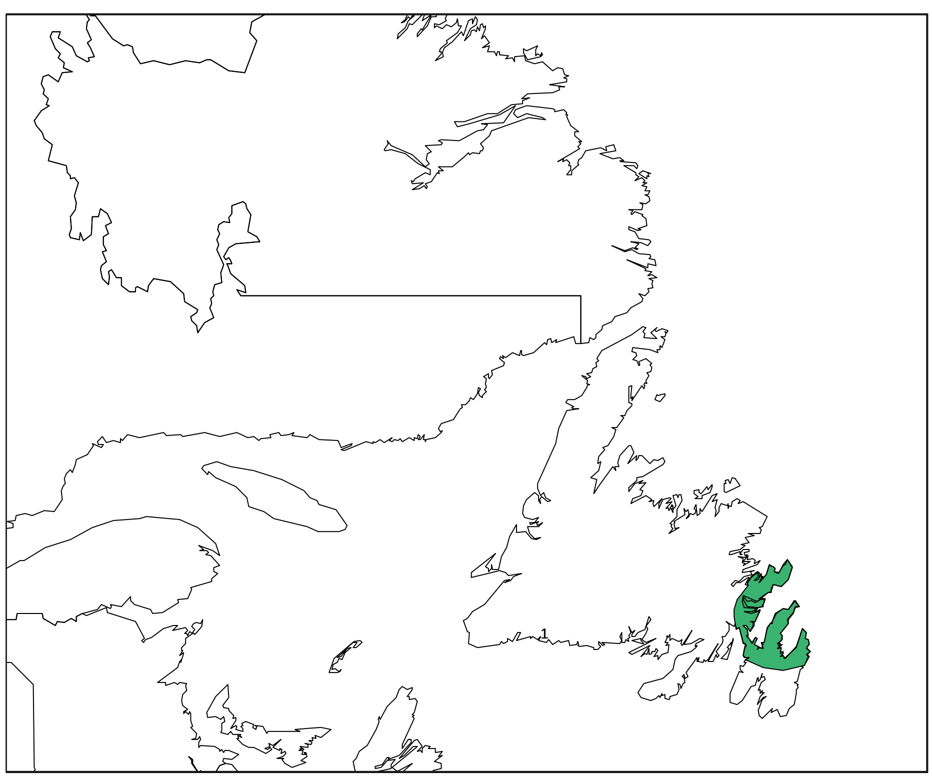
1

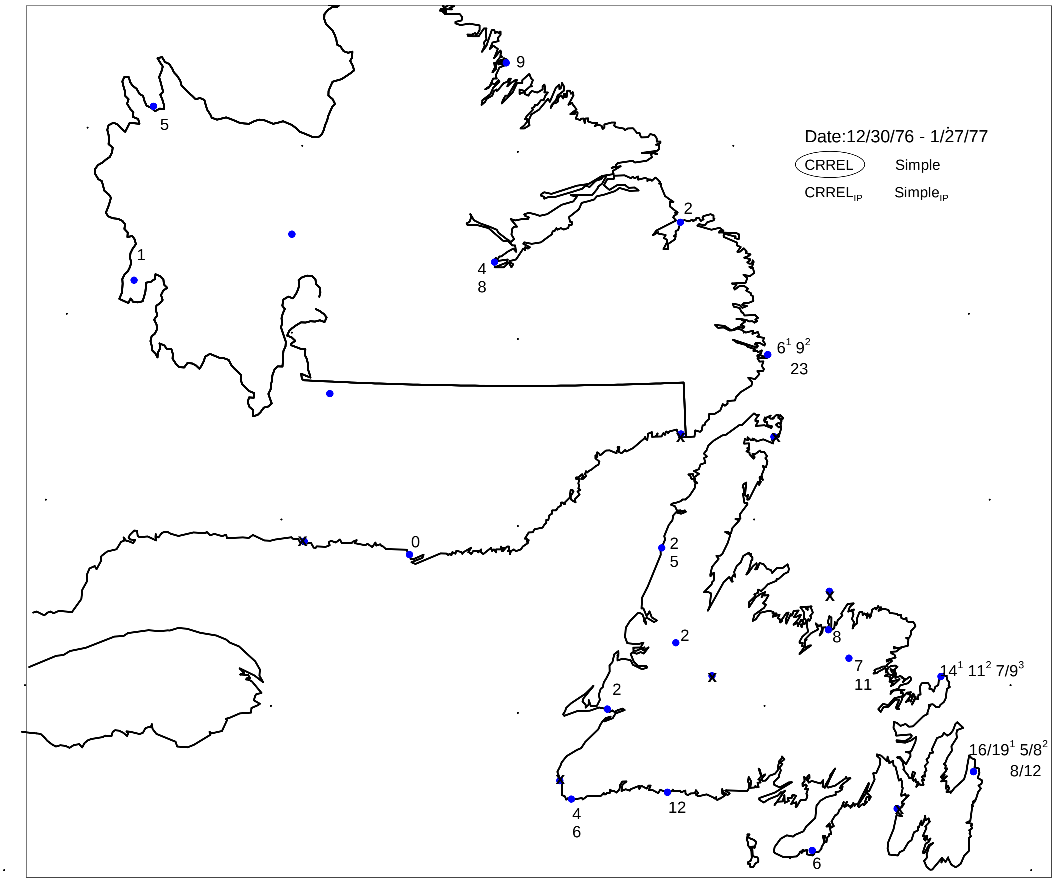
Date:12/30/76 - 1/27/77
CRREL
Simple
CRREL$_{IP}$
Simple$_{IP}$
9
5
1
2
4
8
6[1] 9[2]
23
0
2
5
2
8
7
11
14[1] 11[2] 7/9[3]
2
16/19[1] 5/8[2]
8/12
4
6
12
6

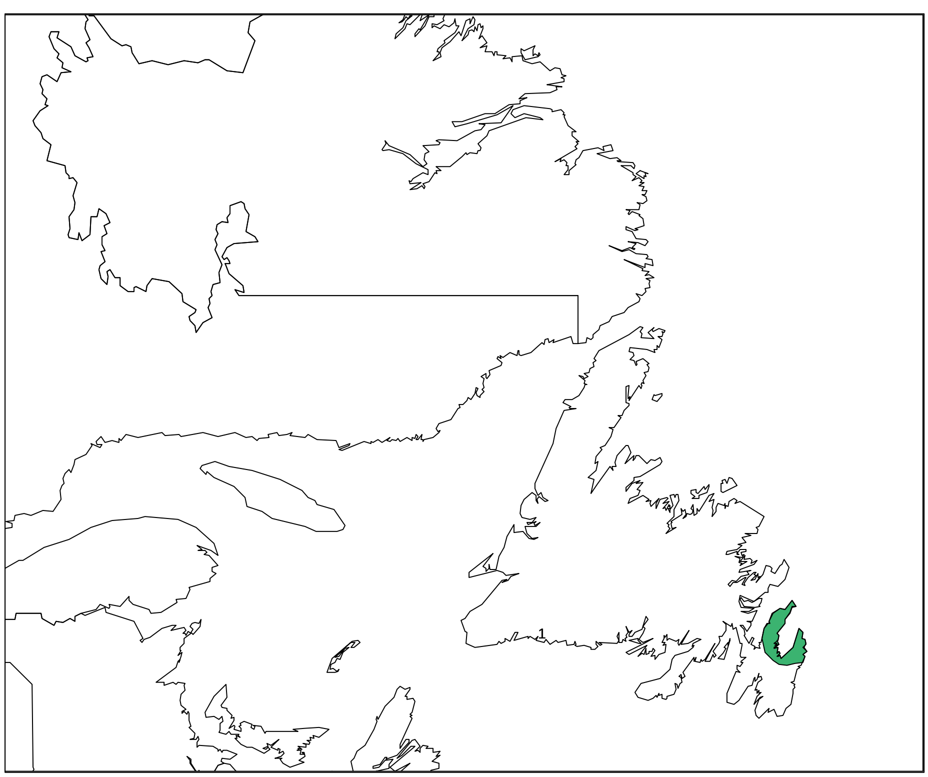

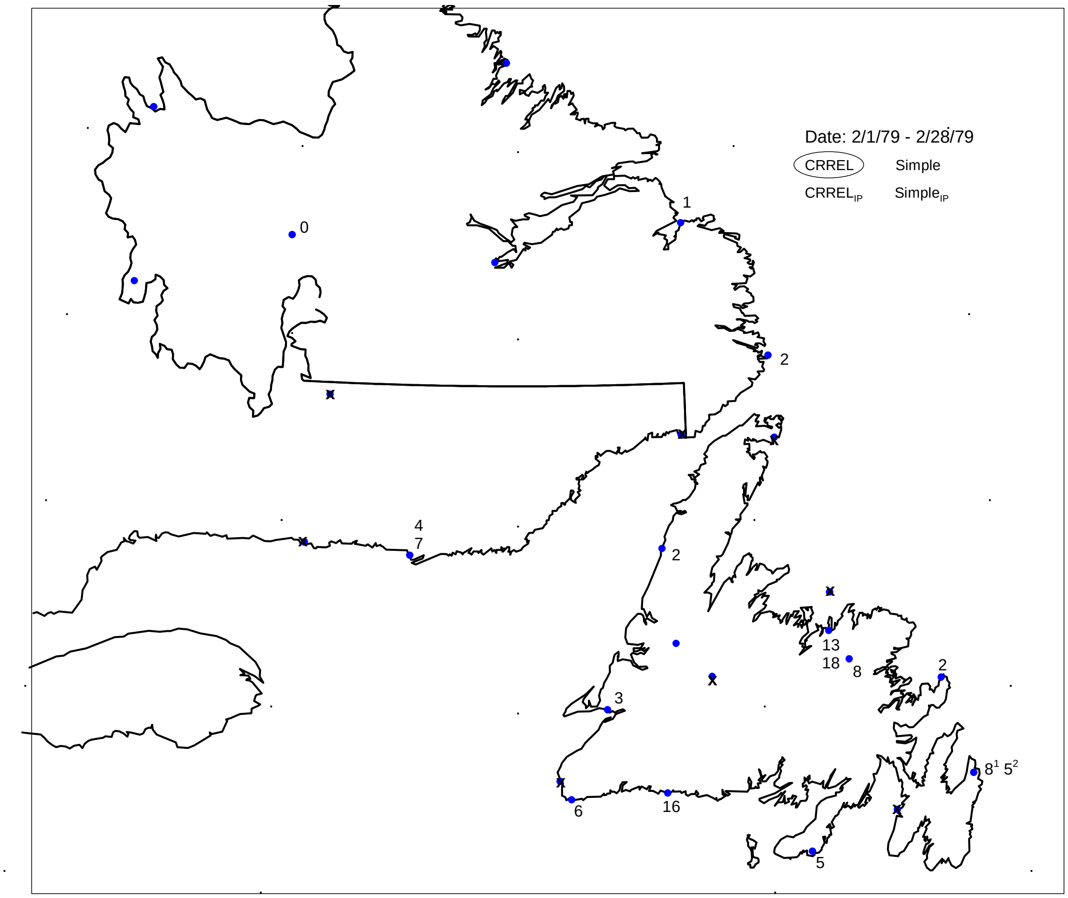
Date: 2/1/79 - 2/28/79
CRREL
Simple
CRREL_IP
Simple_IP
0
1
2
4
7
2
13
18
8
2
3
6
16
5
8^1 5^2

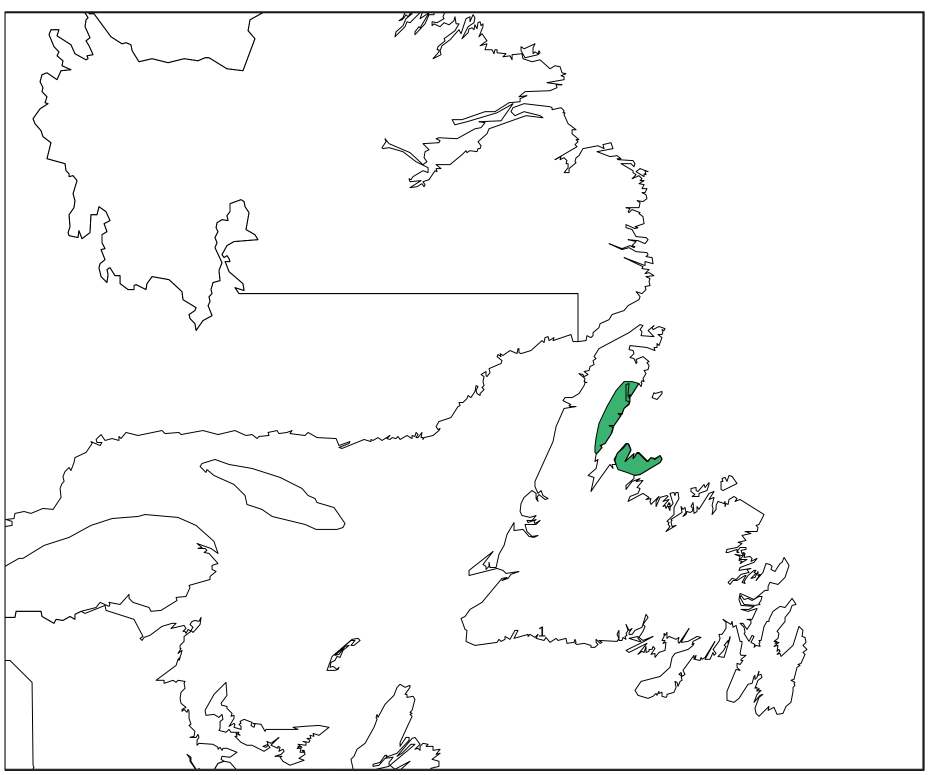
1

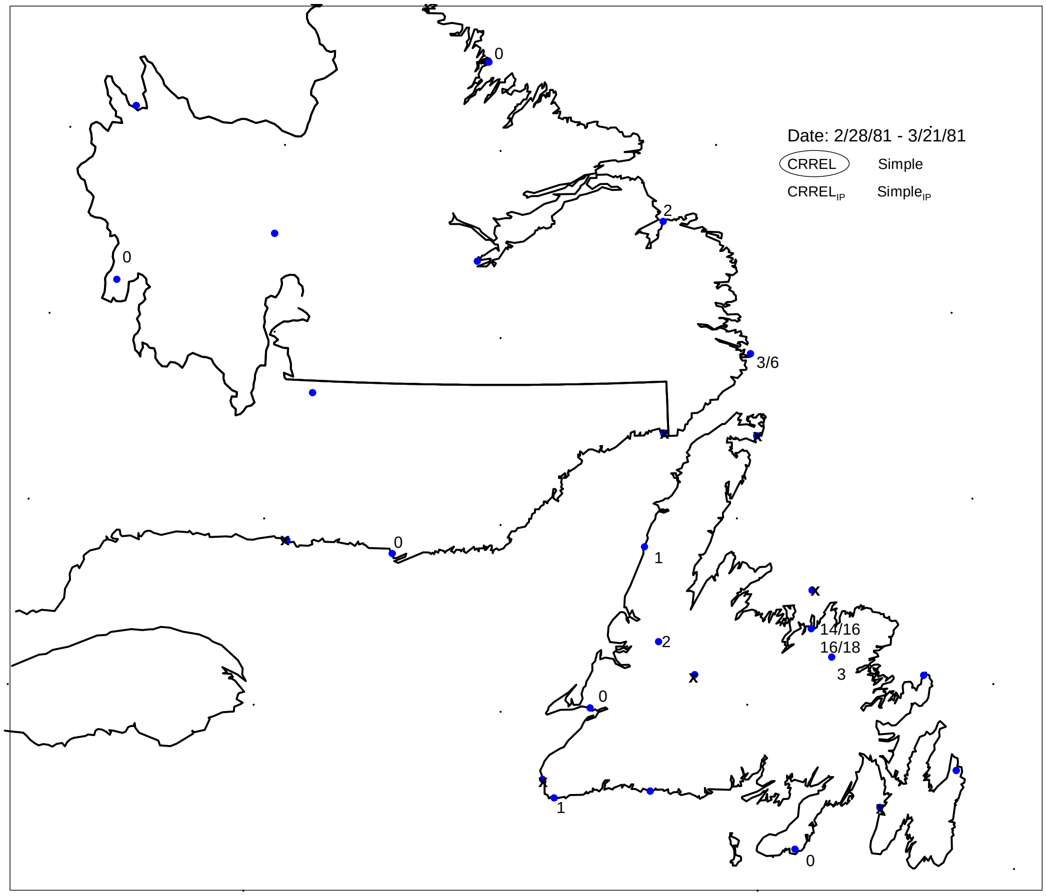
Date: 2/28/81 - 3/21/81
CRREL
Simple
$CRREL_{IP}$
$Simple_{IP}$
0
0
2
3/6
0
1
14/16
16/18
2
3
0
1
0


1

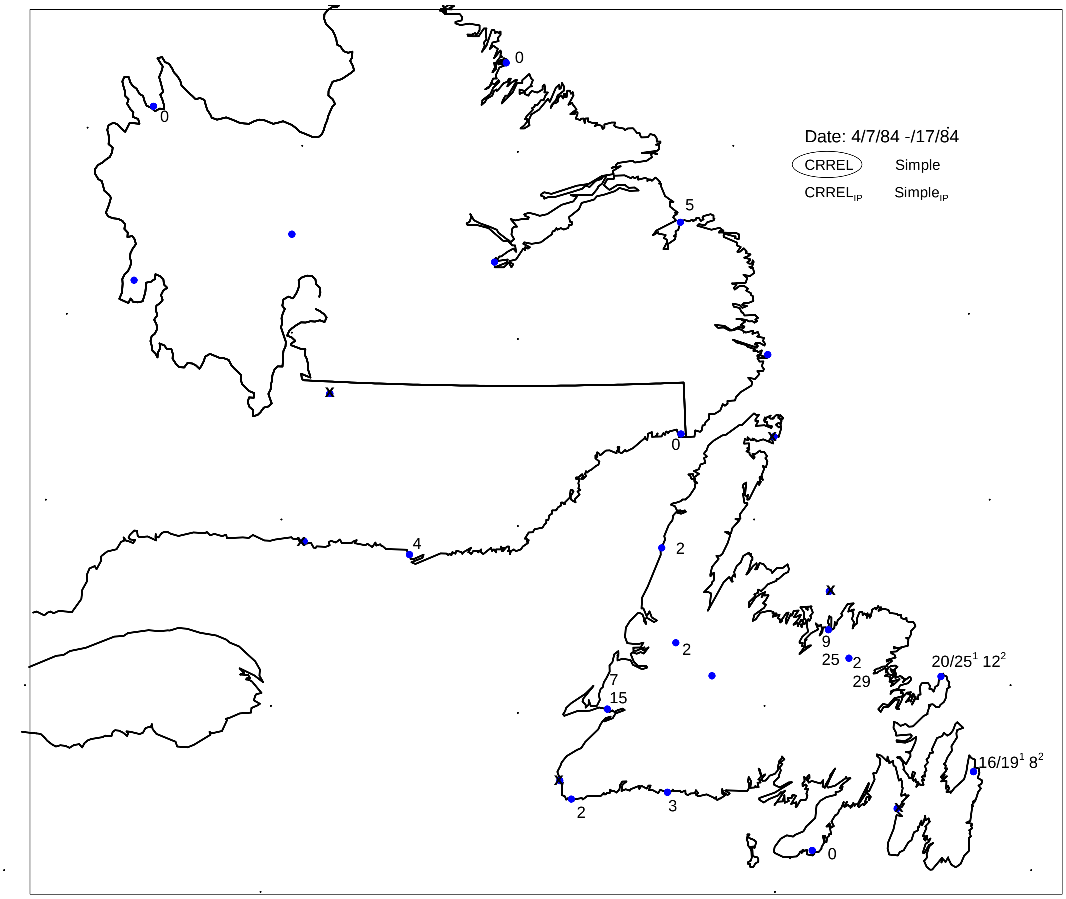
Date: 4/7/84 -/17/84
CRREL
Simple
CRELIP
SimpleIP
0
0
5
0
4
2
2
9
25
2
29
20/25[1] 12[2]
7
15
16/19[1] 8[2]
2
3
0

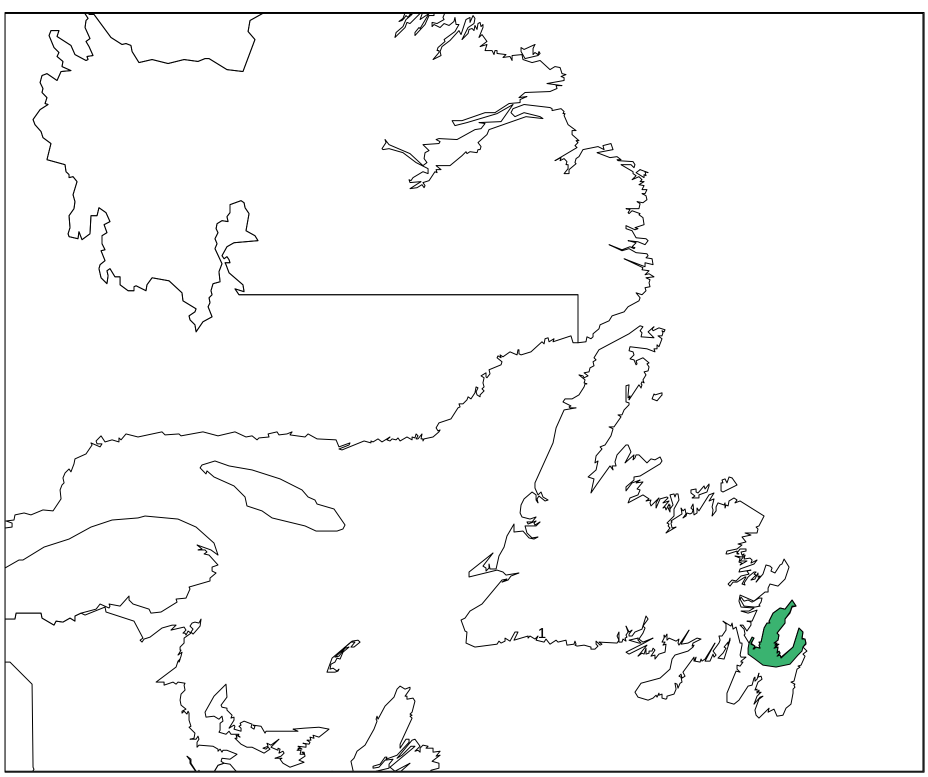
1

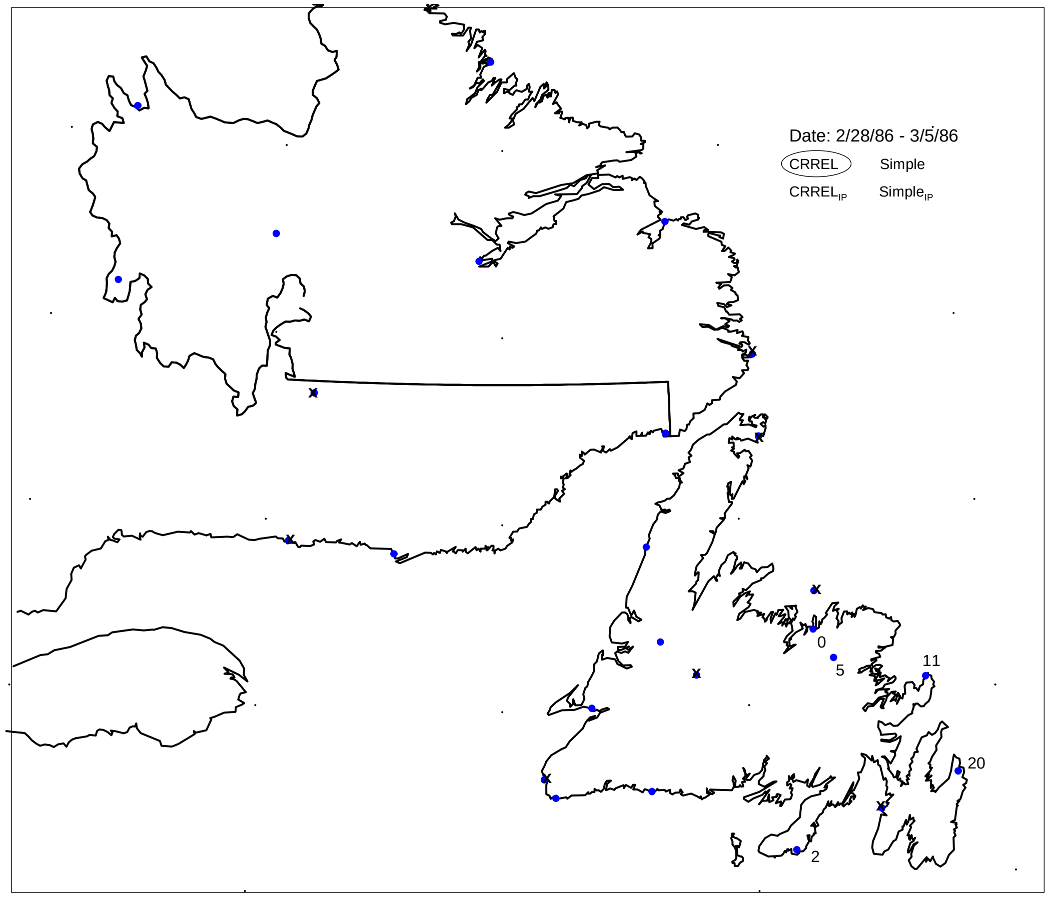
Date: 2/28/86 - 3/5/86
CRREL
Simple
CRREL$_{IP}$
Simple$_{IP}$
0
5
11
20
2

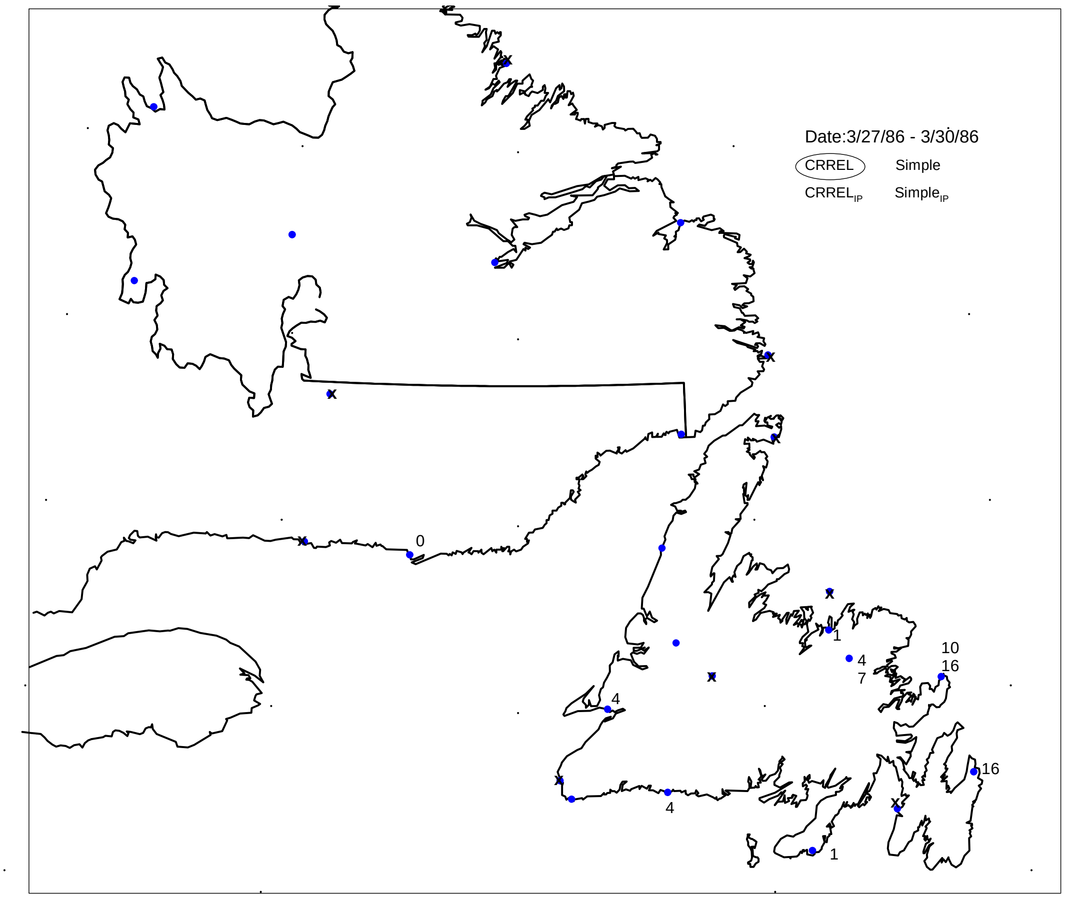
Date:3/27/86 - 3/30/86
CRREL
Simple
CRREL$_{IP}$
Simple$_{IP}$
0
1
4
7
10
16
4
4
16
1


1

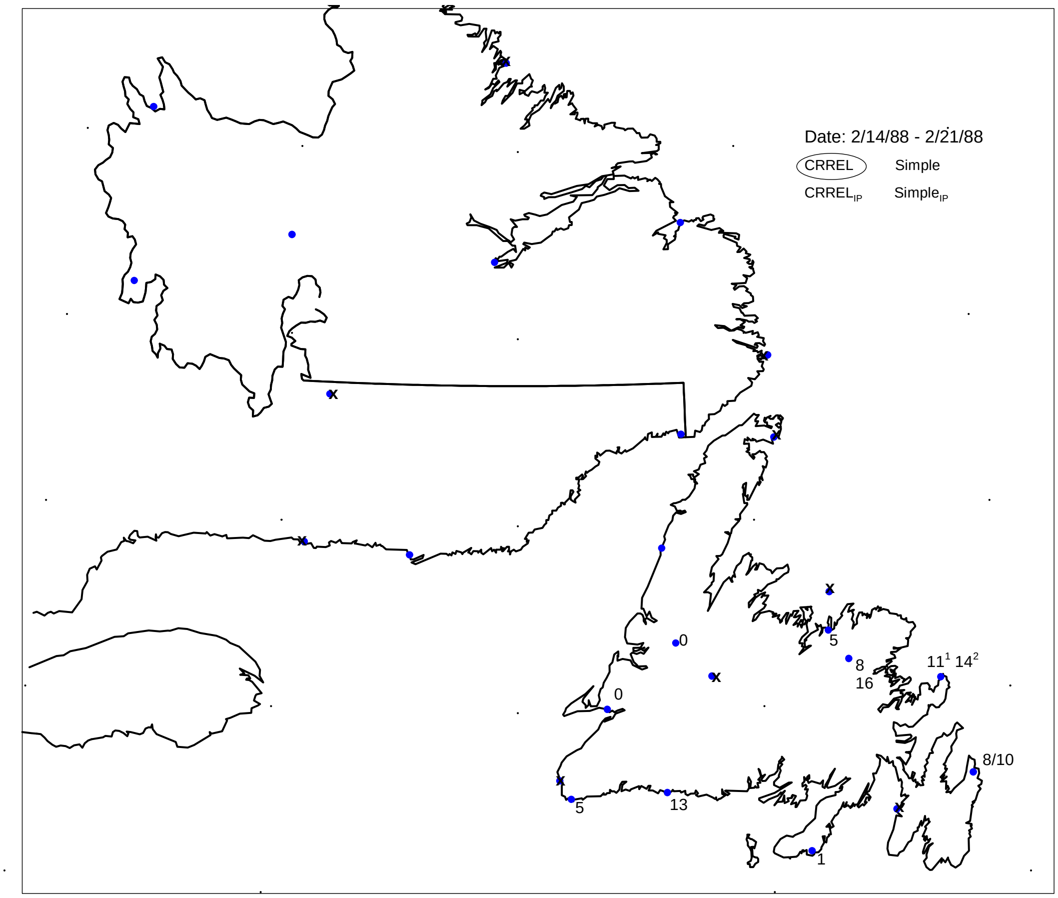
Date: 2/14/88 - 2/21/88
CRREL
Simple
CRREL_IP
Simple_IP
0
5
8
16
11¹ 14²
0
8/10
5
13
1

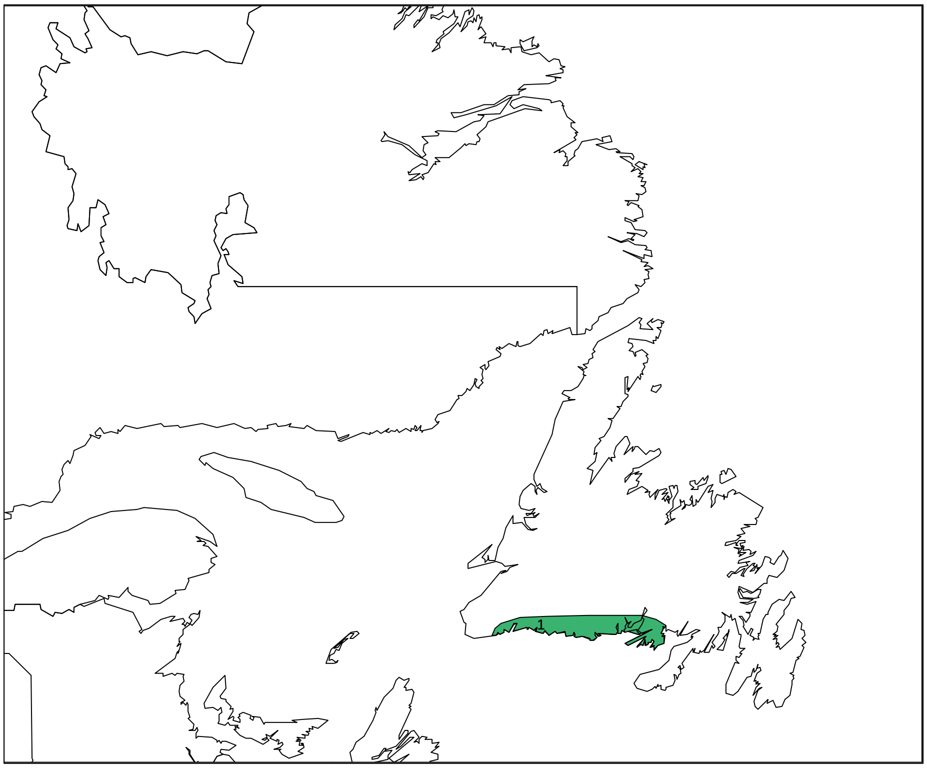
1

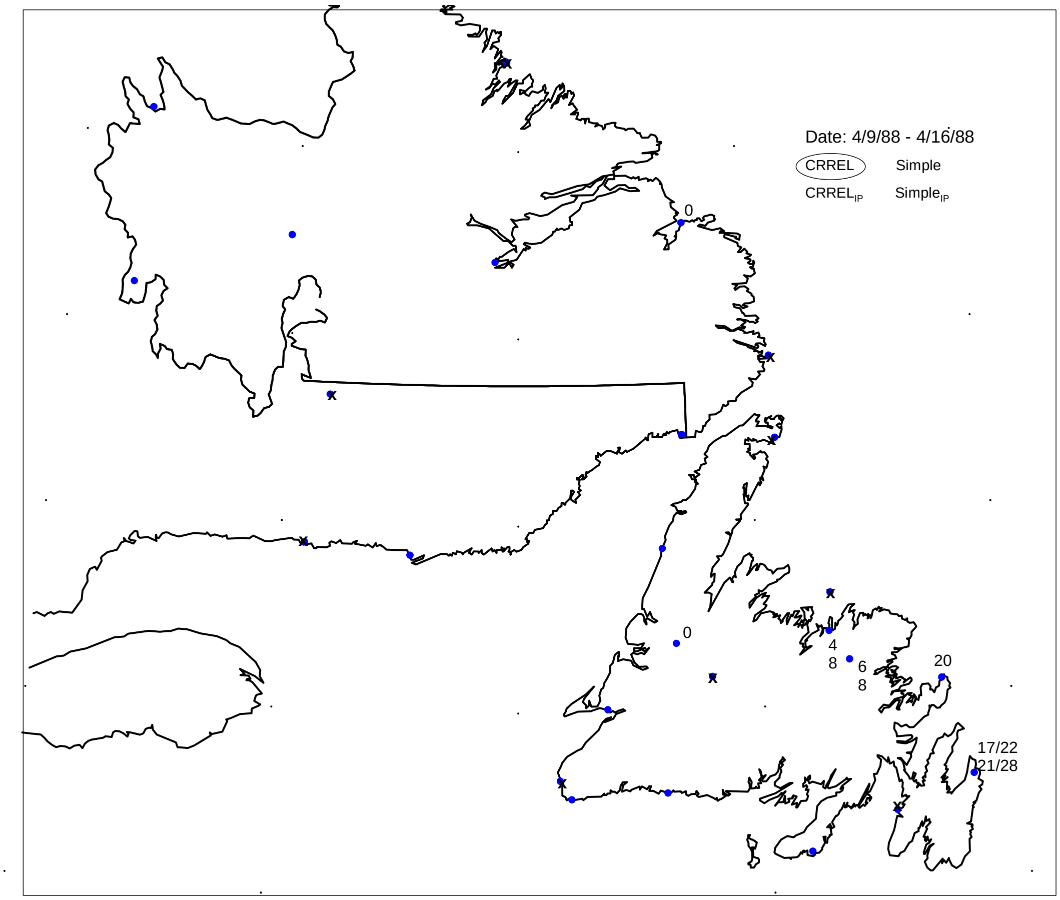
Date: 4/9/88 - 4/16/88
CRREL
Simple
$CRREL_{IP}$
$Simple_{IP}$
0
0
4
8
6
8
20
17/22
21/28


1

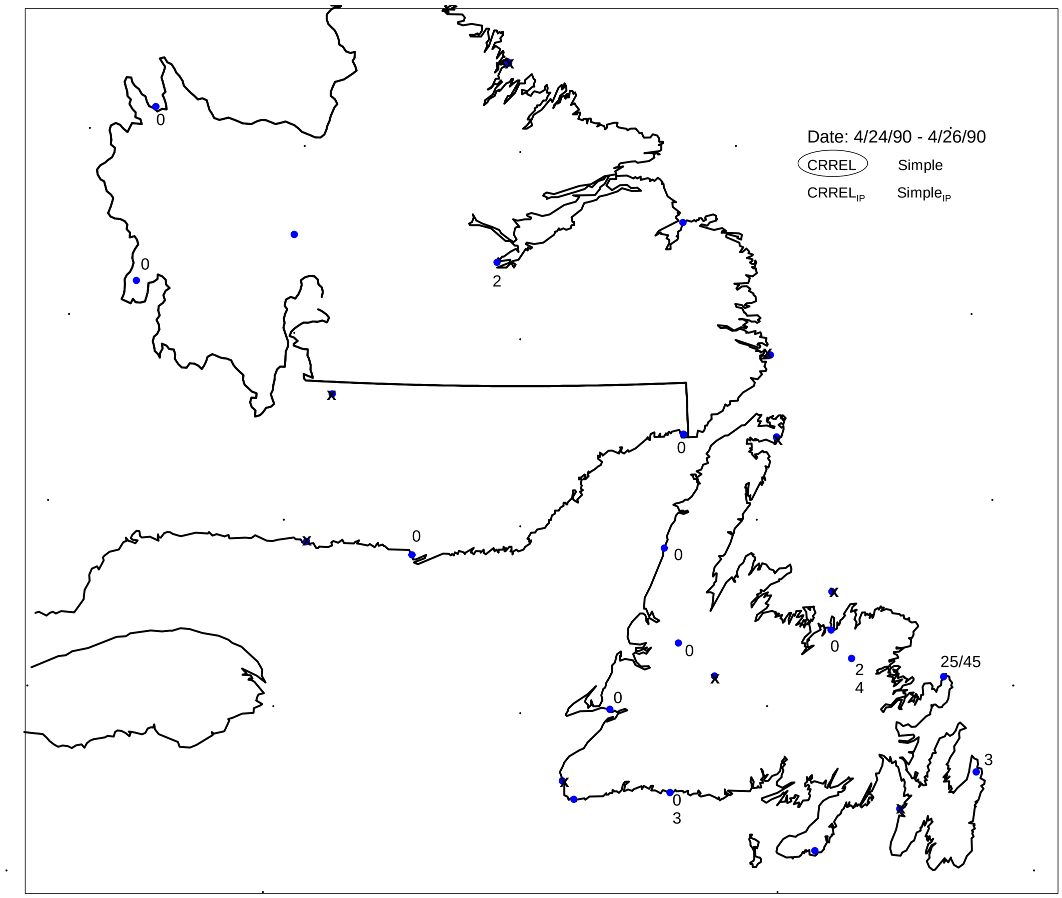
Date: 4/24/90 - 4/26/90
CRREL
Simple
CRELIP
SimpleIP
0
0
2
0
0
0
0
0
2
4
25/45
0
3
0
3

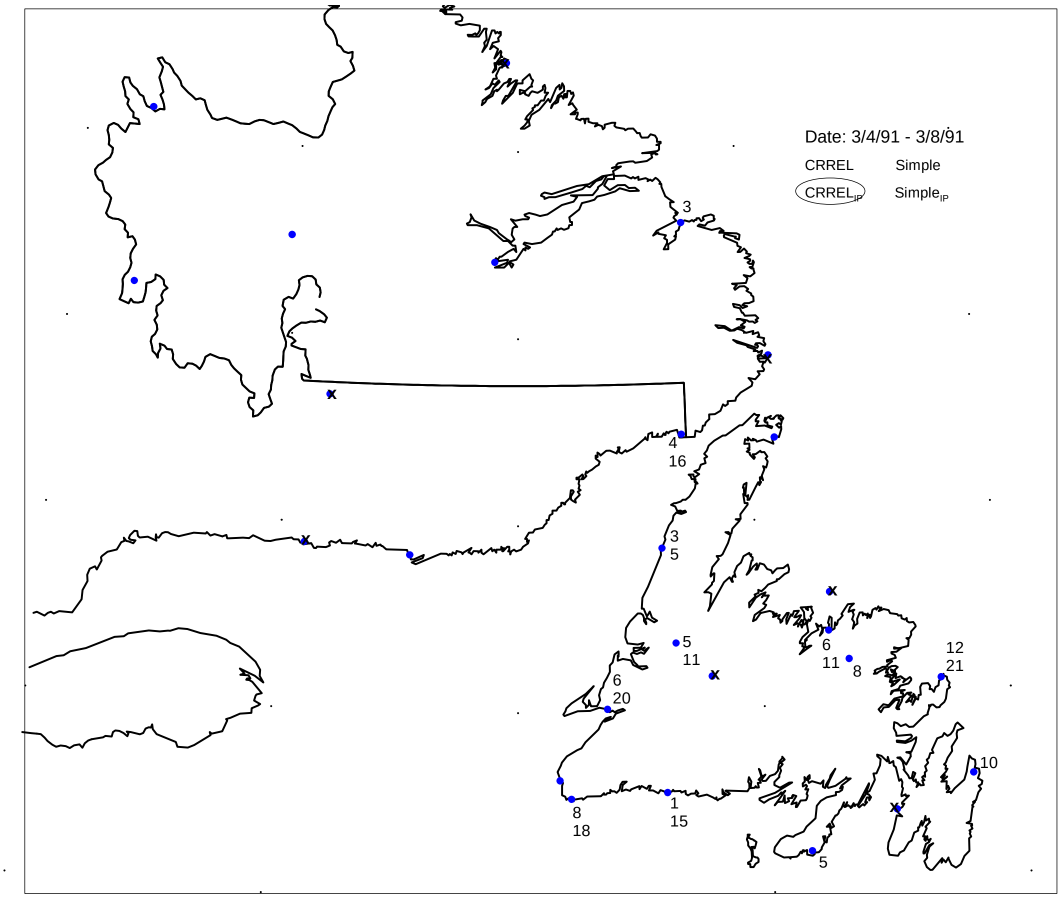
Date: 3/4/91 - 3/8/91
CRREL
Simple
CRREL$_{IP}$
Simple$_{IP}$
3
4
16
3
5
5
11
6
11
8
12
21
6
20
10
8
18
1
15
5


1

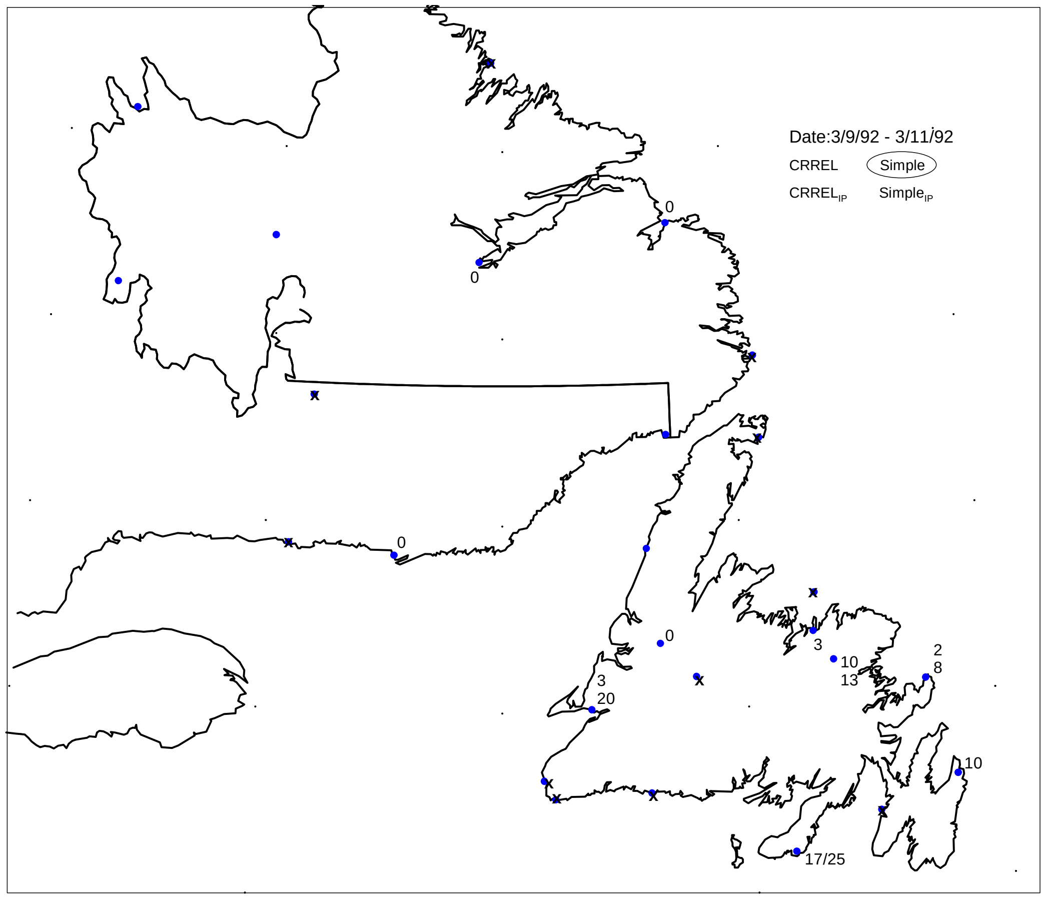
Date:3/9/92 - 3/11/92
CRREL
Simple
CRREL$_{IP}$
Simple$_{IP}$
0
0
0
0
3
10
13
2
8
3
20
10
17/25

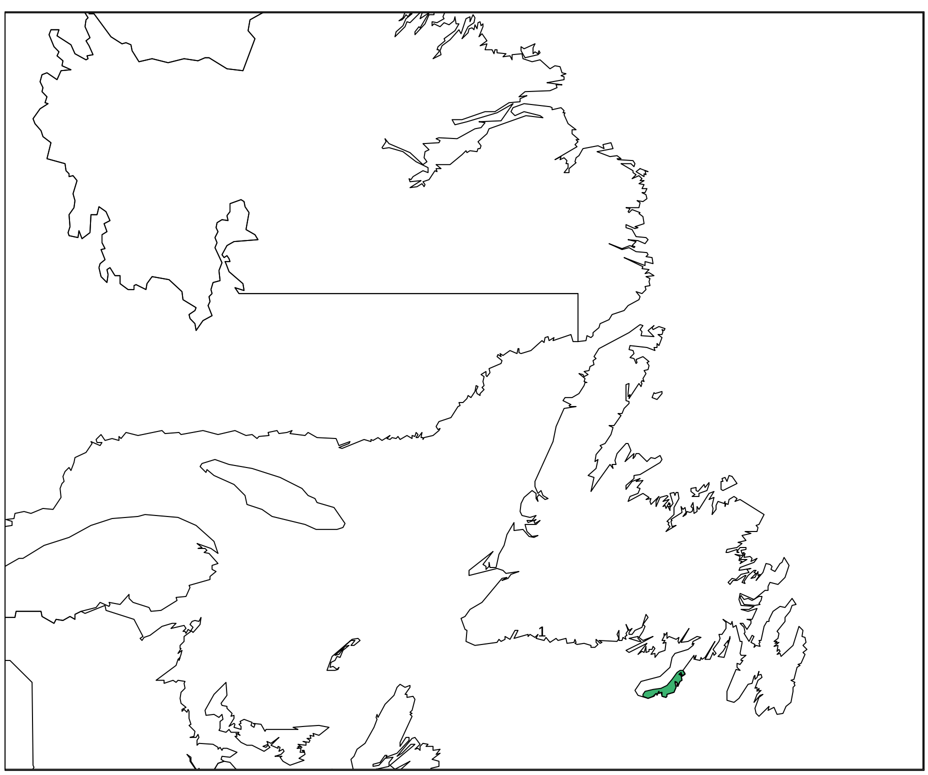
1

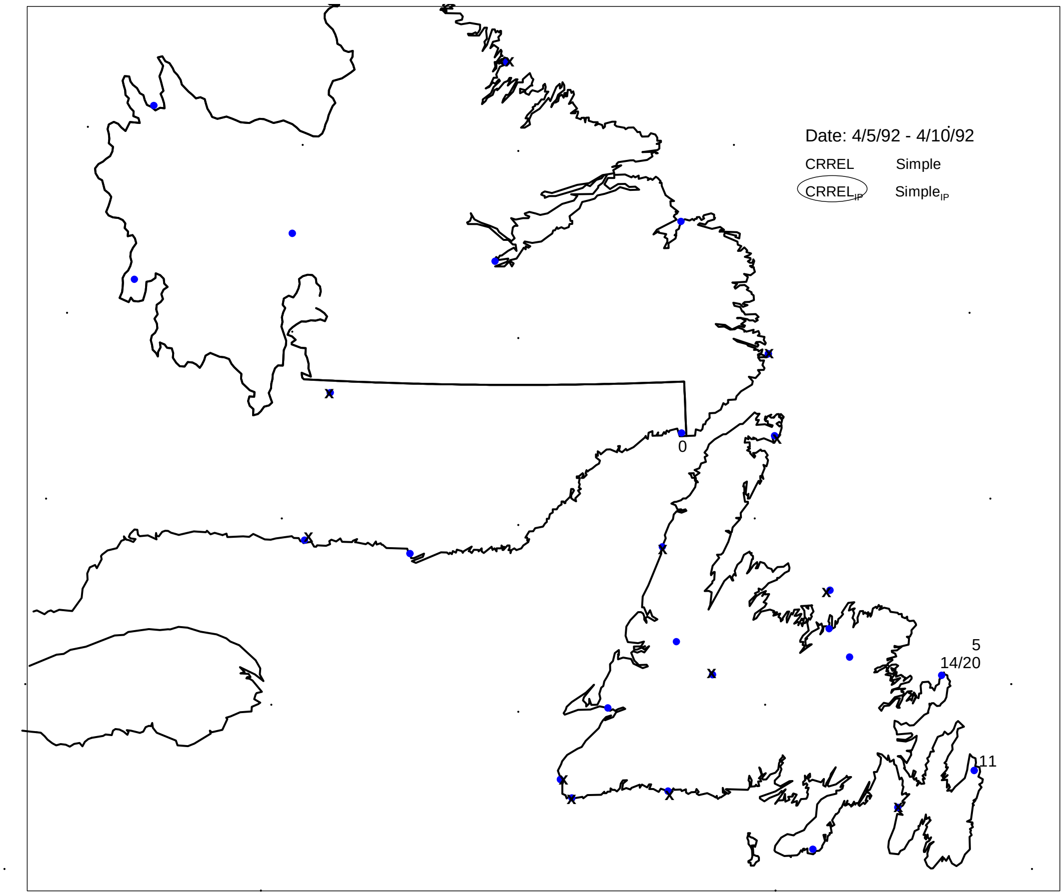
Date: 4/5/92 - 4/10/92
CRREL
Simple
CRREL$_{IP}$
Simple$_{IP}$
0
5
14/20
11


1

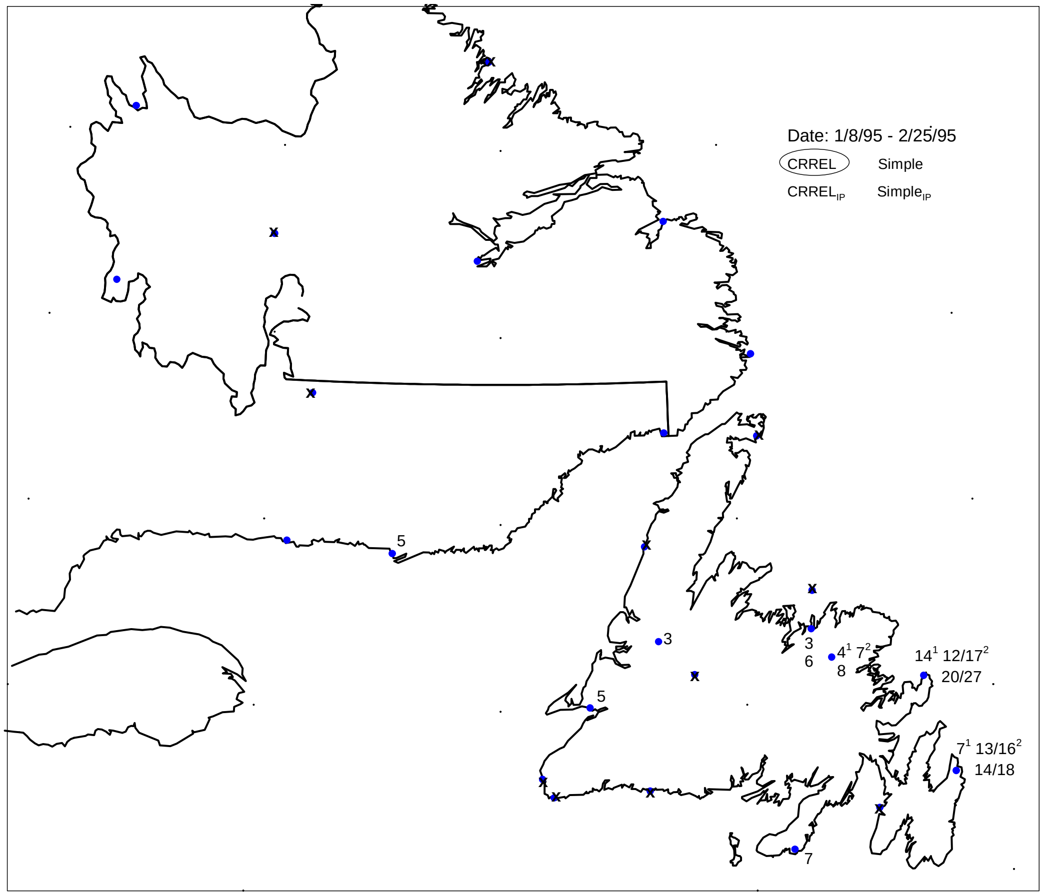
Date: 1/8/95 - 2/25/95
CRREL
Simple
CRREL_IP
Simple_IP
5
3
5
3
6
4¹ 7²
8
14¹ 12/17²
20/27
7¹ 13/16²
14/18
7

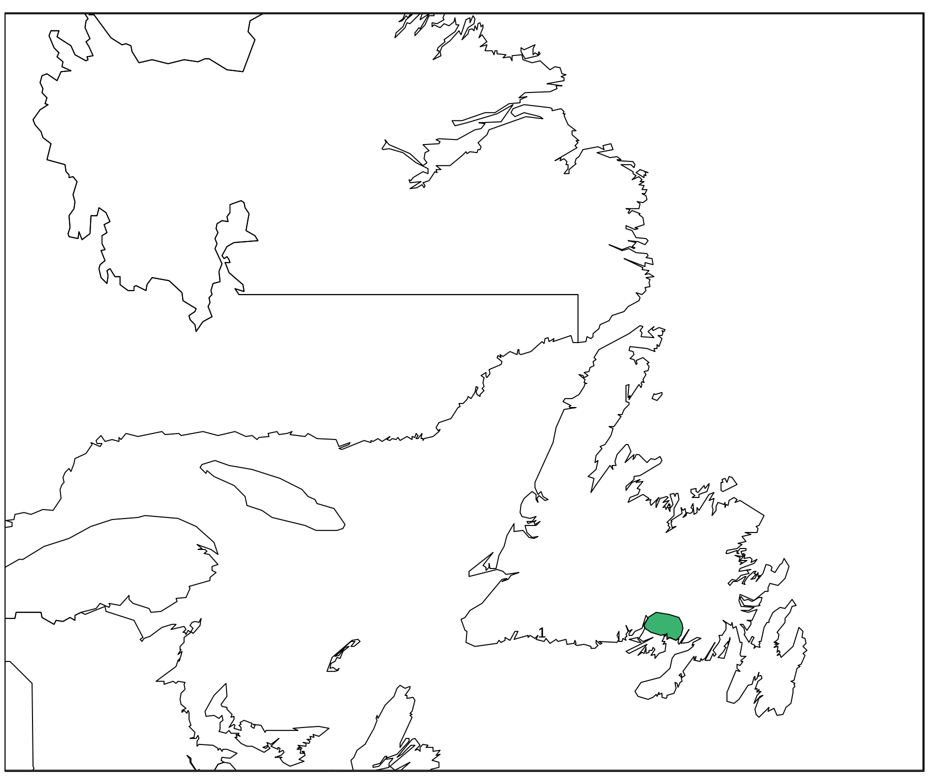
1

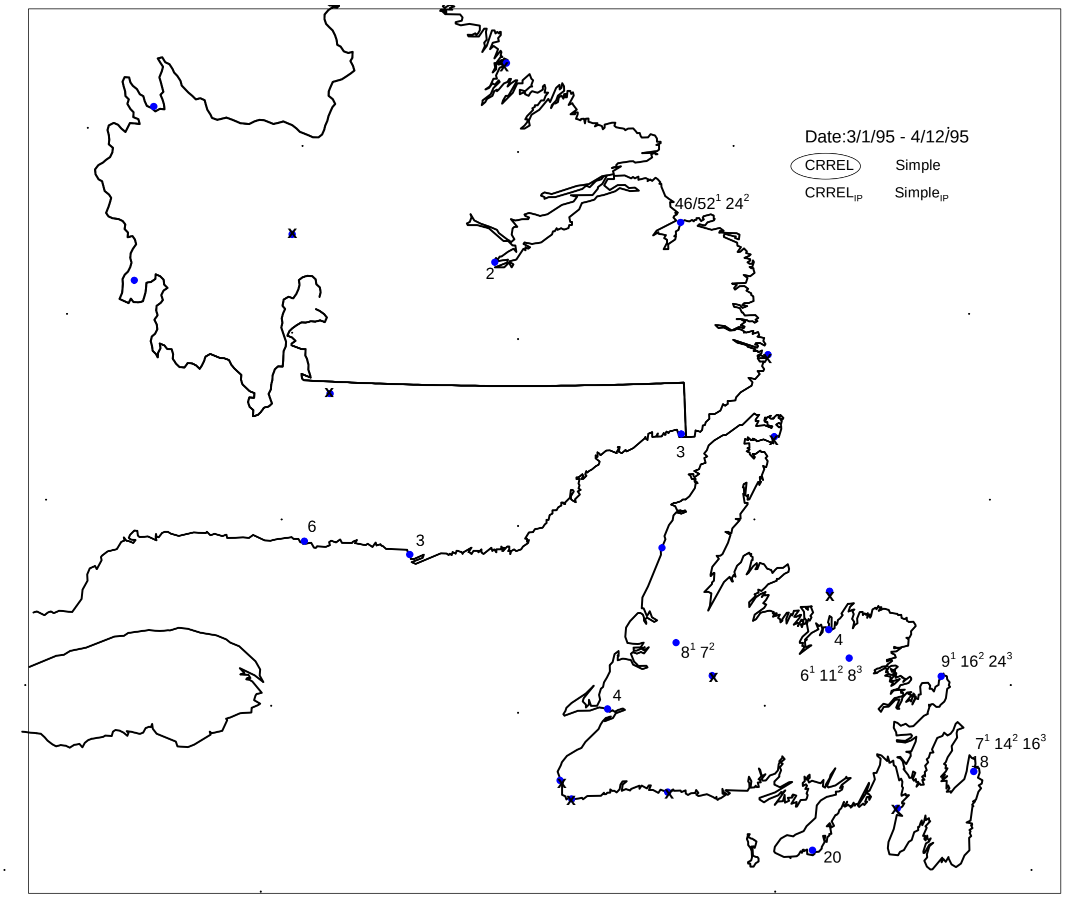
Date:3/1/95 - 4/12/95
CRREL
Simple
CRELIP
SimpleIP
46/52¹ 24²
2
3
6
3
8¹ 7²
4
6¹ 11² 8³
9¹ 16² 24³
4
7¹ 14² 16³
8
20


1

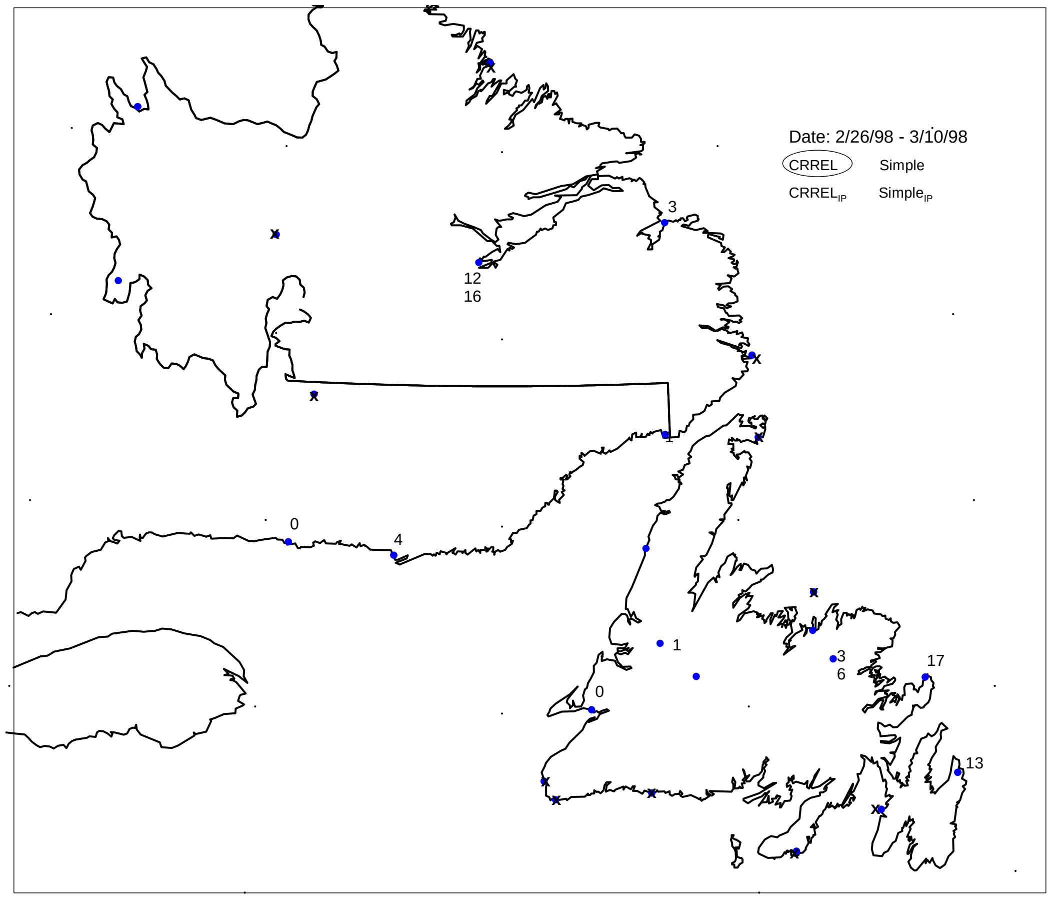
Date: 2/26/98 - 3/10/98
CRREL
Simple
CRELIP
SimpleIP
3
12
16
0
4
1
1
3
6
17
0
13

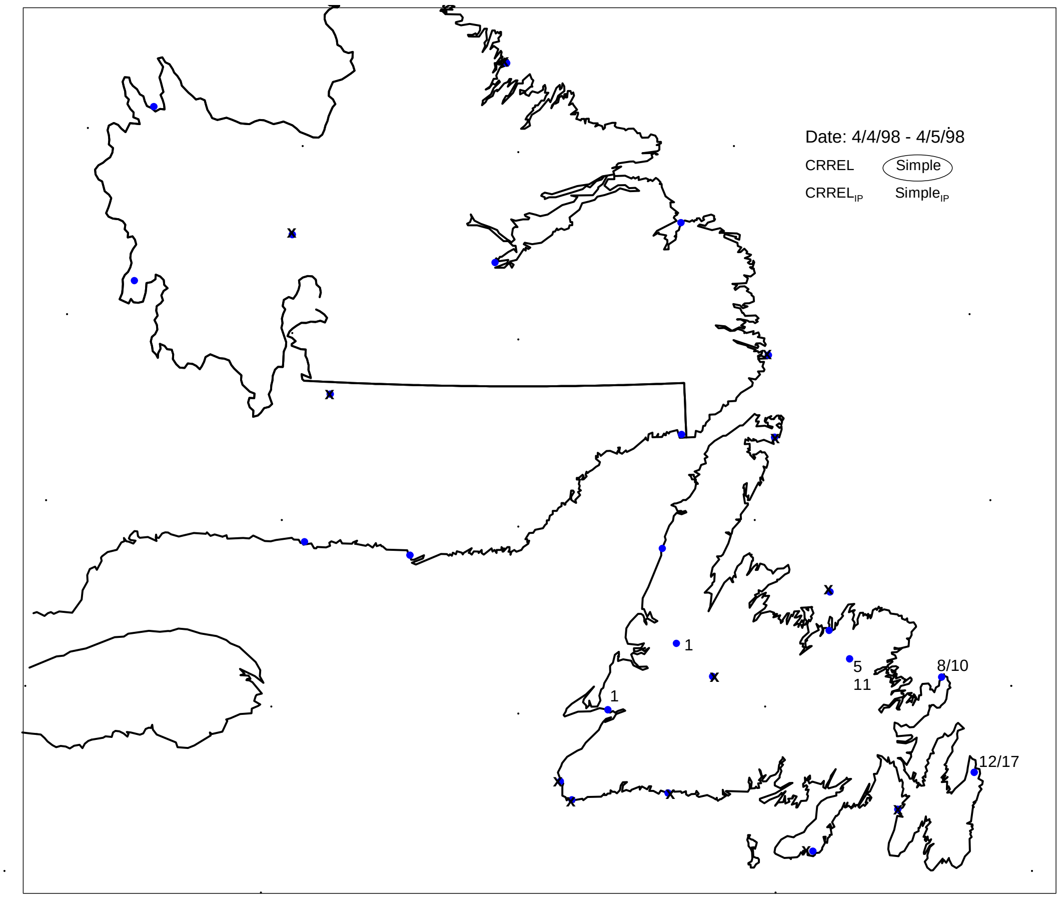
Date: 4/4/98 - 4/5/98
CRREL
Simple
CRELIP
SimpleIP
1
1
5
11
8/10
12/17

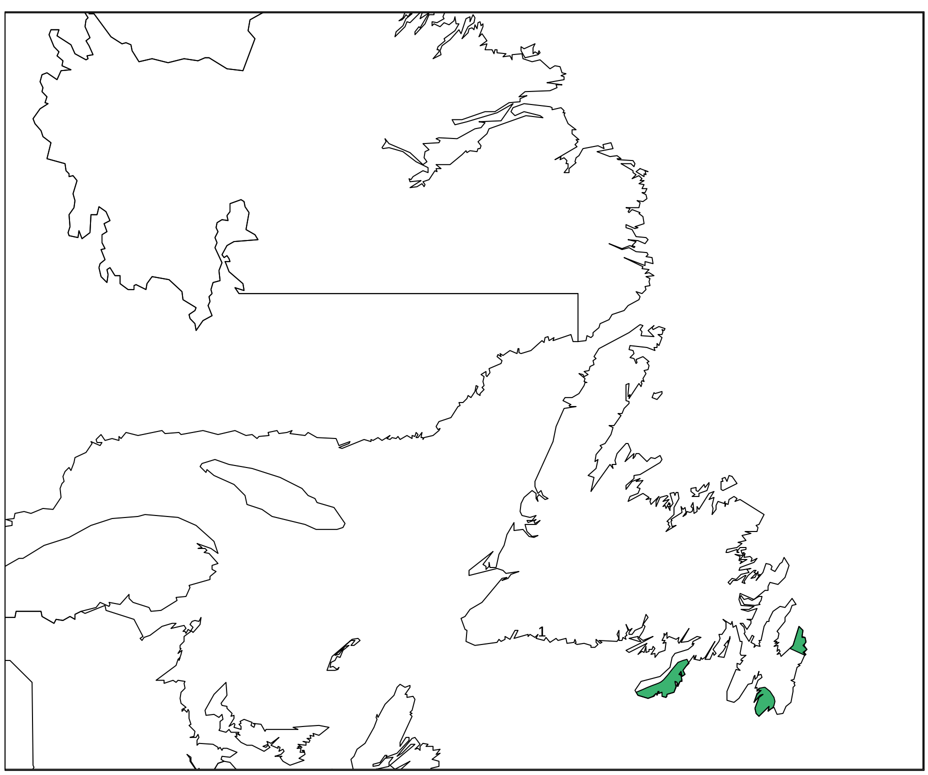
1

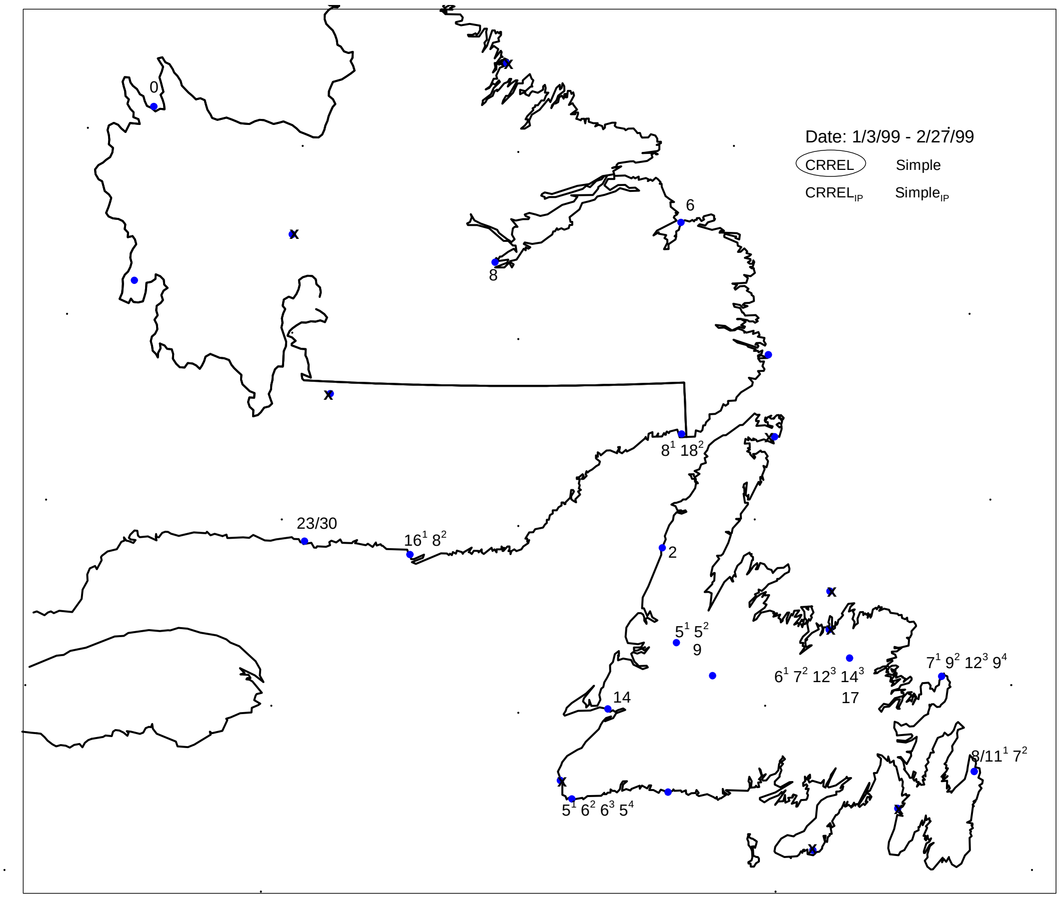
Date: 1/3/99 - 2/27/99
CRREL
Simple
CRELIP
SimpleIP
0
6
8
8¹ 18²
23/30
16¹ 8²
2
5¹ 5²
9
6¹ 7² 12³ 14³
17
7¹ 9² 12³ 9⁴
14
8/11¹ 7²
5¹ 6² 6³ 5⁴

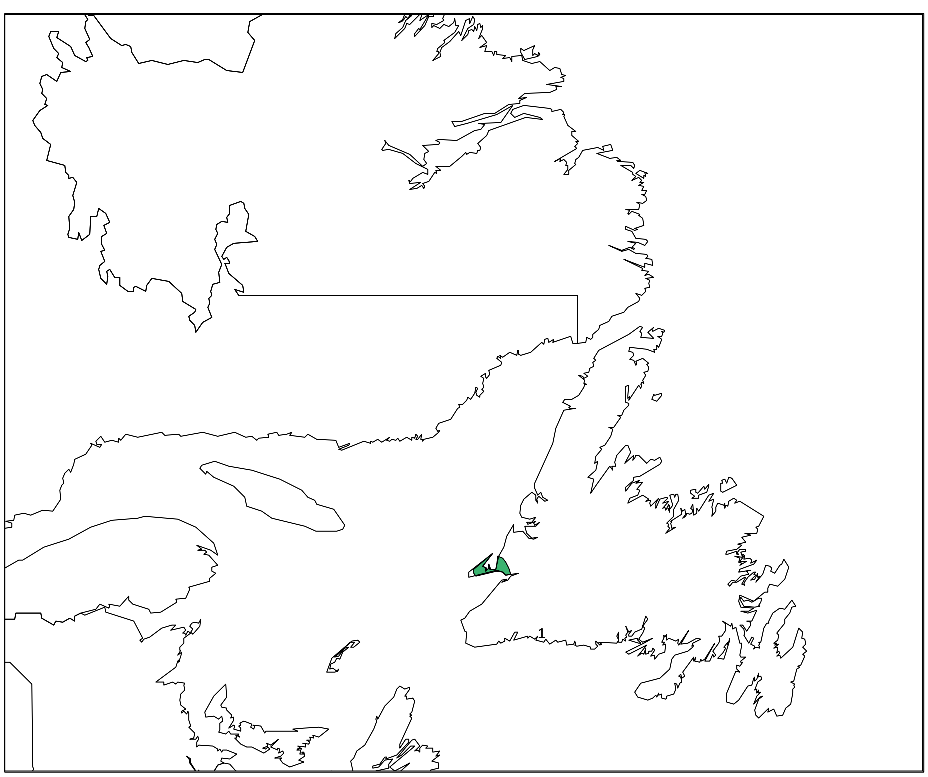

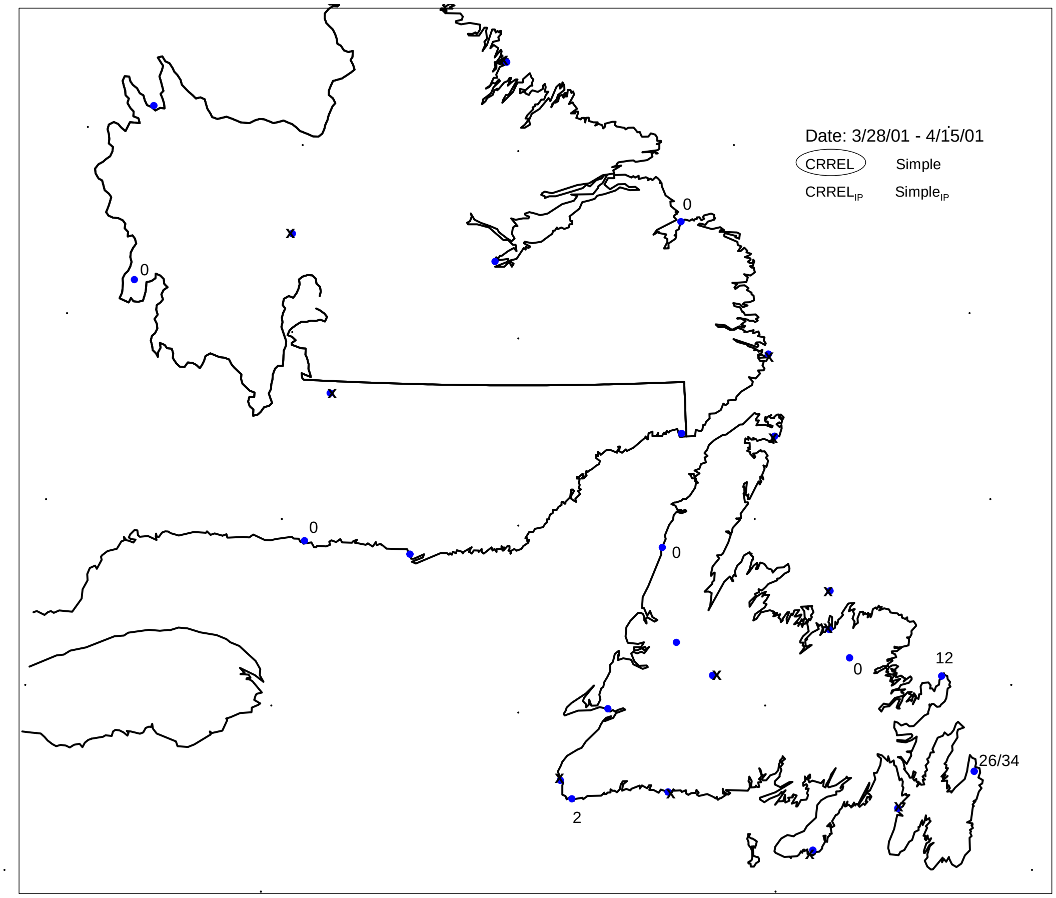
Date: 3/28/01 - 4/15/01
CRREL
Simple
$CRREL_{IP}$
$Simple_{IP}$
0
0
0
0
0
12
26/34
2

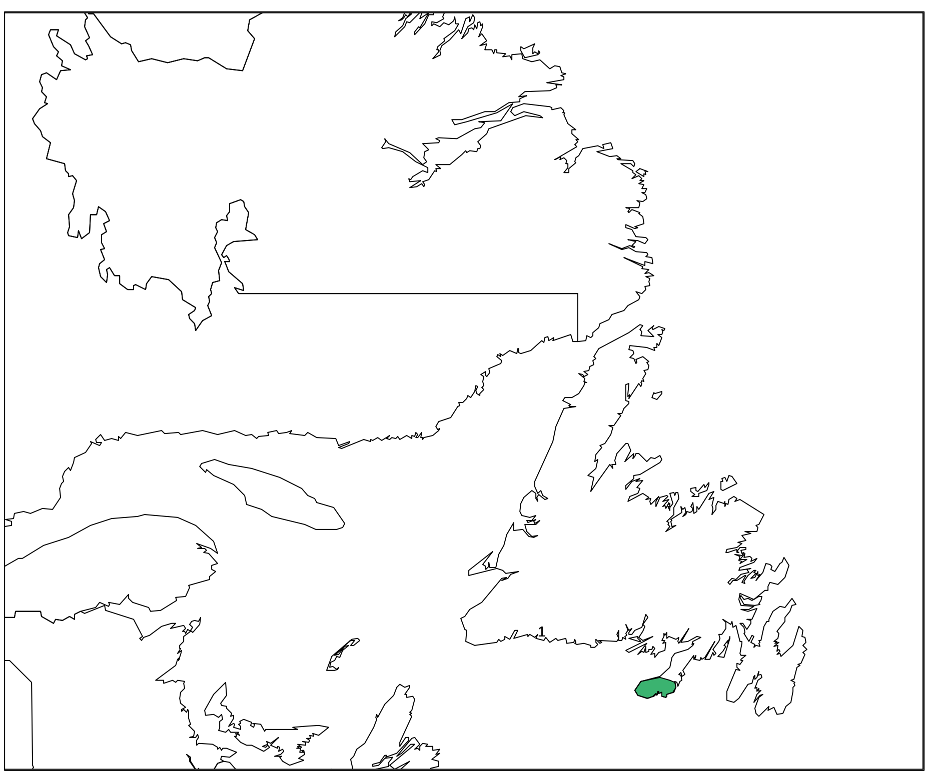

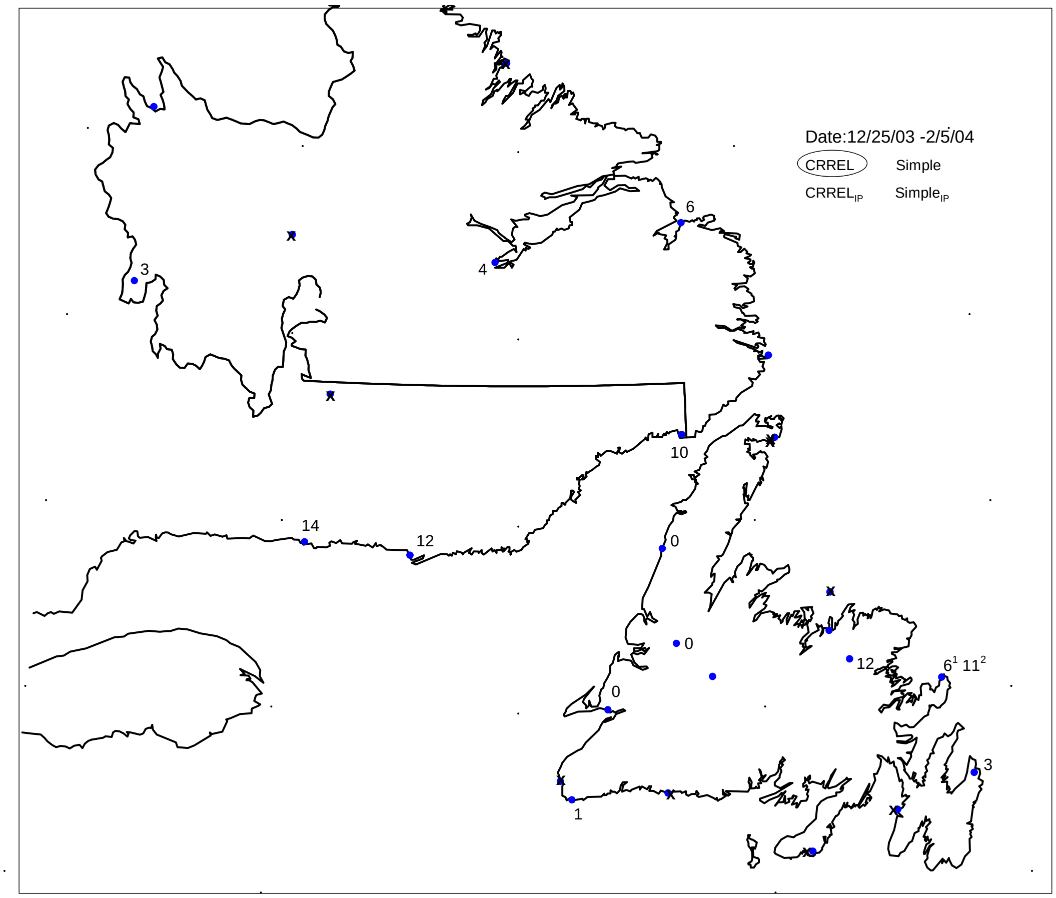
Date:12/25/03 -2/5/04
CRREL
Simple
CRELIP
SimpleIP
6
4
3
10
14
12
0
0
12
6¹ 11²
0
3
1

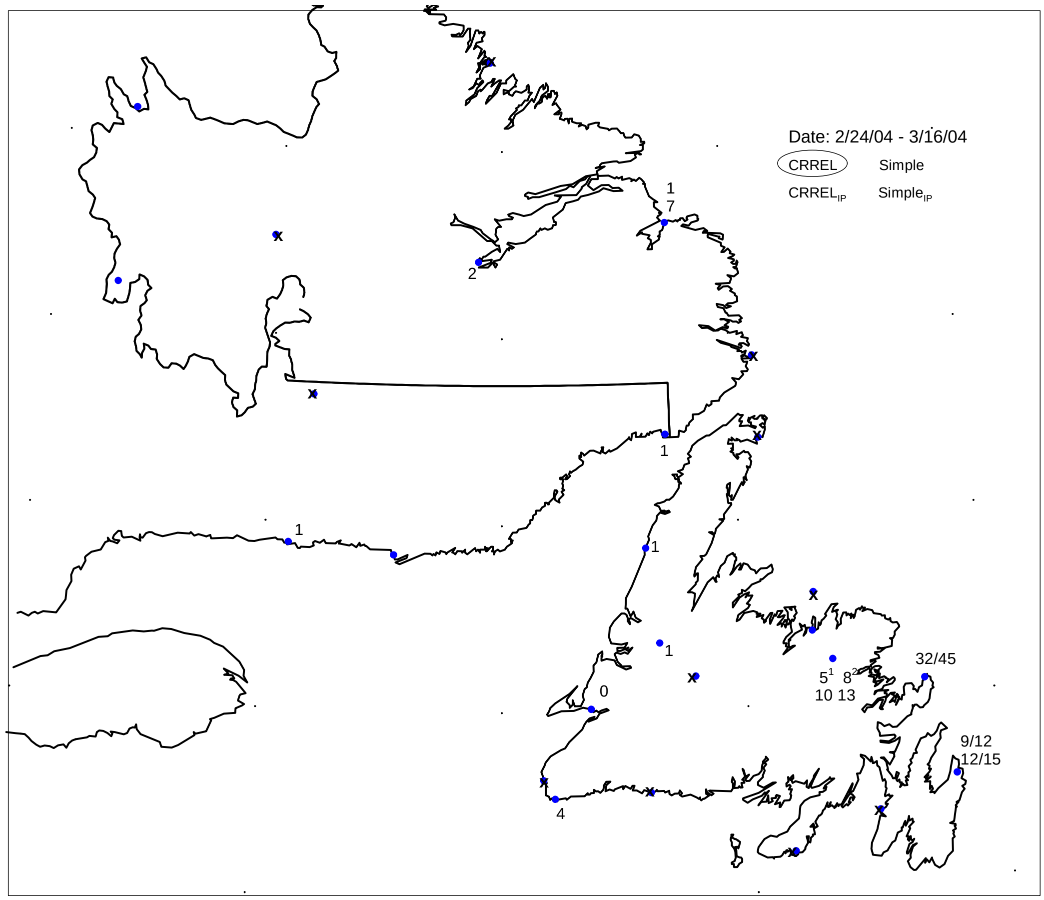
Date: 2/24/04 - 3/16/04
CRREL
Simple
CRELIP
SimpleIP
1
7
2
1
1
1
1
0
4
5
8
10 13
32/45
9/12
12/15

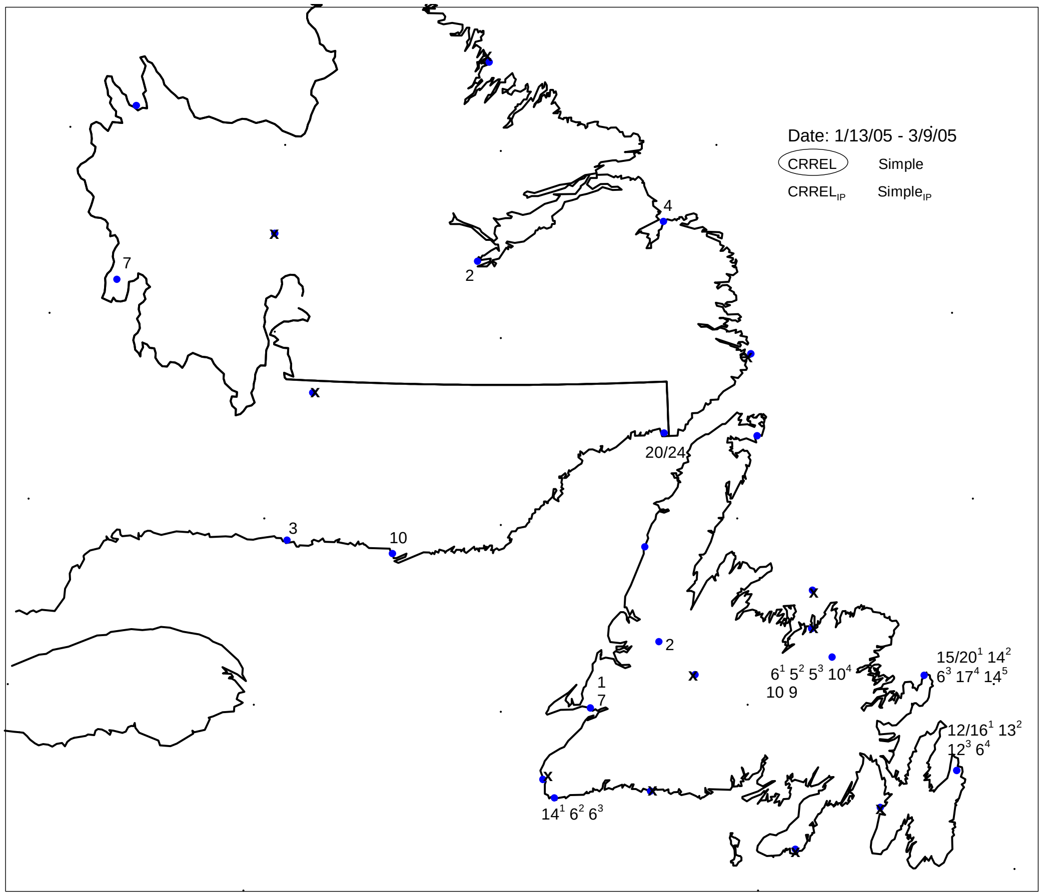
Date: 1/13/05 - 3/9/05
CRREL
Simple
CRELIP
SimpleIP
7
2
4
20/24
3
10
2
1
7
14¹ 6² 6³
6¹ 5² 5³ 10⁴
10 9
15/20¹ 14²
6³ 17⁴ 14⁵
12/16¹ 13²
12³ 6⁴


1

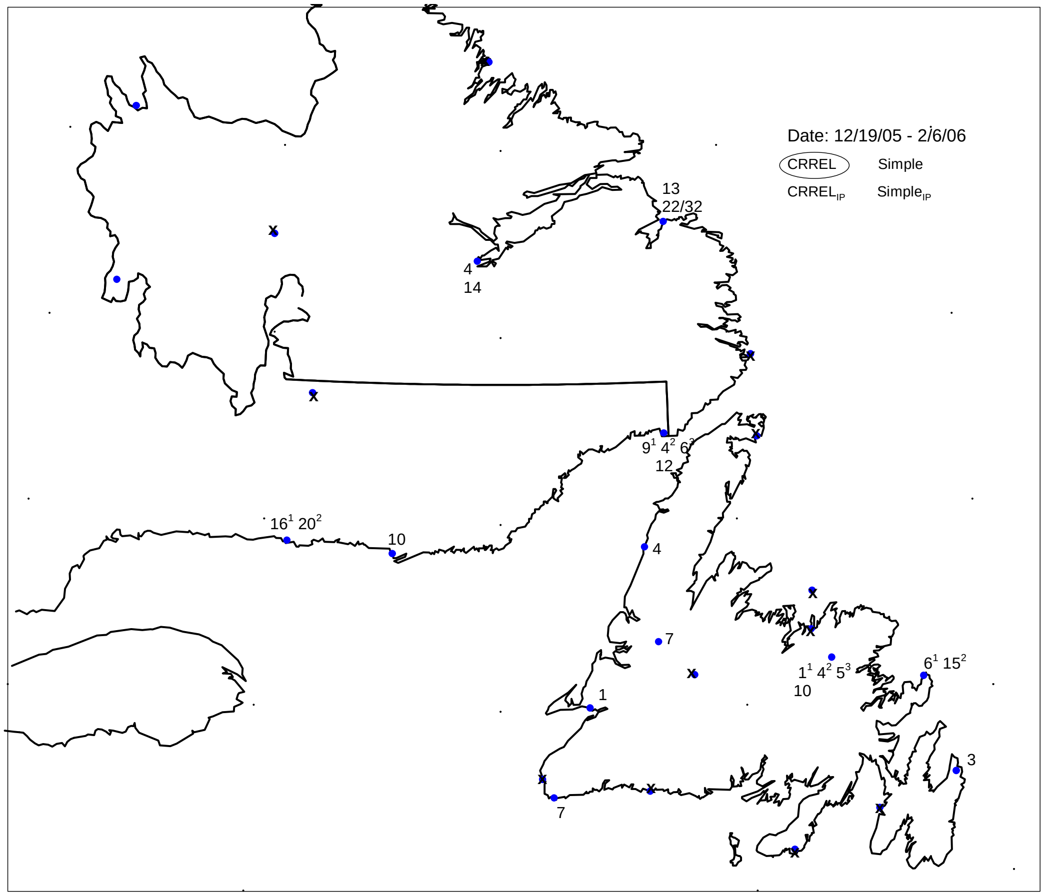
Date: 12/19/05 - 2/6/06
CRREL
Simple
CRELIP
SimpleIP
13
22/32
4
14
9¹ 4² 6²
12
16¹ 20²
10
4
7
1
7
1¹ 4² 5³
10
6¹ 15²
3

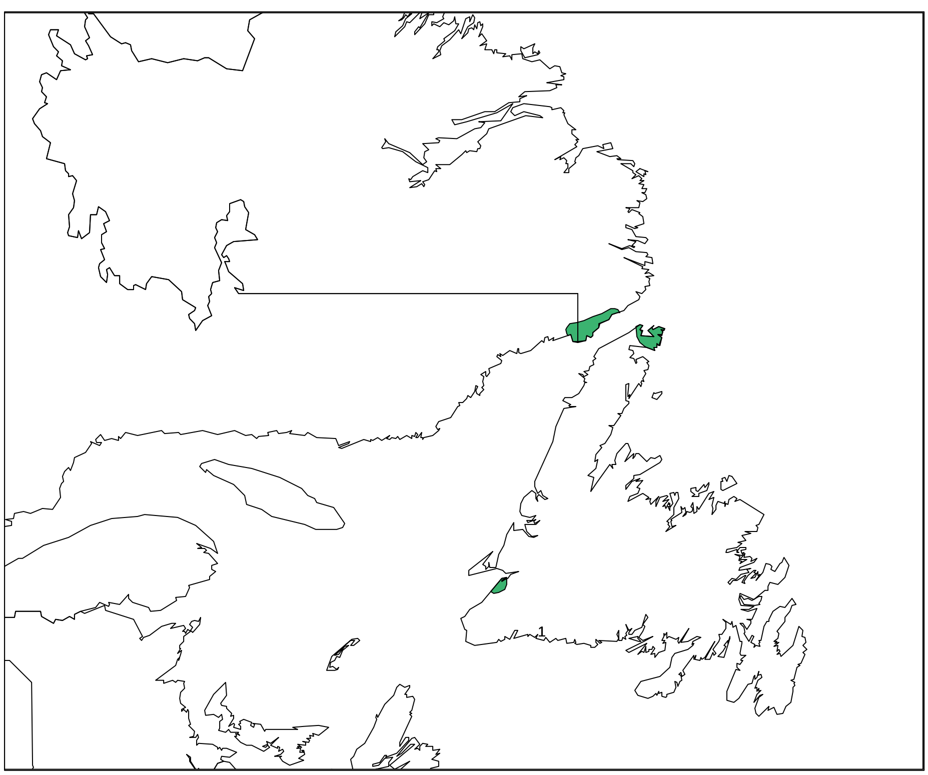
1

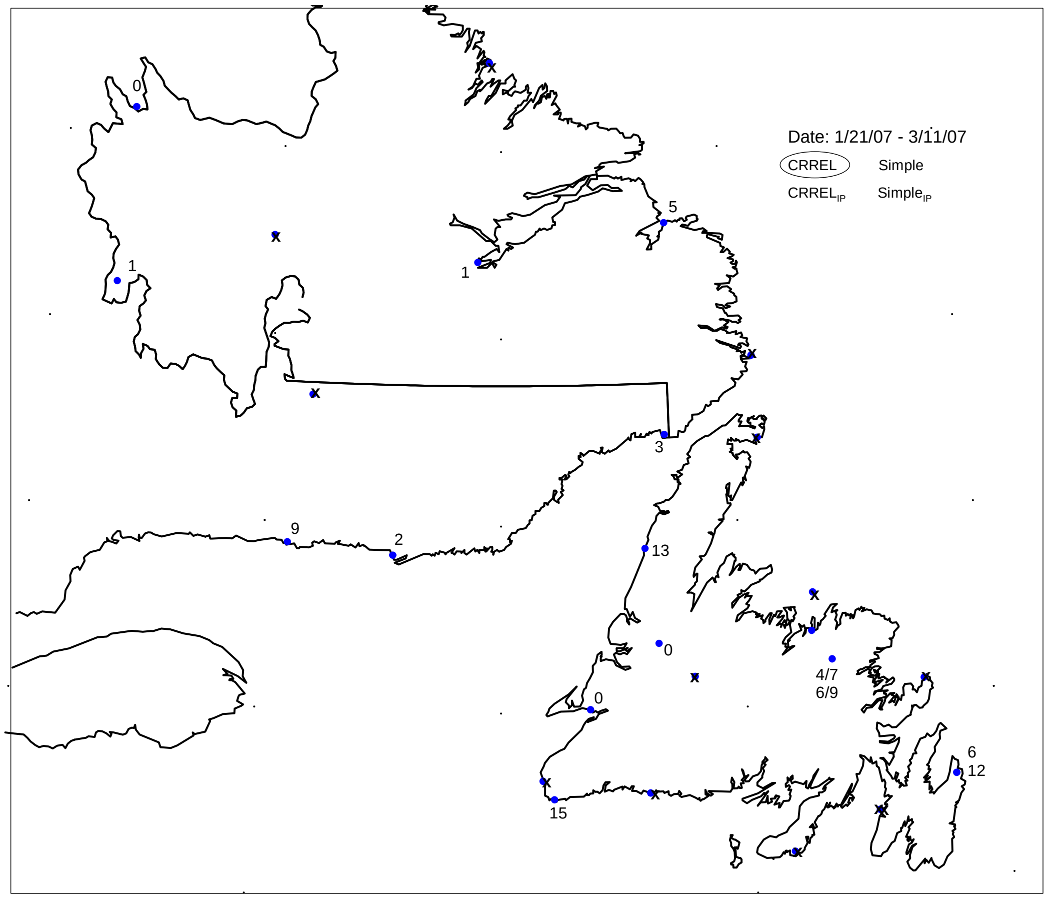
Date: 1/21/07 - 3/11/07
CRREL
Simple
CRELL_IP
Simple_IP
0
1
1
5
3
9
2
13
0
4/7
6/9
0
6
12
15


1

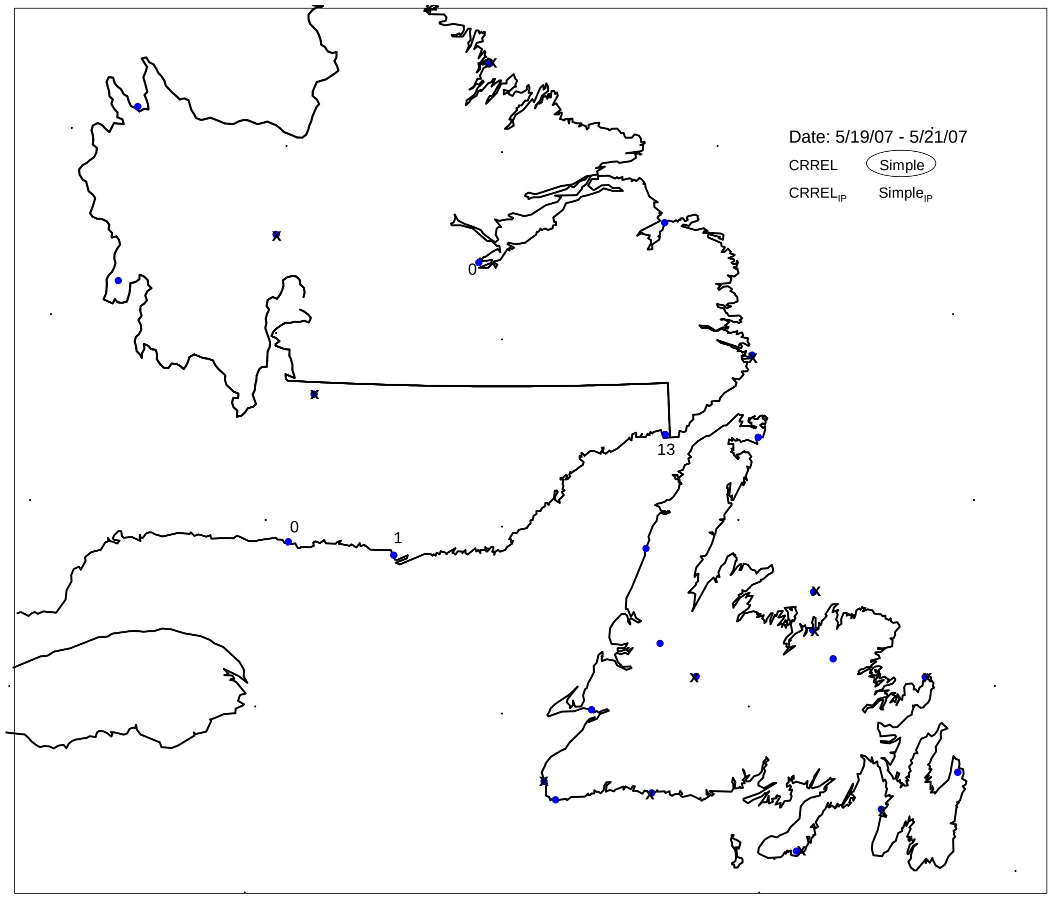
Date: 5/19/07 - 5/21/07
CRREL
Simple
$CRREL_{IP}$
$Simple_{IP}$
0
13
0
1

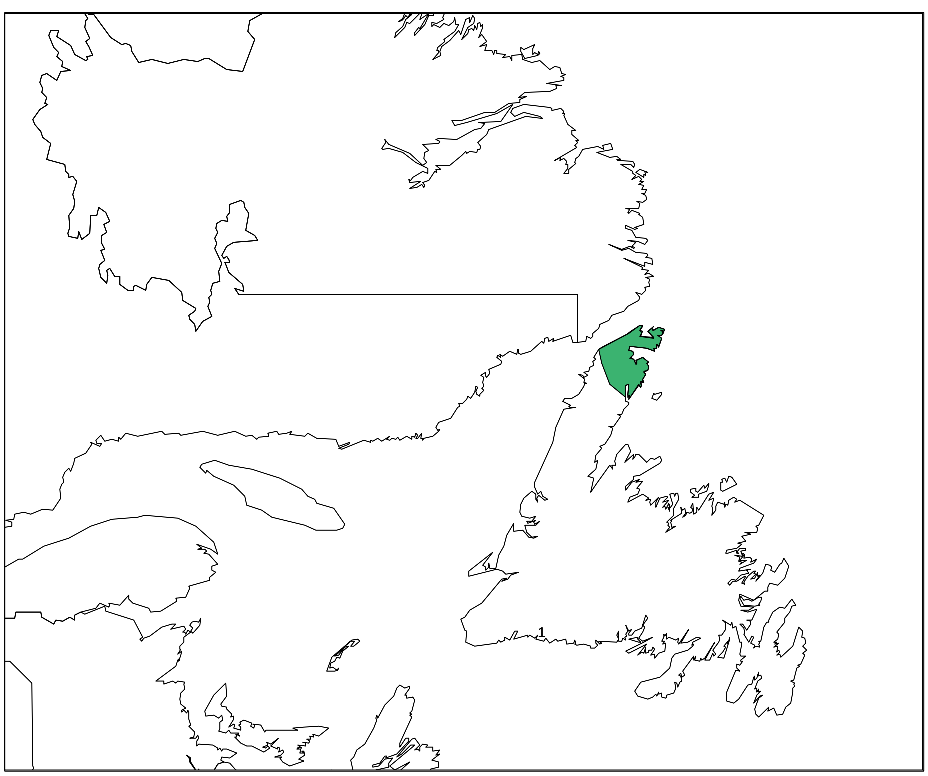
1

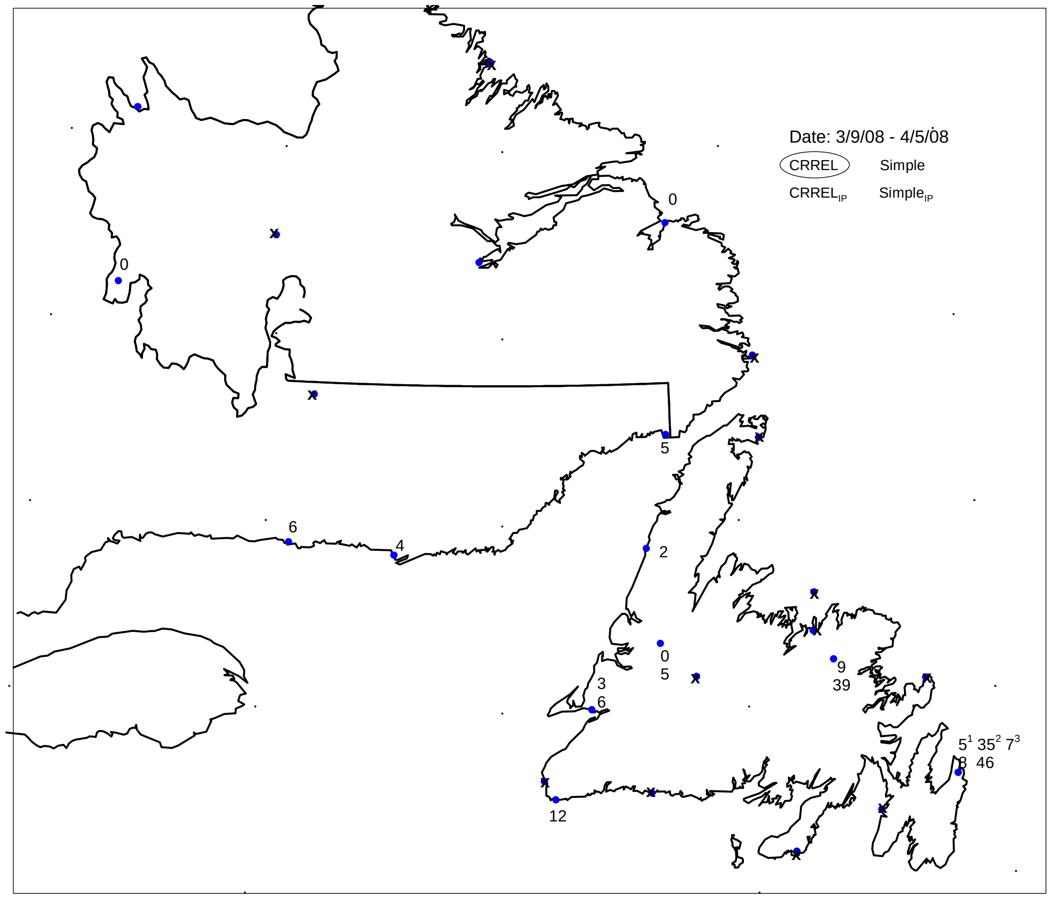
Date: 3/9/08 - 4/5/08
CRREL
Simple
CRELIP
SimpleIP
0
0
5
6
4
2
0
5
9
39
3
6
12
46

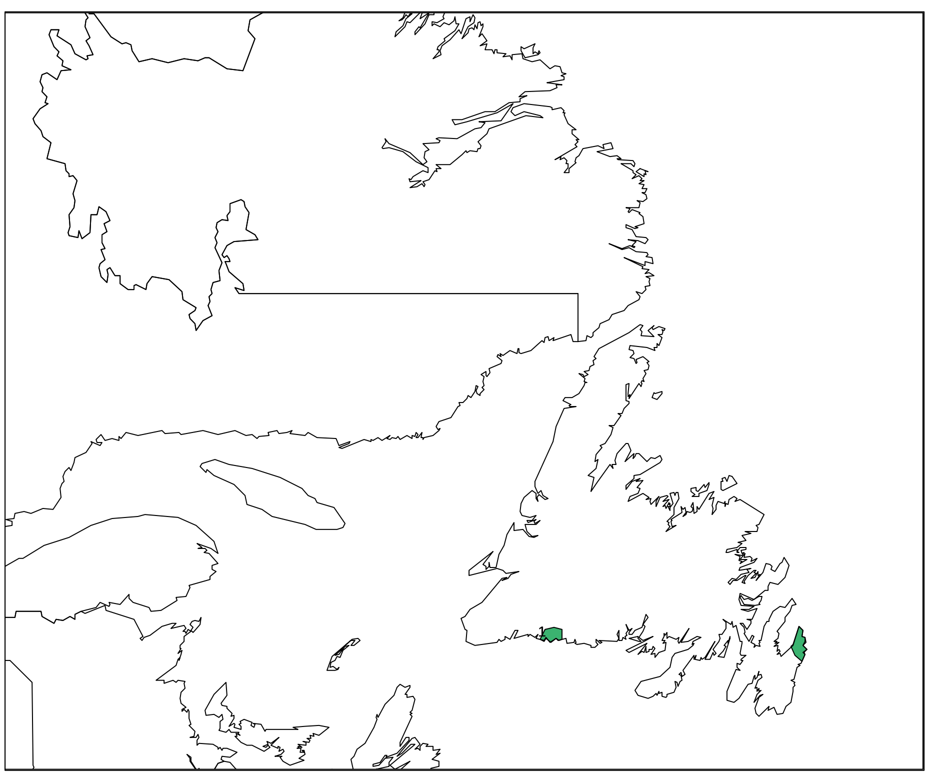

Appendix C. Hawke Hill photos

Kyle Tucker provided these photos from Hawke Hill for 2004 through 2006. Under each photo with a new date, the Simple model equivalent radial ice thicknesses for St. John’s and pseudo Hawke Hill are shown in red.

Fig 1: 2004-02-26 St. John's 4 mm St. John's-Hawke Hill 6 mm

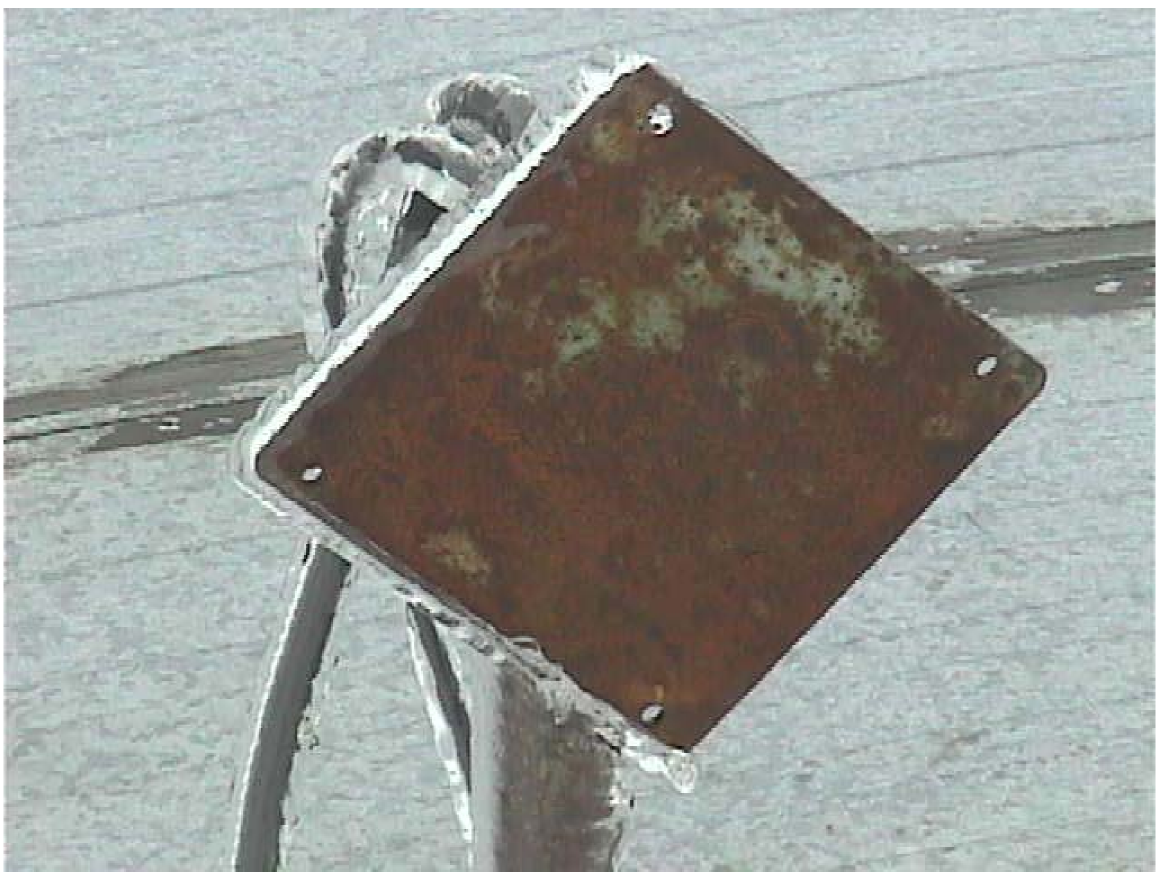

Fig 2: 20040312 St. John's 9 mm St. John's-Hawke Hill 18 mm

Fig 3: 20040312

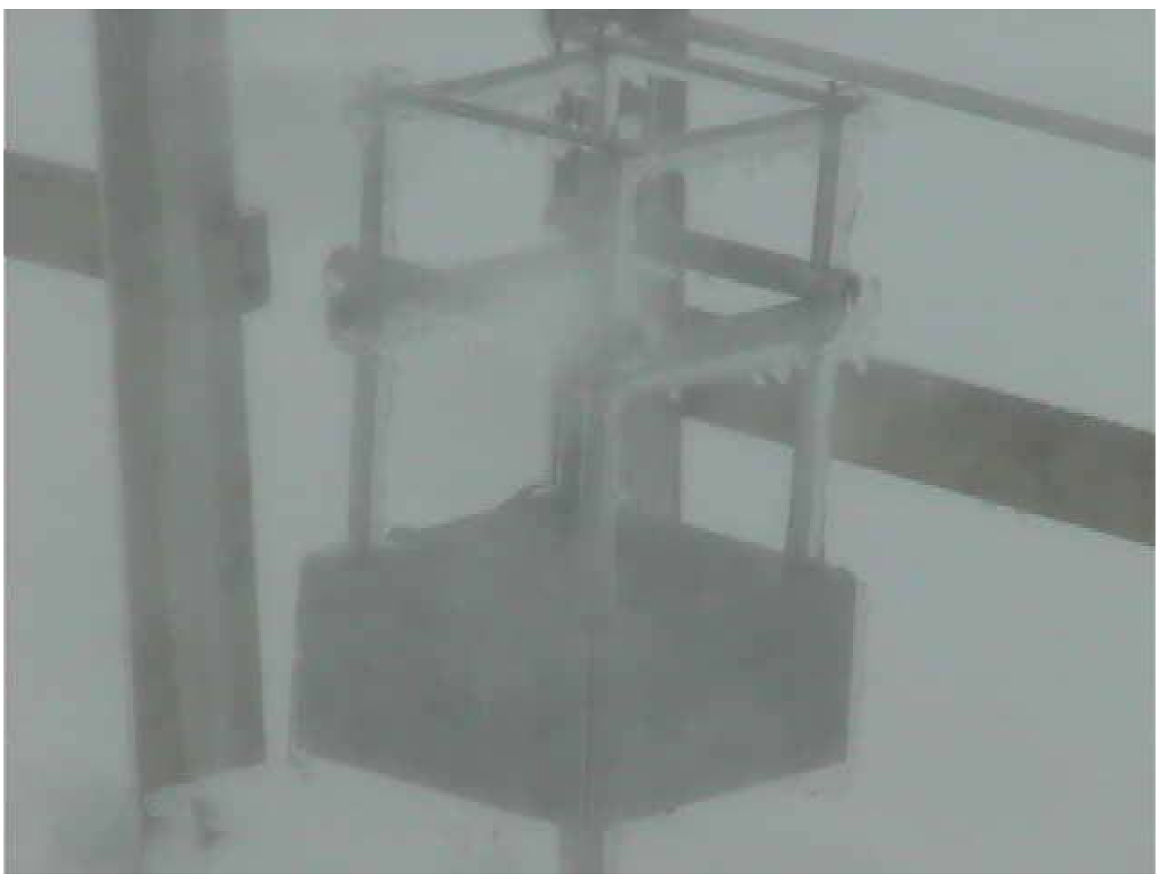

Fig 4: 20040312

Fig 5: 20050124 St. John's 14 mm St. John's-Hawke Hill 18 mm

Fig 6: 20050124

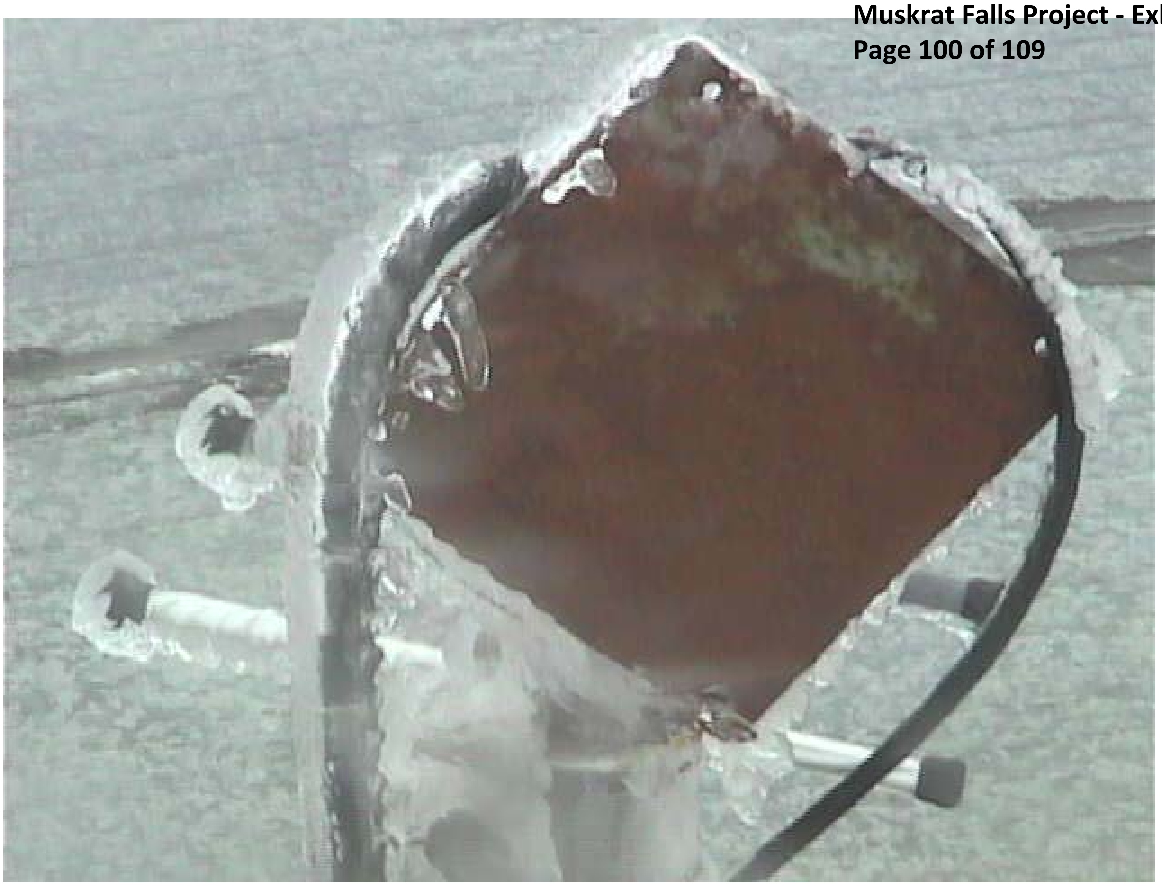

Fig 7: 20050124

Fig 8: 20050124

Fig 9: 20050124

Fig 10: 20050124

Fig 11: 20050124

Fig 12: 20050124

Fig 13: 20050124

Fig 14: 20050302 St. John's 6 mm St. John's-Hawke Hill 9 mm

Fig 15: 20050314 St. John's 3 mm St. John's-Hawke Hill 3 mm

Fig 16: 20060311 St. John's 12 mm St. John's-Hawke Hill 19 mm

Fig 17: 20060312 St. John's 12 mm (same storm) St. John's-Hawke Hill 19 mm (same storm)

Fig 18: 20060312

Fig 19: 20060315 St. John's 7 mm St. John's-Hawke Hill 28 mm (same storm)

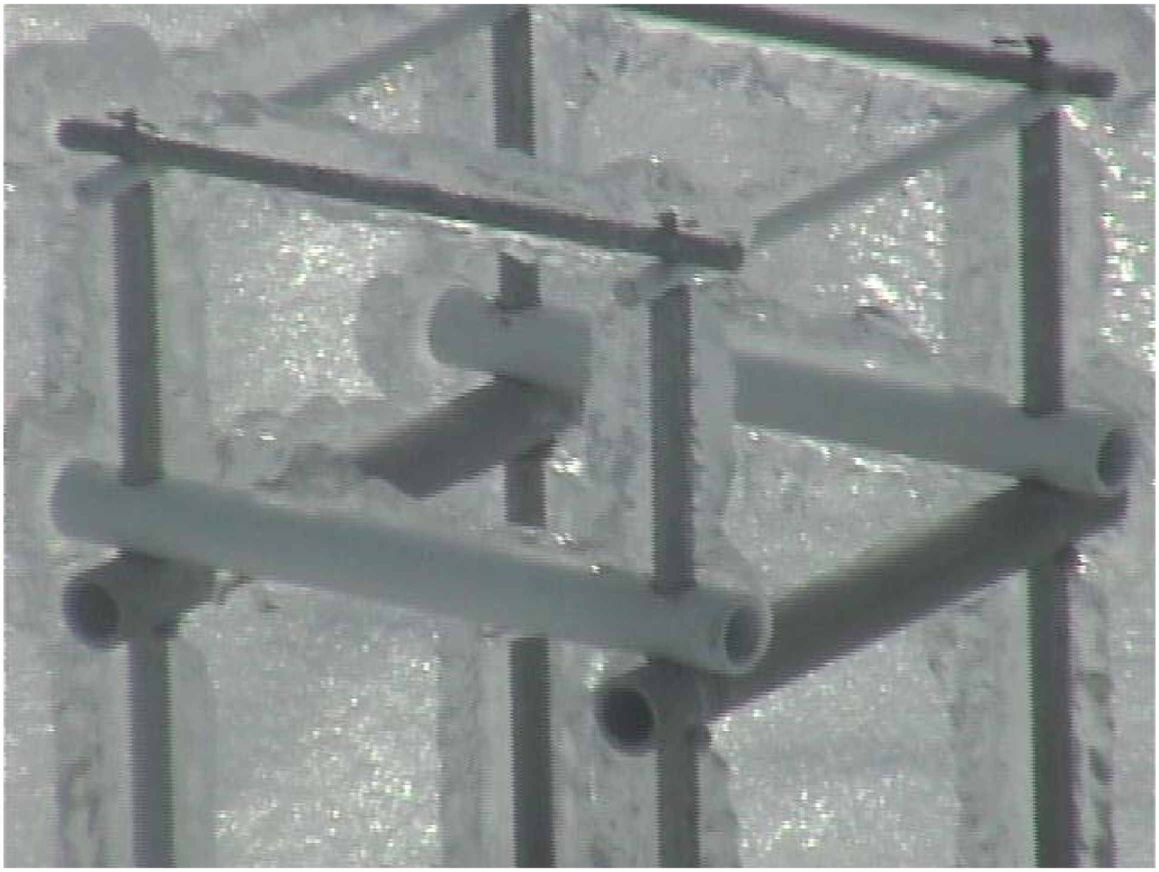

Fig 20: 20060316 St. John's 7 mm (same storm) St. John's-Hawke Hill 28 mm (same storm)

Fig 21: 20060316

Fig 22: 20060321 St. John's 3 mm   St. John's-Hawke Hill 3 mm

Fig 23: 20060328 St. John's 3 mm St. John's-Hawke Hill 7 mm (same storm)

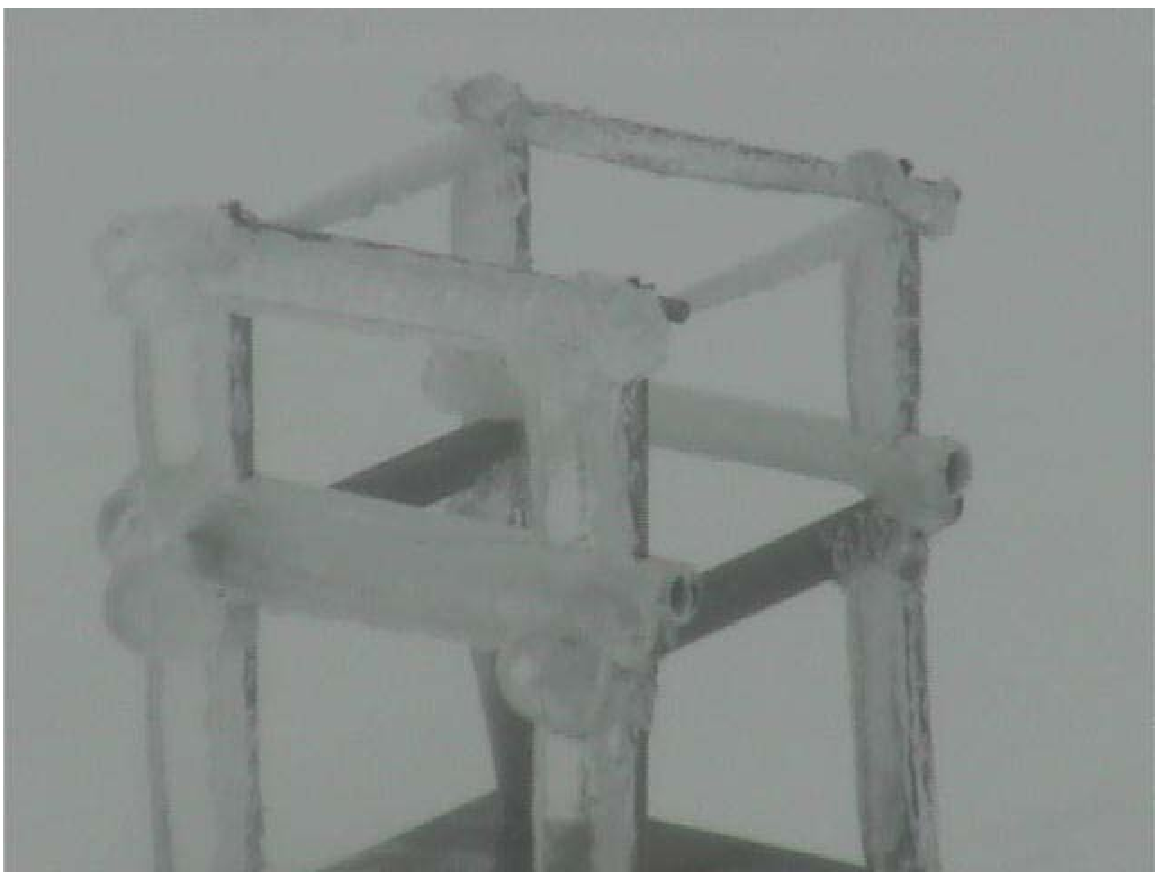

Fig 24: 20060330 St. John's 7 mm (same storm) St. John's-Hawke Hill 13 mm (same storm)

Fig 25: 20060421 St. John's 3 mm St. John's-Hawke Hill 4mm

Fig 26: 20060422 St. John's 3 mm (same storm) St. John's-Hawke Hill 4mm (same storm)